AD-A097 352 SRI INTERNATIONAL MENLO PARK CA F/G 7/4
THERMOCHEMISTRY OF GASEOUS COMPOUNDS OF METALS.(U)
MAR 81 D L HILDENBRAND, K H LAU, R D BRITTAIN F49620-78-C-0033
UNCLASSIFIED AFOSR-TR-81-0330 NL

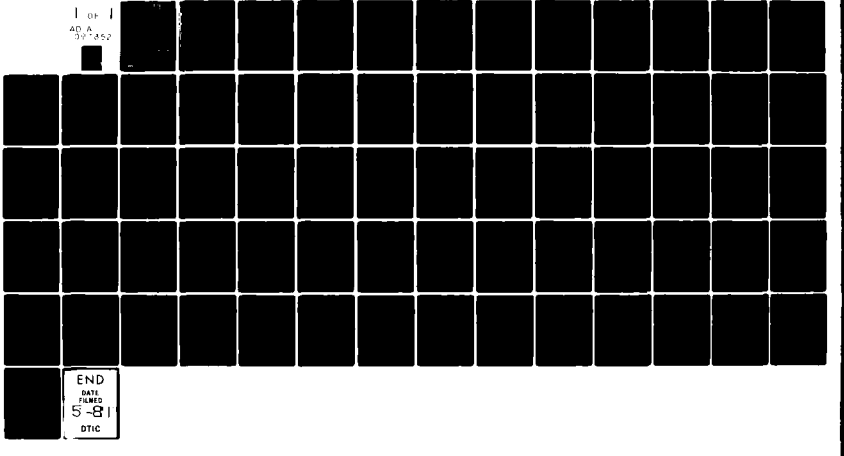

END
DATE FILMED
5-81
DTIC

March 1981

Final Technical Report
5 December 1977 to 4 December 1980

THERMOCHEMISTRY OF GASEOUS COMPOUNDS OF METALS

Prepared by: D. L. Hildenbrand

Work Performed by: D. L. Hildenbrand
K. H. Lau
R. D. Brittain
P. D. Kleinschmidt
R. H. Lamoreaux

Prepared for:

AIR FORCE OFFICE OF SCIENTIFIC RESEARCH
Directorate of Aerospace Sciences (NA)
Building 410
Bolling Air Force Base, DC 20332

Attention: Dr. Caveny

Contract F-49620-78-C-0033

SRI International Project 7028

Approved by:

G. R. Abrahamson, Vice President
Physical Sciences Division

SRI International
333 Ravenswood Ave. • Menlo Park, California 94025
(415) 326-6200 • Cable: SRI INTL MPK • TWX: 910-373-1246

UNCLASSIFIED

SECURITY CLASSIFICATION OF THIS PAGE (When Data Entered)

REPORT DOCUMENTATION PAGE

READ INSTRUCTIONS BEFORE COMPLETING FORM

1. REPORT NUMBER: AFOSR-TR-81-0330	2. GOVT ACCESSION NO.: AD-A097352
3. RECIPIENT'S CATALOG NUMBER	
4. TITLE (and Subtitle): Thermochemistry of Gaseous Compounds of Metals.	5. TYPE OF REPORT & PERIOD COVERED: Final rept. 5 Dec 77 - 4 Dec 80
	6. PERFORMING ORG. REPORT NUMBER
7. AUTHOR(s): D. L. Hildenbrand, K. H. Lau, R. D. Brittain, P. D. Kleinschmidt, R. H. Lamoreaux	8. CONTRACT OR GRANT NUMBER(s): F49620-78-C-0033
9. PERFORMING ORGANIZATION NAME AND ADDRESS: SRI International, 333 Ravenswood Avenue, Menlo Park, CA 94025	10. PROGRAM ELEMENT, PROJECT, TASK AREA & WORK UNIT NUMBERS: 61102F 2308/B1
11. CONTROLLING OFFICE NAME AND ADDRESS: Air Force Office of Scientific Research, Bldg. 410, Bolling AFB, DC 20332	12. REPORT DATE: Mar 1981
	13. NUMBER OF PAGES: 45
14. MONITORING AGENCY NAME & ADDRESS (if different from Controlling Office)	15. SECURITY CLASS. (of this report): Unclassified
	15a. DECLASSIFICATION DOWNGRADING SCHEDULE

16. DISTRIBUTION STATEMENT (of this Report)

Approved for public release; distribution unlimited

17. DISTRIBUTION STATEMENT (of the abstract entered in Block 20, if different from Report)

18. SUPPLEMENTARY NOTES

19. KEY WORDS (Continue on reverse side if necessary and identify by block number)

Thermochemistry
Reaction equilibria
Mass spectrometry
Enthalpies of formation
Dissociation energies
Entropies
Metal oxides
Metal oxyhalides
High temp. chemistry
Metal halides

20. ABSTRACT (Continue on reverse side if necessary and identify by block number)

See reverse side.

410281

UNCLASSIFIED

DD FORM 1473

The results obtained during a three-year program of thermochemical studies of gaseous inorganic metal compounds are summarized in this report. The metal compounds studied were primarily the fluorides, oxides, and oxyfluorides of the transition and lanthanide metals, potential hot corrosion products and/or reaction products of chemical pumping steps in potential lasing processes. Specific chemical systems studied were the gaseous fluorides of Mo, Ta, Zr, B, Sc, Y, La, Ni, Sm, Eu, and Tm; the oxides of Lu and Tm; and the oxyfluorides of Ta and W. Derived thermochemical data include the standard enthalpies of formation, bond dissociation energies, ionization energies, and in most cases absolute entropy data that can be used to check the assignment of spectroscopic and molecular constants; the latter proved to be particularly important for the scandium group lanthanide group metal compounds, which have large but uncertain electronic contributions to the entropy and Gibbs energy function. The entropy and enthalpy data can be used together to evaluate the equilibrium behavior of these systems over wide temperature ranges. Bond dissociation energy data for the scandium-group and lanthanide fluorides, which have sufficient ionic bonding for valid comparisons, correlate well with the predictions of the polarizable ion model, providing further corroboration for the usefulness of this model in generating thermochemical data for species not studied experimentally. The thermochemical data for the tantalum fluorides provide a clear explanation for the observed resistance of tantalum to attack by fluorine at high temperatures and low pressures.

TABLE OF CONTENTS

ABSTRACT

The results obtained during a three-year program of thermochemical studies of gaseous inorganic metal compounds are summarized in this report. The metal compounds studied were primarily the fluorides, oxides, and oxyfluorides of the transition and lanthanide metals, potential hot corrosion products and/or reaction products of chemical pumping steps in potential lasing processes. Specific chemical systems studied were the gaseous fluorides of Mo, Ta, Zr, B, Sc, Y, La, Ni, Sm, Eu, and Tm; the oxides of Lu and Tm; and the oxyfluorides of Ta and W. Derived thermochemical data include the standard enthalpies of formation, bond dissociation energies, ionization energies, and in most cases absolute entropy data that can be used to check the assignment of spectroscopic and molecular constants; the latter proved to be particularly important for the scandium group and lanthanide group metal compounds, which have large but uncertain electronic contributions to the entropy and Gibbs energy function. The entropy and enthalpy data can be used together to evaluate the equilibrium behavior of these systems over wide temperature ranges. Bond dissociation energy data for the scandium-group and lanthanide fluorides, which have sufficient ionic bonding for valid comparisons, correlate well with the predictions of the polarizable ion model, providing further corroboration for the usefulness of this model in generating thermochemical data for species not studied experimentally. The thermochemical data for the tantalum fluorides provide a clear explanation for the observed resistance of tantalum to attack by fluorine at high temperatures and low pressures.

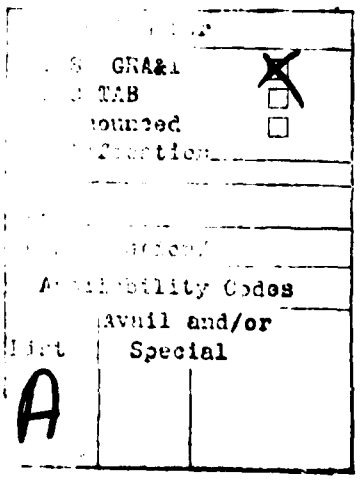

Research Objectives

The objective of this program is to provide reliable thermochemical data [enthalpies, entropies, and Gibbs energies of formation, bond dissociation energies (BDE), ionization energies] for high temperature chemical species of interest in aerospace technological applications. Data of this type are used by the engineer, scientist, and designer concerned with the analysis of a variety of processes such as combustion, chemical corrosion, propulsion, and chemically pumped lasing reactions. Sophisticated computer codes based on both equilibrium and nonequilibrium chemistry have been developed for the parametric analysis of a number of such processes, but the lack of basic molecular property data as well as the lack of reliable methodologies for estimating these properties often make the results of these computations highly uncertain and of dubious value.

In this program, we have been concerned primarily with the generation, identification, and thermochemical characterization of technologically relevant gaseous compounds of the metals for which information is missing, incomplete, or conflicting. A secondary goal is the correlation of the results with the predictions of various chemical bonding models so that significantly improved schemes for making molecular property estimates can be developed. The recurring demands for such data always exceed the capabilities of the scientific community for producing new experimental results, so that the development of reliable models for both present and future use is quite important.

During the last year of the program, we have investigated gaseous fluorides of boron and zirconium, and gaseous oxyfluorides of tantalum and tungsten. These species are potential products of the corrosive interaction of fluorine and its compounds with structural materials such as lanthanum hexaboride, zirconia, zirconium boride, and the

refractory metals tantalum and tungsten. Materials in this group have, for example, been considered for service in combustion-driven HF and DF lasers, in which structural members are exposed to atomic and molecular fluorine at temperatures of 1500 to 2000 K. The results of the thermochemical studies can be used with appropriate kinetic models such as the quasi-equilibrium model of gas-solid reactions[1] to estimate the degree of corrosive interaction and, therefore, the suitability of these materials under the required conditions. The thermochemical results are summarized below.

Technical Approach

The primary experimental technique utilized in this work has been high temperature mass spectrometry. Our magnetic deflection instrument and high temperature beam source arrangement, together with the experimental procedure and data treatment methods, have been described in the literature.[2,3] The accuracy of the pyrometric temperature measurement, a critical parameter in thermochemical studies, is checked routinely by calibration against a laboratory standard lamp. Preliminary measurements to check the reaction chemistry on some of the systems reported here were made with a similarly-equipped quadrupole mass filter, but all of the final equilibrium measurements were obtained with the magnetic instrument. The performance of the magnetic spectrometer has been substantially upgraded in the last year by installation of a faster pumping system on the effusion source chamber and by installation of an electrically driven tuning fork for modulation of the neutral effusion beam to improve sensitivity for permanent gases by synchronous detection.

Equilibrium vapor pressures were determined by the torsion-effusion method, as described previously.[4,5] The performance of the torsion apparatus is checked periodically with a vapor pressure standard, and the absolute pressures are estimated to be accurate to within five percent. Slope data normally have an accuracy of about one percent.

Results

Many of the results obtained from this research program have already been published in scientific journals and need not be recounted here. These include studies of the Mo-F, Ta-F, B-F, Lu-O, Tm-O, Sm-F, Eu-F, and Tm-F systems, along with papers on calculational methods and experimental technique. Reprints of these papers are given in Appendices to this report. Other results not yet published are summarized below.

A. Scandium Yttrium and Lanthanum Fluorides

Extensive second law measurements of gaseous equilibria involving the MF, MF_2, and MF_3 species were made using Ba and BaF as reaction partners. Effusion beams of the desired composition were generated by fluorination of the pertinent metals with SF_6 or other metal fluorides, or by partial reduction of the IIIB metal trifluorides. The gaseous beam species were unambiguously identified from ionization threshold appearance potentials, and equilibrium data were evaluated from ion abundances measured with low energy electrons. The vaporization thermodynamics of the trifluorides were also studied by the torsion-effusion method.

A summary of the gaseous reactions studied and the derived enthalpy and bond dissociation energy (BDE) data are given in Table I. Data for the one Sc-Ba-F reaction studied here were coupled with similar second law results reported previously[6] for reactions involving Sc, ScF, and ScF_2 species to evaluate the BDE's listed in Table I. Our results for the Sc-F system and some of those for the Y-F system are in fair agreement with the BDE values reported by Zmbov and Margrave[7], which are uncertain by 6-10 kcal/mole, but the new data indicate D_0°(YF) to be about 20 kcal/mole larger. And the new BDE data for the La-F species differ by 10-20 kcal/mole from previous estimates in the literature.[8]

From reasonably complete spectroscopic and structural data, the entropies and other thermodynamic functions of the MF, MF_2, and MF_3 gaseous species were calculated, exclusive of the electronic contributions, which are uncertain or unknown for all but perhaps the MF_3 species.

It is expected that the valence-saturated MF_3 species would have singlet electronic ground states and no significant low-lying states, but this is not certain. These calculated entropies were then compared with experimental second law entropies of the metal fluoride species evaluated from the accurate reaction thermochemistry summarized in Table I, plus the earlier data for ScF and ScF_2.[6] The experimental entropies of the ScF, YF, and LaF diatomic species are all larger than those calculated from the translational, rotational, and vibrational contributions; these differences are believed to be due to the presence of low-lying $^3\Delta$ states in the ScF-YF-LaF series. The entropy comparisons indicate the energies of these $^3\Delta$ states to be approximately 500 to 1000 cm^{-1} in ScF, 2500 cm^{-1} in YF, and 4000 cm^{-1} in LaF.

Actually the experimental entropy of ScF at 2100 K agrees to within 0.5 cal/deg mol with that calculated from the low-lying state assignments $X\ ^1\Sigma$, $^3\Delta$ (T_e = 461 cm^{-1}), and $^1\Delta$ (T_e = 2612 cm^{-1}) derived from ab initio calculations by Carlson and Moser,[9] and suggested by the analysis of Brewer and Green.[10] And the indications from the entropy data of an increasing separation of the $X\ ^1\Sigma$ and $^3\Delta$ states in going from ScF to YF to LaF are in accord with the photoluminescence results of Broida and co-workers[11,12] on the low-lying states of the isoelectronic molecules TiO and ZrO; these studies[11,12] showed the energy increments of these states above ground to increase in going down the series from TiO to ZrO. Likewise, the analysis of Weltner and McLeod[13] indicates that this separation increases still further in going from ZrO to HfO.

Electronic entropies of the order of several cal/deg mole at 2200 K are also indicated for ScF_2 and YF_2, while the experimental entropies of LaF_2 and the metal trifluoride species are compatible with those calculated solely from the translational, rotational, and vibrational contributions. The entropy data provided by these second law measurements are especially valuable, since they provide the additional information needed in evaluating the high temperature equilibrium behavior of chemical systems in many technological and engineering applications.

The equilibrium vapor pressures of crystalline ScF_3, YF_3, and LaF_3 were measured by the torsion-effusion method using graphite effusion cells, with the following results:

$ScF_3(s)$: log P(atm) = 9.310 - (19000/T) (1220 to 1400 K)

$YF_3(s)$: log P(atm) = 8.890 - (20750/T) (1350 to 1430 K)

$LaF_3(s)$: log P(atm) = 9.510 - (21620/T) (1330 to 1500 K)

Absolute pressures are estimated to be accurate within ten percent; there is considerable scatter among data in the literature, but the new results will clarify the issue and will be useful, for example, in quantitatively evaluating the thermal stability of protective films of the solid and liquid trifluorides on substrates containing Sc, Y, and La.

For ScF, YF, and LaF, where the internuclear distances are known accurately, dissociation energies predicted by the Rittner electrostatic bonding model using reasonable M^+ ion polarizabilities are in good agreement with the experimental values. Using this ionic model, the calculated value for YF_3 (where the internuclear Y-F distance has been determined by electron diffraction) also agrees well with the experimental heat of atomization. Lack of adequate data on bond distances precludes extension of the Rittner model to the other Sc, Y, and La species. Estimated bond distances of uncertain accuracy are of no help here; a change of only 3.5% in the estimated La-F distance in LaF_3, for example, leads to a difference of 30 kcal/mole in the calculated binding energy. The comparison between calculated and measured dissociation energies underlines the extreme usefulness of the Rittner model in estimating thermochemical data, but at the same time points up the sensitivity of the calculated values to the quality of the input parameters such as internuclear distance. A more complete discussion of the ionic model calculations is given in Appendix C.

Attempts to corroborate the equilibrium thermochemical data by means of electron impact measurements on the trifluorides were unsuccessful because an unexpected low energy process obscured the threshold for

the major dissociative process $MF_3 + e \rightarrow MF_2^+ + F + 2e$. This additional low energy process is believed to be the ion pair process $MF_3 + e \rightarrow MF_2^+ + F^- + e$, since the negative ion F^- was detected along with ScF_2^+ in the studies of ScF_3, and the threshold energy is compatible with this interpretation. The intensity of the low energy tail on the MF_2^+ ion yield curve was strongest for YF_3, and weakest for LaF_3.

B. Nickel Fluorides

Reaction equilibria involving gaseous NiF and NiF_2 were studied by mass spectrometry, using Cu and CuF as reaction partners. Beams of the appropriate composition were generated by the reaction of NiF_2 vapor with a Cu-Ni alloy. The reactions studied and the derived thermochemical data are summarized in Table II. There are no previous thermochemical determinations on NiF; the new experimental value of D(NiF) is 5 to 20 kcal/mole higher than estimates that have appeared in the literature. The second-law reaction entropy data are consistent with $^2\pi$ and $^3\Phi$ electronic ground states for NiF and NiF_2, respectively. These ground state configurations lead to electronic entropies of 2.8 and 3.6 cal/deg mole, and the inclusion of these terms yields calculated entropies agreeing to within one cal/deg mole with the experimental entropies.

C. Zirconium Fluorides

The gaseous species ZrF_4, ZrF_3, ZrF_2, and ZrF, along with Zr, Ba, and BaF were generated from an equilibrium effusion beam source by the the reaction of BaF_2 vapor with Zr powder or sheet. After the species were carefully characterized from their ionization threshold energies, several series of equilibrium measurements were made over wide temperature ranges by means of mass spectrometry, using ion intensities measured at low electron energies to evaluate neutral species abundances. Results are summarized in Table III; as can be seen, third law enthalpies evaluated from thermodynamic functions in the JANAF Tables[14] are in fairly good agreement with the second law values, indicating that estimated spectroscopic constants of ZrF_3, ZrF_2, and ZrF are reasonable. At present the second law values are preferred, and derived data are based on these.

The derived bond dissociation energies in Table III vary between 148 and 166 kcal/mole and their sum, 631 ± 6 kcal/mole, is in reasonable agreement with the heat of atomization 620 ± 2 calculated from the enthalpy of formation of $ZrF_4(s)$ and the enthalpy of sublimation of $ZrF_4(g)$. Derived thermochemical data for gaseous ZrF, ZrF_2, and ZrF_3 differ by 5-6 kcal/mole from JANAF Table values based on early preliminary work, but the new results are considered to be much more reliable, and they allow the gaseous thermochemistry of the Zr-F system to be defined clearly.

D. The Ta-O-F System

In previous studies, Zmbov and Margrave[15] investigated gas-solid equilibria involving $TaOF_3(g)$ and used the results to derive thermochemical data for this species and an estimate for $TaOF_2(g)$. Since oxyfluorides of this type are quite stable and will be prominent when oxygen or water impurities are present in Ta-F systems, we carried out additional equilibrium studies of Ta-O-F species by fluorinating a solid mixture of Ta_2O_5, SiO_2, and Ta with a gaseous mixture of SF_6 and SiF_4. At cell temperatures above 2000 K, the gaseous species involved in the reaction equilibria

$$TaOF_3(g) + SiF(g) = TaF_4(g) + SiO(g) \qquad (1)$$

$$TaOF_2(g) + SiF(g) = TaF_3(g) + SiO(g) \qquad (2)$$

were clearly identified, and equilibrium measurements were made over the range 2024 to 2306 K by mass spectrometry, with the second-law results shown in Table IV. Standard enthalpies of formation and bond dissociation energies of the Ta-O-F species were derived as shown. The accuracy of these thermochemical values is on the order of ± 5 kcal/mole, due to uncertainties in the data[14,16] for SiF, SiO, TaF_3, and TaF_4, as well as uncertainties in the equilibrium data.

To aid in carrying out high temperature equilibrium calculations involving the Ta-O-F species, the possibility of estimating the thermodynamic functions of $TaOF_3$ and $TaOF_2$ was explored. It seemed reasonable

to assume that the vibrational contributions to the functions of $TaOF_3$ and $TaOF_2$ would approximate those of TaF_4 and TaF_3, respectively, and that the rotational contributions would differ mainly in the symmetry factors: $TaOF_3$ (C_{3v}); TaF_4 (T_d); TaF_3 (C_{3v}); and $TaOF_2$ (C_{2v}). Also the estimated electronic statistical weights would be one for $TaOF_3$ and TaF_3, and two for $TaOF_2$ and TaF_4. With these assumptions and the estimated functions for TaF_3 and TaF_4 shown previously to be in accord with the equilibrium data,[16] values for $TaOF_3$ and $TaOF_2$ were estimated as noted above. The resulting third law enthalpies, shown in Table IV, are in fair agreement with the second law values, indicating that thermodynamic functions of $TaOF_3$ and $TaOF_2$ so estimated can be used effectively in practical equilibrium calculations.

The derived bond dissociation energies $D(F_3Ta\text{-}O)$ and $D(F_2Ta\text{-}O)$ given in Table IV are intermediate between the values D(Ta-O) = 200 $\pm$ 15 kcal/mole and D(OTa-O) = 154 $\pm$ 15 kcal/mole taken from the JANAF Tables.[14] Likewise the derived BDE $D(OF_2Ta\text{-}F)$ is comparable to the values $D(F_2Ta\text{-}F)$ = 144 kcal/mole, $D(F_3Ta\text{-}F)$ = 130 kcal/mole, and $D(F_4Ta\text{-}F)$ = 138 kcal/mole.[16] Corresponding BDE values in the Ta-O-F species thus appear quite reasonable, and one can extend the analysis to estimate data for TaOF as shown in Table IV. The derived standard enthalpy of formation of $TaOF_3(g)$ corroborates the values -315 $\pm$ 10 kcal/mole and -321 $\pm$ 10 kcal/mole recalculated from the equilibrium data of Zmbov and Margrave[15] with more recent auxiliary information.

E. The W-O-F System

For reasons similar to those underlying the Ta-O-F studies, new investigations were undertaken to characterize significant gaseous species in the W-O-F system. Here, too, Zmbov, Uy, and Margrave[17] have studied reaction equilibria involving gaseous WOF_4 and WO_2F_2, and reported thermochemical data for these species. We have now extended this work by examining several gaseous equilibria involving WO_2F_2, and the additional species WOF_3, WOF_2, and WOF. This work again was carried out by high temperature mass spectrometry; the species were identified primarily from their ionization threshold energies, and equilibrium data were

obtained with low-energy ionizing electrons using GeO, GeF, and several of the W-F species as reaction partners. The equilibrium mixtures were generated by reaction of $WF_6(g)$ containing a $WOF_4(g)$ impurity with $GeO_2(s)$ and W(s) in a tungsten effusion cell. It was not possible to generate sufficiently strong signals over the wide temperature range required for reliable second law analysis, so that results were derived entirely from third law analysis. The preceding work on $TaOF_3$ and $TaOF_2$ shows that the systematic approach used there in estimating the thermodynamic functions of the M-O-F species is reasonable, so that the derived third law reaction enthalpies are estimated to be accurate to within 3 kcal/mole. Results are summarized in Table V. Data for the reference compounds GeO and GeF used in analyzing the data were taken from reference 18, while those for the W-F species are from our earlier work.[19]

The various W-O and W-F BDE's derived for the W-O-F species again appear reasonable when compared to the values $D(O_2W-O)$ = 148 kcal/mole, D(OW-O) = 143 kcal/mole, and D(W-O) = 161 kcal/mole evaluated from data in the JANAF Tables,[14] and to values for the corresponding W-F species ranging from 106 to 120 kcal/mole.[19] The observed trends permit one to make a reliable estimate of $D(F_4W-O)$ and, therefore, of the standard enthalpy of formation of $WOF_4(g)$, not observed in this work. Thermochemical properties of gaseous WO_2F_2 and WOF_4 derived from this work differ from some of the earlier values by significant amounts, but the present results are believed to be more reliable, and all of the new data together can be used to define the equilibrium vapor phase chemistry of the W-O-F system.

F. The La-O-F System

Possible vapor species in the La_2O_3-LaF_3 system were investigated by vaporizing a mixture of these two phases from a Knudsen cell and examining the vapor by quadrupole mass spectrometry. No gaseous species other than LaF_3 could be detected, and it is concluded that gaseous oxyfluorides are not of importance in this system.

G. Derived Standard Enthalpies of Formation

The thermochemical results of primary interest in these studies, the standard enthalpies of formation, are summarized in Table VI. This table serves as a summary of those systems studied successfully during the program.

Professional Personnel

The professional personnel associated with the program were the following:

Dr. D. L. Hildenbrand, Senior Research Scientist
(Principal Investigator)
Dr. K. H. Lau, Materials Chemist
Dr. R. D. Brittain, Postdoctoral Chemist
Dr. P. D. Kleinschmidt, Postdoctoral Chemist
Dr. R. H. Lamoreaux, Materials Chemist

Publications

In addition to the seven publications shown in the Appendices, the following additional manuscripts are planned or are in preparation:

"Mass Spectrometric Studies of the Thermochemistry of the Scandium, Yttrium, and Lanthanum Fluorides," by P. D. Kleinschmidt, K. H. Lau, and D. L. Hildenbrand, to be submitted to the Journal of Chemical Physics.

"Dissociation Energies of NiF and NiF_2," K. H. Lau and D. L. Hildenbrand, to be submitted to High Temperature Science.

"Thermochemical Characterization of the Gaseous Zirconium Fluorides by Mass Spectrometry," by K. H. Lau and D. L. Hildenbrand, to be submitted to the Journal of Physical Chemistry.

"Thermochemistry of the Gaseous Oxyfluorides of Tantalum and Tungsten," by R. D. Brittain, K. H. Lau, and D. L. Hildenbrand, to be submitted to the Journal of the Electrochemical Society.

REFERENCES

1. J. C. Batty and R. E. Stickney, J. Chem. Phys. 51, 4475 (1969).

2. D. L. Hildenbrand, J. Chem. Phys. 48, 3657 (1968); 52, 5751 (1970).

3. D. L. Hildenbrand, Int. J. Mass Spectrom. Ion Phys. 4, 75 (1970); 7, 255 (1971).

4. D. L. Hildenbrand and W. F. Hall, J. Phys. Chem. 67, 888 (1963).

5. D. L. Hildenbrand and D. T. Knight, J. Chem. Phys. 51, 1260 (1969).

6. D. L. Hildenbrand, P. D. Kleinschmidt, and K. H. Lau, Report AFOSR-TR-78-0163, January 1978.

7. K. F. Zmbov and J. L. Margrave, J. Chem. Phys. 47, 3122 (1967).

8. K. F. Zmbov and J. L. Margrave, in Mass Spectrometry in Inorganic Chemistry, Adv. Chem. Ser. 72, Am. Chem. Soc., Wash., DC, 1968, p. 267.

9. K. D. Carlson and C. Moser, J. Chem. Phys. 46, 35 (1967).

10. L. Brewer and D. W. Green, High Temp. Sci. 1, 26 (1969).

11. J. M. Brom, Jr., and H. P. Broida, J. Chem. Phys. 63, 3710 (1975).

12. L. J. Lauchlan, J. M. Brom, Jr., and H. P. Broida, J. Chem. Phys. 65, 2672 (1976).

13. W. Weltner, Jr., and D. McLeod, Jr., J. Phys. Chem. 69, 3488 (1965).

14. JANAF Thermochemical Tables, NSRDS-NBS 37 (1971), and supplements.

15. K. F. Zmbov and J. L. Margrave, J. Phys. Chem. 72, 1099 (1968).

16. K. H. Lau and D. L. Hildenbrand, J. Chem. Phys. 71, 1572 (1979).

17. K. F. Zmbov, O. M. Uy, and J. L. Margrave, J. Phys. Chem. 73, 3008 (1969).

18. Thermodynamic Data for Individual Substances, V. P. Glushko and L. V. Gurvich, Eds., Vol. II, Institute for High Temperatures, Academy of Science, Moscow, 1979.

19. D. L. Hildenbrand, J. Chem. Phys. 62, 3074 (1975).

Table I

THERMOCHEMISTRY OF GROUP IIIB METAL FLUORIDE REACTIONS AND DERIVED BOND DISSOCIATION ENERGIES

Gaseous Reaction	Range, K	$\Delta H_T^\circ(II)$* kcal/mole	$\Delta H_{298}^\circ(II)$* kcal/mole
$ScF_3 + Ba = ScF_2 + BaF$	1470-1663	22.3 ± 1.1	24.4
$YF + Ba = Y + BaF$	1553-1733	21.0 ± 0.9	23.2
$YF_2 + Ba = YF + BaF$	1553-1715	1.3 ± 0.9	-0.7
$YF_3 + Ba = YF_2 + BaF$	1490-1696	19.3 ± 0.6	21.6
$LaF + Ba = La + BaF$	1984-2131	22.3 ± 1.2	22.0
$LaF_2 + Ba = LaF + BaF$	1891-2131	17.8 ± 0.4	17.0
$LaF_3 + Ba = LaF_2 + BaF$	1805-1978	9.4 ± 0.7	12.6
$La + LaF_2 = 2LaF$	2008-2270	-5.4 ± 0.4	-6.0

Bond	D_{298}°, kcal/mole	Bond	D_{298}°, kcal/mole	Bond	D_{298}°, kcal/mole
Sc-F	139.4	Y-F	161.9	La-F	160.7
FSc-F	145.8	FY-F	138.0	FLa-F	155.7
F_2Sc-F	163.1	F_2Y-F	160.3	F_2La-F	151.3

*II signifies second law value.

Table II

THERMOCHEMISTRY OF Ni-F REACTIONS AND DERIVED RESULTS

Gaseous Reaction	Range, K	ΔH_T°(II)* kcal/mole	ΔH_{298}°(II)* kcal/mole
NiF + Cu = Ni + CuF	1463-1664	5.4 ± 0.3	6.1
Ni + NiF_2 + 2NiF	1463-1664	6.4 ± 1.0	9.8

D_{298}°(NiF) = 109.0 ± 2 kcal/mole

D_{298}°(FNi-F) = 118.8 ± 3 kcal/mole

*II signifies second law value.

Table III

THERMOCHEMISTRY OF Zr-F REACTIONS AND DERIVED DATA

Gaseous Reaction	Range, K	ΔH_T°(II) kcal/mole	ΔH_{298}°(II) kcal/mole	ΔH_{298}°(III)* kcal/mole
$Zr + BaF = ZrF + Ba$	2102 - 2353	-10.1 ± 2	- 9.6 ± 2	-12.1 ± 3
$ZrF + BaF = ZrF_2 + Ba$	2102 - 2353	-20.1	-21.1	-21.0
$ZrF_2 + BaF = ZrF_3 + Ba$	1790 - 2173	-24.2	-27.4	-23.0
$ZrF_3 + BaF = ZrF_4 + Ba$	1423 - 1767	-15.8	-18.2	-19.3

Bond	D_{298}°, kcal/mole
Zr-F	148 ± 3
FZr-F	160
F_2Zr-F	166
F_3Zr-F	157

*Calculated with thermal functions from JANAF Tables.

Table IV

REACTION THERMOCHEMISTRY AND DERIVED THERMOCHEMICAL DATA
FOR Ta-O-F SPECIES

Gaseous Reaction	ΔH°_{298}(II) kcal/mole	ΔH°_{298}(III) kcal/mole
$TaOF_3 + SiF = SiO + TaF_4$	$- 1.0 \pm 2$	$- 4.2 \pm 3$
$TaOF_2 + SiF = SiO + TaF_3$	-16.5 ± 2	-19.9 ± 3

Bond	D°_{298}, kcal/mole
(F_3Ta-O)	189.0
(F_2Ta-O)	187.6
(OF_2Ta-F)	145.6
(FTa-O)	(185)

Table V

REACTION THERMOCHEMISTRY AND DERIVED THERMOCHEMICAL DATA FOR W-O-F SPECIES

Gaseous Reaction	ΔH°_{298}(III), kcal/mole
$WOF_3 + GeF = WF_4 + GeO$	-5.0 ± 3
$WO_2F_2 + GeF = WOF_3 + GeO$	5.0 ± 3
$WOF_2 + GeF = WF_3 + GeO$	10.0 ± 3
$WOF + GeF = WF_2 + GeO$	-4.0 ± 5

Bond	D°_{298}, kcal/mole
$(F_3W\text{-}O)$	148.5
$(F_2W\text{-}O)$	163.3
(FW-O)	161.3
$(F_2OW\text{-}O)$	143.5
$(F_4W\text{-}O)$	(145)
$(F_2OW\text{-}F)$	104.7
(FOW-F)	133.5

Table VI

DERIVED STANDARD ENTHALPIES OF FORMATION (kcal/mole)

Gaseous Species	ΔHf°_{298}	Uncertainty	Gaseous Species	ΔHf°_{298}	Uncertainty
MoF_5	-297	1	YF	- 41	2
			YF_2	-160	2
TaF	69	3	YF_3	-301	2
TaF_2	- 69	3			
TaF_3	-194	3	LaF	- 38	2
TaF_4	-305	3	LaF_2	-175	2
TaF_5	-425	3	LaF_3	-307	2
TmO	- 8	3	NiF	13	2
LuO	2	3	NiF_2	- 87	2
BF_2	-120	4	ZrF	14	2
			ZrF_2	-127	2
SmF	- 67	2	ZrF_3	-269	2
SmF_2	-183	2			
SmF_3	-302	2	$TaOF_3$	-323	5
			$TaOF_2$	-197	5
EuF	- 69	2	TaOF	(- 63)	5
EuF_2	-181	2			
EuF_3	-281	2	WO_2F_2	-208	5
			WOF_3	-210	5
TmF	- 47	2	WOF_2	-124	5
TmF_2	-162	2	WOF	- 10	5
TmF_3	-292	2	WOF_4	(-307)	5
ScF	- 30	2			
ScF_2	-157	2			
ScF_3	-301	2			

J. Chem. Thermodynamics 1979, 11, 765–772

The thermodynamic stability of gaseous molybdenum pentafluoride*

P. D. KLEINSCHMIDT, K. H. LAU, and D. L. HILDENBRAND

SRI International, Menlo Park, California 94025, U.S.A.

(*Received 12 June 1978; in revised form 20 November 1978*)

The heterogeneous reaction equilibrium (5/6)MoF_5(g)+(1/6)Mo(s) = MoF_3(g) was studied by mass spectrometry over the range 460 to 525 K, and values of $\Delta_r H°/R$ at 298.15 K derived by the second-law (6.9 ± 0.5) kK and third-law (6.4 ± 1.0) kK procedures are in close agreement. From the preferred second-law result, one derives $\Delta_f H°/R$ of MoF_5(g) at 298.15 K to be −(149.3 ± 0.5) kK, in good agreement with a value obtained previously from gaseous equilibrium measurements in the Mo+S+F system. Another value for MoF_5(g) derived from the vapor pressure of MoF_5(l) appears to be in error because of an incorrect evaluation of the partial pressure of monomer. The primary bond-dissociation function, $\{D(F_4Mo–F)\}/R$, is found to be 47.6 kK, compared with the average value of 53.8 kK in MoF_6. Gas-solid equilibrium in the MoF_6+MoF_5+Mo system is attained rapidly at the low temperatures and pressures of our experiments, once a "clean" Mo surface is generated.

1. Introduction

In previous studies of the Mo+F system by high-temperature mass spectrometry, gaseous equilibria among the lower fluorides were investigated, with S and SF as reaction partners for the Mo+F species.[1] All of the gaseous lower fluorides were observed and characterized, pentafluoride through monofluoride, and standard enthalpies of formation were derived from the reaction thermochemistry, using the thermochemical properties of SF as reference. Results for the higher Mo fluorides are based on derived results for the preceding lower fluorides, so that uncertainties propagate up the chain. Thus the reported[1] $\Delta_f H°/R$ of MoF_5(g) at 298.15 K, −(149.3 ± 4.3) kK, contains a relatively large uncertainty, perhaps overly generous. Subsequently, Douglas[2] reported the results of an independent evaluation of the thermodynamic properties of MoF_5 vapor, based on measurements of the vapor pressure and vapor density of MoF_5(l).[3] The key to the interpretation of the vaporization data was the determination of saturated vapor composition. The vapor densities indicated an overall degree of association very close to 2, suggesting saturated MoF_5 vapor to be largely dimeric. Douglas[2] combined this information with a vapor mass spectrum reported by Falconer *et al.*,[4] and with certain assumptions about fragmentation patterns and relative ionization efficiencies, to estimate the molecular abundances

* Research sponsored by the Air Force Office of Scientific Research (AFSC), United States Air Force, under Contract F 49620-78-C0033. The United States Government is authorized to reproduce and distribute reprints for Governmental purposes notwithstanding any copyright notation hereon.

of MoF_5 monomer, dimer, and trimer. From the estimated partial pressures, Douglas[2] derived the value $\Delta_v H^\circ/R = (9.6 \pm 1.5)$ kK for the vaporization process $MoF_5(l) = MoF_5(g)$ at 298.15 K. This value can be combined with the standard enthalpy of formation[5,6] and the enthalpy of fusion[3] of $MoF_5(s)$ to obtain the corresponding value for gaseous MoF_5: $\{\Delta_f H^\circ(298.15\ K)\}/R = -(157.0 \pm 2)$ kK. This latter value is some 7.5 kK more negative than our mass spectrometric result[1] and, even considering the large uncertainties, the two independent results do not overlap.

It seemed important to resolve this difference so as to increase our understanding of complex metal-halide chemistry, and to provide accurate thermochemical quantities for the lower fluoride species. It also seemed desirable to carry out the redetermination *via a route* that was independent of the previous determinations.[1,2] In considering the various possibilities for equilibrium studies, determinations referred to MoF_6 appeared most attractive, in view of the accurately known thermochemical properties of $MoF_6(l)$ and $MoF_6(g)$.[7,8] A rough thermochemical calculation showed that the heterogeneous reaction equilibrium:

$$(5/6)MoF_6(g) + (1/6)Mo(s) = MoF_5(g), \qquad (1)$$

might be suitable for study, especially since the two different enthalpies of formation of $MoF_5(g)$ led to widely divergent values of the equilibrium constant K°. For example at 500 K, K° for reaction (1) is calculated to be about 7×10^{-4} if $\{\Delta_f H^\circ(MoF_5, g, 298.15\ K)\}/R = -149.3$ kK and about $3 \times 10^{+3}$ if -157.0 kK. It certainly should be possible to determine which of these values is more nearly correct and to carry out new and independent studies on $MoF_5(g)$ *via* reaction (1), if the partial pressures of $MoF_6(g)$ and $MoF_5(g)$ in equilibrium with Mo(s) can be monitored separately and if it can be demonstrated that chemical equilibrium is achieved at the relatively low temperatures and low pressures likely to prevail. Although reaction (1) is one of the main routes for preparing $MoF_5(s)$,[5] there appear to be no previous equilibrium studies of this process. In this paper we report the results of a mass-spectrometric study of reaction (1) that yielded new thermochemical quantities for $MoF_5(g)$.

2. Experimental

All of the experiments described here were done with the $\pi/3$ sector, 30.5 cm radius, direction-focusing mass spectrometer described previously.[9] The effusion-beam source was very similar to that used earlier for the Mo+F studies,[1] namely a molybdenum cell fitted with a gas inlet tube at the base. The cell contained several coils of molybdenum wire separated by a thin Mo disc that was perforated with a number of 0.5 mm holes. Temperatures were measured with a Pt-to-(Pt+13 mass per cent Rh) thermocouple, the junction of which was attached to the outside surface of the cell top with a tight-fitting nickel band. When the cell was heated above 1000 K for outgassing and cleanup, temperatures measured with the thermocouple agreed to within a few K of those determined by optical pyrometry, when sighting on a black-body cavity in the lid.

The MoF_6 sample was obtained from Research Organic/Inorganic Chemical Corp., Sun Valley, California. A steel reservoir tank was filled to a pressure of about

7 kPa with gas from the MoF_6 supply cylinder. Gas from the reservoir was then metered into the effusion cell with a variable-flow leak valve. The room-temperature mass spectrum indicated the presence of a small $MoOF_4$ impurity, much less than that observed in other samples from various suppliers. However, the $MoOF_4$ impurity did not interfere with the studies of reaction (1).

3. Results

When MoF_6 from the reservoir bulb was admitted to the effusion cell at room temperature, the major ion observed in the electron impact mass spectrum was MoF_5^+, with a threshold appearance potential E_A of (15.2 ± 0.3) V. The MoF_5^+ signal responded sharply to movement of the molecular-beam defining slit and to adjustment of the leak valve. This room temperature $E_A(MoF_5^+)$ is in agreement with the value reported earlier,[1] and is clearly in accord with ion formation by the fragmentation process: $MoF_6 + e^- = MoF_5^+ + F + 2e^-$. As is often the case with valence-saturated metal halides, the parent ion is not observed; removal of a valence electron from MoF_6 apparently yields an unstable molecular ion that dissociates to $MoF_5^+ + F$ on a time scale that is short compared with the approximately μs flight time of the ion from ion source to collector. In any event, the ion MoF_5^+ appearing at a threshold energy of 15.2 V can be used to monitor the MoF_6 abundance in the effusion-cell beam.

When the cell temperature was increased to 450 K or higher, the E_A of MoF_5^+ dropped to (10.7 ± 0.3)V, in agreement with the value (10.60 ± 0.10) V reported previously[1] for parent MoF_5^+. A check of the mass spectrum at several temperatures and MoF_6 flow rates indicated MoF_5^+ to be the major ion product of MoF_5, also. By judicious choice of ionizing electron energies, the MoF_5^+ abundance can be used as a measure of both MoF_5 and MoF_6. The unfolding of these two neutral contributions to MoF_5^+ can be done most accurately when the neutral abundance mole ratio $n(MoF_5)/n(MoF_6)$ is small. Under such conditions, the MoF_5^+ parent signal a few V above threshold can be determined quite accurately, but its extrapolated contribution to the total ion yield a few V above the MoF_5^+/MoF_6 fragment-ion threshold is relatively small. Therefore extrapolation of the MoF_5^+ parent-ion curve is not critical, and both MoF_5 and MoF_6 ion yields can be determined reliably. An ionization efficiency curve measured at 450 K showing both parent and MoF_5^+/Mo_6 fragment contributions is seen in figure 1. In the ensuing discussion, the quantities $I(MoF_5^+/MoF_5)$ and $I(MoF_5^+/MoF_6)$ represent the MoF_5^+ ion current yields from MoF_5 and MoF_6, respectively.

As a test for the attainment of chemical equilibrium, the ion current quotient $\{I(MoF_5^+/MoF_5)\}/\{I(MoF_5^+/MoF_6)\}^{5/6}$, which is proportional to the equilibrium constant of reaction (1), was determined at a series of MoF_6 flow rates at constant temperature. For these studies, the MoF_5^+ parent and fragment-ion abundances were evaluated at an ionizing potential 3 V above the respective thresholds. Initially, the calculated equilibrium quotients were found to vary somewhat with flow rate, with a change by a factor of 10 in MoF_6 abundance leading to a change by a factor of about 2 in the quotient. Since this type of behavior could have resulted from the coverage of reactive molybdenum surface sites by an adherent oxide film, the cell

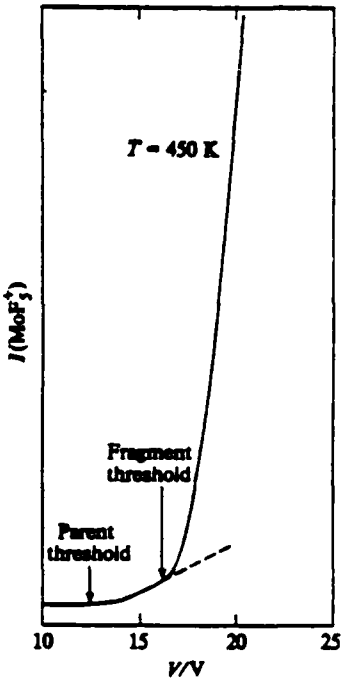

FIGURE 1. Ionization-efficiency curve of MoF_5^+ at cell temperature 450 K, showing parent and fragment contributions. Energy scale is uncorrected.

was heated to 1300 K and held there for several hours under a vacuum of about 7×10^{-5} Pa. Subsequent measurements showed that the equilibrium quotient shifted to a slightly lower absolute value as a result of this treatment, but that the quotient was now virtually independent of MoF_6 flow rate. A representative set of results illustrating the effect of flow rate on the calculated equilibrium quotient at 440K is given in table 1. The results show that, after vacuum degassing of the Mo surfaces at high temperatures, the ion-current quotient is essentially independent of flow rate and partial-pressure variations, so that chemical equilibrium is established within the cell. Subsequently, the equilibrium quotient at any given temperature could be reproduced closely, provided that the "clean" molybdenum surface was maintained.

TABLE 1. Effect of MoF_6 flow rate on ion abundances (in arbitrary units) and calculated equilibrium quotients at 440 K

$I(MoF_6^+/MoF_6)$	$I(MoF_5^+/MoF_6)$	$\frac{\{I(MoF_6^+/MoF_6)\}}{\{I(MoF_5^+/MoF_6)\}^{6/6}}$	$I(MoF_6^+/MoF_6)$	$I(MoF_5^+/MoF_6)$	$\frac{\{I(MoF_6^+/MoF_6)\}}{\{I(MoF_5^+/MoF_6)\}^{6/6}}$
11.3	0.047	6.28×10^{-6}	50.5	0.191	7.27×10^{-6}
12.4	0.051	6.26×10^{-6}	106.1	0.365	7.48×10^{-6}
36.4	0.151	7.55×10^{-6}	108.4	0.396	7.98×10^{-6}
45.0	0.162	6.79×10^{-6}			

Two independent series of measurements of the temperature dependence of the reaction equilibrium quotient were made, using an excess ionizing potential (ΔV) of 3 V in one instance and 2 V in the other. These measurements were made at a constant flow rate, since the attainment of equilibrium had already been verified. The two different values of ΔV were used to check on possible interference from the dimer fragmentation process: $Mo_2F_{10}+e^- = MoF_5^+ + MoF_5 + 2e^-$, since the dimer was observed in relatively high abundance above 500 K. For an enthalpy of dimerization of 20 to 40 R kK, dimer fragmentation could contribute to the MoF_5^+ ion yield a few V above the MoF_5^+ parent threshold. Some preliminary experiments with $\Delta V = 4$V yielded second-law plots for reaction (1) that exhibited an increase in slope above about 480 K. The results taken with lower excess ionizing energies showed no such effects and are free of interference from dimer. The two second-law slopes, derived from least-squares analysis of $\log_{10}K'$ against $1/T$ where

$$K' = \{I(MoF_5^+/MoF_5)\}T^{1/6}/\{I(MoF_5^+/MoF_6)\}^{5/6},$$

yielded $\{\Delta_r H°(492\text{ K})\}/R = (6.89 \pm 0.05)$ kK for $\Delta V = 2$ V and $\{\Delta_r H°(460\text{ K})\}/R = (7.15 \pm 0.25)$ kK for $\Delta V = 3$ V. A plot of the two sets is shown in figure 2. Although the two second-law enthalpies are in close agreement, the value obtained with the smaller ΔV is believed to be more reliable, and these results were used in the final analysis.

In order to check for internal consistency *via* a corresponding third-law calculation, values of the constant K' were converted to standard equilibrium constants $K°$ using

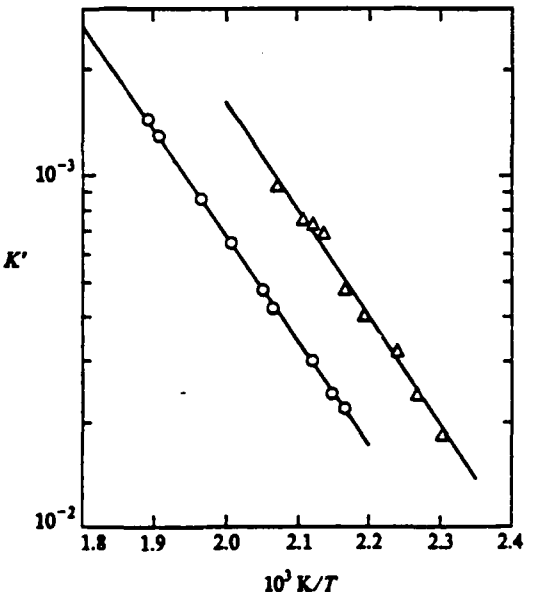

FIGURE 2. Plot of equilibrium quotient K' for reaction: $(5/6)MoF_6(g)+(1/6)Mo(s) = MoF_5(g)$ as function of temperature at two different excess ionizing potentials. ○, $\Delta V = 2$ V; △, $\Delta V = 3$ V.

an instrument-sensitivity constant determined for the pertinent ionizing energy by a gold vapor-pressure calibration. Relative ionization cross sections of MoF_5 and MoF_6 were estimated from additivity of the atomic cross sections,[10] these estimates should introduce relatively little uncertainty, however. The observed ion intensities, values of K' and K'', and the derived third law enthalpies are summarized in table 2.

TABLE 2. Ion abundances and derived equilibrium quantities for reaction (1)[a]

T/K	$I(MoF_5^+)$ (13 V)	$I(MoF_5^+)^b$ (17.5 V)	$K' \times 10^4$	$K'' \times 10^4$	$\Delta_r H°(298.15\ K)/R$ kK
462.0	0.090	19.3	2.19	3.98	6.45
465.7	0.102	20.2	2.40	4.36	6.46
471.8	0.123	19.6	3.02	5.47	6.43
484.1	0.162	18.8	4.17	7.57	6.44
487.8	0.180	18.7	4.71	8.55	6.43
497.8	0.240	18.8	6.40	11.6	6.41
509.0	0.318	19.2	8.60	15.6	6.40
525.2	0.441	18.8	12.9	23.4	6.39
527.8	0.486	19.1	14.3	25.9	6.36
				Mean:	6.42
				Second law (298.15 K):	6.89 ± 0.05

[a] Excess ionizing potential: 2 V.
[b] $I(MoF_5^+/MoF_6)_{17.5\,V} = I(MoF_5^+)_{17.5\,V} - 8.0I(MoF_6^+)_{15.5\,V}$.

Thermodynamic functions of Mo(s) and MoF_6(g) used in the third-law analysis were taken from the JANAF Tables,[7] while those of MoF_5(g) were taken from tables prepared by Douglas *et al.*[11] The functions for Mo(s) and MoF_6(g) are based on well established thermal and molecular data, and are of relatively high accuracy. For MoF_5(g), the calculated functions are derived from the spectroscopic data of Acquista and Abramowitz[12] plus two estimated fundamentals.[11] This set of functions for MoF_5(g) is preferred over other possible assignments because of the high degree of compatibility with the extensive second-law data on MoF_5 gaseous equilibria.[1] These sources lead to values of $\Delta\Phi°(298.15\ K)/R$ of 6.14 and 6.09 at 400 and 500 K, respectively, for reaction (1).† Additionally, the thermal functions indicate that the enthalpic correction of the second-law slope enthalpy to 298.15 K is essentially negligible. As shown in table 2, the average third-law value $\{\Delta_r H°(298.15\ K)\}/R = 6.44$ kK for reaction (1) compares favorably with the second-law value of (6.89 ± 0.05) kK. On the whole, the agreement is satisfactory.

Of the several derived values, the second-law result obtained with the lower ionizing potential is considered the most reliable, leading to the selected value from the present work: $\{\Delta_r H°(298.15\ K)\}/R = (6.89 \pm 0.40)$ kK for reaction (1). By combining this with data for MoF_6(g),[7] one derives $\{\Delta_f H°(MoF_5, g, 298.15\ K)\}/R = \{6.9 + (5/6)(-187.4)\}$ kK $= -(149.3 \pm 0.5)$ kK, in fortuitously close agreement with the earlier mass-spectrometric value $-(149.3 \pm 4.3)$ kK. It would seem that, together, these two determinations establish the enthalpy of formation of MoF_5(g) with reasonable certainty.

† $\Phi°(T) = -\{G°(T) - H°(T)\}/RT$.

Combination of the new results for the gas with the average of the two determinations for the enthalpy of formation of MoF_5(s),[5,6] yields $\Delta_f H°/R$ = 18 kK for the sublimation of MoF_5 monomer at 298.15 K, close to the corresponding values for WF_5 (18.6 kK),[5,13] and UF_5 (17 kK).[14] From the enthalpy of fusion of MoF_5(s),[3] one then evaluates $\Delta_f H°/R$ = 17 kK for the vaporization of the liquid to gaseous monomer at 298.15 K, compared with the value (9.6 ± 1.5) kK inferred by Douglas[2] from the pressure, density, and mass spectrum of saturated MoF_5 vapor, as described earlier. The large discrepancy almost certainly stems from the difficulty in estimating the abundance of MoF_5 monomer from the saturated-vapor mass spectrum of Falconer *et al.*[4] In particular, detailed information on the variation of mass spectrum with ionizing energy is required; as already indicated, fragmentation of Mo_2F_{10} can contribute to the MoF_5^+ ion yield at ionizing potentials only a few V above the parent-ion threshold, so that one could easily overestimate the monomer partial pressure in saturated vapor from the limited mass spectral data.[4] In fact, Falconer *et al.*[4] warned that "since neither the cross sections nor the fragmentation patterns are known, a quantitative assessment of the population of neutral species in the vapor cannot be made from the existing data."

An alternate interpretation consistent with the data is that saturated MoF_5 vapor is essentially dimeric, with a small percentage of trimer and an insignificant amount of monomer. In fact, our new value for the enthalpy of formation of MoF_5(g) can be combined with data for MoF_5(s),[5,6] and MoF_5(l),[2,3] to evaluate the partial pressure of MoF_5 monomer at 400 K as 5×10^{-6} Pa, while the total vapor pressure is 1×10^3 Pa. Although insignificant in the saturated vapor, the monomer will be the dominant pentafluoride species in most high-temperature applications; hence its properties must be established accurately. Additionally, value $\Delta_f H°/R$ = 17 kK for the vaporization of monomer noted above, together with the corresponding dimer value of 8 kK,[2] leads to the value $\Delta_f H°/R$ = 26 kK for the dissociation of dimer at 298.15 K, *i.e.* for the process: $Mo_2F_{10}(g) = 2MoF_5(g)$. This value, uncertain by at least several kK, is consistent with a recent determination[15] of (20.6 ± 1) kK for the dissociation of uranium pentafluoride dimer; the latter is believed to be the only direct thermochemical measurement on a metal pentafluoride dimer. Note that our reinterpretation of the MoF_5 monomer data requires that Douglas' derived data[2] be modified so as to increase the stability of dimer and to decrease the stability of trimer.

From the new results on MoF_5(g), one can evaluate the primary bond-dissociation energy in MoF_6, *i.e.* the enthalpy change for the process: $MoF_6 = MoF_5 + F$, within narrow limits. At 298.15 K, this value, designated $\{D(F_5Mo\text{–}F)\}/R$, is calculated to be $\{9.5 - 149.3 - (-187.4)\}$ kK = (47.6 ± 0.6) kK, compared with the average value in MoF_6(g) of 53.9 kK. Since $\{D(F_4Mo\text{–}F)\}/R$ = 44 kK and the average value in MoF_4(g) is 57.9 kK,[1] it is apparent that the fluorine ligands tend to stabilize the Mo^{4+} tetravalent state. Therefore, the gaseous tetrafluoride generally will be more important than the hexafluoride or the pentafluoride in the high temperature chemistry of the Mo+F system.

One aspect of the present work that seemed at the time rather surprising was the rapid and complete attainment of chemical equilibrium in the $Mo + MoF_5 + MoF_6$ system at 400 to 500 K, when the Mo(s) surface was maintained free of films of foreign

substances. It might have been expected that the bond-breaking and rearrangement steps leading to product formation would be the rate-limiting processes at these relatively low temperatures. However, the chemical step is apparently much faster than the surface accommodation of the incoming MoF_6 molecule, especially when a retarding film is present. In this respect, the behavior is in accord with the quasi-equilibrium (QE) model of gas-solid reactions proposed by Batty and Stickney.[16] The QE model, which seems to be in accord with the results of several metal + oxygen reactions, is based on the assumption that reaction products are in equilibrium with the solid substrate and with one another, and that the rate of emission of products is limited by the kinetics of adsorption of the incoming reactive species.

REFERENCES

1. Hildenbrand, D. L. *J. Chem. Phys.* 1976, 65, 614.
2. Douglas, T. B. *J. Chem Thermodynamics.* 1977, 9, 1165.
3. Krause, R. F., Jr.; Douglas, T. B. *J. Chem. Thermodynamics* 1977, 9, 1149.
4. Falconer, W. E.; Jones, G. R.; Sunder, W. A.; Vasile, M. J.; Muenter, A. A.; Dyke, T. R.; Klemperer, W. *J. Fluorine Chem.* 1974, 4, 213.
5. Burgess, J.; Haigh, L.; Peacock, R. D. *J. Chem. Soc. Dalton Trans.* 1974, 1062.
6. Nuttall, R. L.; Kilday, M. V.; Churney, K. L. *Natl. Bur. Stand. Report NBSIR* 73–281 (1 July 1973).
7. JANAF Thermochemical Tables, NSRDS–NBS 37. D. R. Stull; H. Prophet: editors. U.S. Govt. Printing Office: Washington, D. C. Second edition. 1971.
8. Dellien, I.; Hall, F. M.; Hepler, L. G. *Chem. Rev.* 1976, 76, 283.
9. Hildenbrand, D. L. *J. Chem. Phys.* 1968, 48, 3657; *ibid.* 1970, 52, 5751.
10. Mann, J. B. *J. Chem. Phys.* 1967, 46, 1646.
11. Douglas, T. B.; Krause, R. F., Jr.; Acquista, N.; Abramowitz, S. *National Bureau of Standards Report NBSIR* 73–280 (1 January 1973).
12. Acquista, N.; Abramowitz, S. *J. Chem. Phys.* 1973, 58, 5484.
13. Hildenbrand, D. L. *J. Chem. Phys.* 1975, 62, 3074.
14. Hildenbrand, D. L. *J. Chem. Phys.* 1977, 66, 4788.
15. Kleinschmidt, P. D.; Hildenbrand, D. L. unpublished results.
16. Batty, J. C.; Stickney, R. E. *J. Chem. Phys.* 1969, 51, 4475.

Thermochemical properties of the gaseous tantalum fluorides[a)]

K. H. Lau and D. L. Hildenbrand

SRI International, Menlo Park, California 94025
(Received 30 January 1979; accepted 8 May 1979)

The gaseous tantalum fluoride species TaF_n, with $n = 1$ to 5, were generated under equilibrium conditions by admitting $SF_6(g)$ to a tantalum effusion cell at temperatures in the range 1000–2500 K. Mass spectrometry was utilized to establish the species identities and then to study several reaction equilibria. Reaction enthalpies were derived primarily by second law analysis, from which the standard enthalpies of formation at 298 K of TaF_5 (-424.6 kcal/mol), TaF_4 (-305.2 kcal/mol), TaF_3 (-194.0 kcal/mol), TaF_2 (-68.7 kcal/mol) and TaF (69.2 kcal/mol) were derived, all ± 3 kcal/mol. Estimated thermodynamic functions of the Ta–F species, based on data for the neighboring tungsten fluorides, were found to be quite compatible with the equilibrium data. Equilibrium gas phase compositions in the Ta–F system, calculated over a range of temperatures for several pressures using the data reported here, correlate closely with kinetic data on the reaction of Ta with F atoms. The sharp decline in reaction rate above 2000 K can be accounted for on purely thermodynamic grounds.

INTRODUCTION

The chemical interaction of the refractory metal tantalum with fluorine at elevated temperatures is of interest in chemical vapor deposition technology, in the analysis of metal fluorination kinetics, and in the evaluation of the susceptibility of tantalum and its refractory compounds to corrosive attack by fluorine and fluorides. All of these applications require a knowledge of the thermochemical properties of the gaseous tantalum fluorides. In particular, Nordine[1] has pointed out the role of thermochemical data in treating the kinetics of the gasification of refractory metals by atomic fluorine, and has discussed the Ta + F reaction system in depth. The treatment of the kinetics of gas–solid reactions of this type by the quasiequilibrium (QE) model of Batty and Stickney[2] has been quite successful, but since the QE model is based on emission of gaseous products in thermodynamic equilibrium distributions, the lack of thermochemical data for these species severely restricts its application. Other studies of the Ta–F reaction have been carried out by Machiels and Olander[3] and by Philippart *et al.*,[4] but again interpretation is somewhat hindered for the same reason.

Feber[5] and Zmbov and Margrave[6] have made estimates of the enthalpies of formation of the gaseous Ta–F species, but these estimates differ by 10 to 20 kcal/mol and there is no satisfactory way to judge their reliability. Furthermore, there are no experimental spectroscopic and molecular constant data needed for evaluating entropies used in high temperature equilibrium calculations. The objective of the present study was to devise suitable experimental conditions for generating and identifying the gaseous tantalum fluorides, and to make comprehensive measurements of reaction equilibria among these species. If sufficiently accurate and extensive, these measurements will yield the enthalpies, entropies, and Gibbs energies of formation needed in calculating the high temperature equilibrium properties of the Ta–F system. We report here the results of such studies, carried out by high temperature mass spectrometry.

EXPERIMENTAL

Gaseous TaF_n species, where $n = 1$–5, were generated by fluorinating Ta metal with gaseous SF_6. For this purpose, SF_6 from an external reservoir was admitted to the base of a tantalum effusion cell of the type used in earlier work.[7] The cell was 1.27 cm o.d. and 2.20 cm long, with an internal cavity 0.80 cm i.d. and 1.25 cm long; a 0.55 cm o.d. gas inlet tube entered the base of the cell. A coil of tantalum wire was placed in the lower section of the cell, and a thin tantalum diaphragm containing several 0.5 mm diameter holes around the periphery was placed between the upper and lower sections to increase the number of reactive gas–solid collisions. The beam exit orifice was 0.15 cm in diameter and 0.35 cm long. Total pressure in the cell was always less than 1×10^{-6} atm, so that molecular flow conditions prevailed throughout. A few measurements were made with $CaF_2(s)$ in the cell, and also with WF_6 as the reactive gas. Reaction products were sampled with a mass spectrometer, and ion abundances evaluated at low ionizing electron energies were used in deriving the desired equilibrium data. The magnetic mass spectrometer, the experimental technique, and the data evaluation methods have been described in previous publications.[7]

Below about 1200 K, TaF_5 was the only readily detectable Ta–F product, but above that temperature, increasing abundances of the lower-valent Ta fluorides were observed. The attainment of chemical equilibrium within the effusion oven source was checked by varying the gas flow rate and applying the mass action test to the resulting equilibrium data. All other details concerning measurements of ionization efficiency curves, temperature determination by optical pyrometry, etc. have been described previously.[7]

[a)] Research sponsored by the Air Force Office of Scientific Research (AFSC), United States Air Force, under Contract F 49620-78-C-0033. The United States Government is authorized to reproduce and distribute reprints for Governmental purposes notwithstanding any copyright notation hereon.

 0021-9606/79/161572-06$01.00

TABLE I. Appearance potentials and neutral precursors of ions observed in Ta–F studies.

Ion	Threshold A. P. (eV)[a]	Cell temperature (K)	Neutral precursor
TaF_4^+	14.7	1100	TaF_5
TaF_4^+	8.5	1500	TaF_4
TaF_3^+	8.2	1750	TaF_3
TaF_2^+	8.0	2100	TaF_2
TaF^+	11.0	2130	TaF_2
TaF^+	8.0	2430	TaF
$TaSF_3^+$	10.4	1200	$TaSF_3$
CaF^+	5.5	1800	CaF
Ca^+	6.0	1800	Ca
WF_5^+	10.0	1600	WF_5
WF_4^+	10.0	1600	WF_4

[a]Estimated uncertainty ±0.3 eV, vanishing current method.

Gaseous SF_6 and WF_6 were obtained from the Matheson Co. and from Alfa Division/Ventron Corp., while the $CaF_2(s)$ sample was of typical reagent grade quality.

RESULTS

The threshold appearance potentials (A. P.'s) of ions observed at various effusion cell temperatures are listed in Table I, along with the neutral species assigned as precursors. Threshold energies were evaluated by the vanishing current method, with the energy scale calibrated by reference to the A. P. of background Hg^+. Interpretation of the A. P. data is straightforward, with the lowest threshold of each ion clearly associated with simple ionization of the corresponding neutral. There are no previous threshold data for any of the lower-valent tantalum fluorides; the threshold A. P.'s of parent Ca^+, CaF^+, WF_4^+, and WF_5^+ are in good agreement with earlier determinations,[4,5] while the dissociative threshold for TaF_3^+/TaF_5 agrees with the value 14.8 ± 0.3 eV resulting from measurements on TaF_5 vapor.[6] As expected, the ionization energies of the lower TaF_n species are converging on the spectroscopic ionization potential (I. P.) of Ta (7.89 eV) with removal of successive F atoms. This type of behavior has been observed with the W and Mo fluorides[9,10] and seems characteristic of transition metal halides. The behavior of nontransition halides is quite different, with the I. P.'s of the odd-electron molecules several eV lower than those of the neighboring even-electron species.

TABLE II. Equilibrium constants for the reaction $TaF_5(g) + TaF_3(g) = 2\ TaF_4(g)$ (1).

T (K)	K_1	T (K)	K_1
1515	0.408	1633	0.513
1515	0.438	1660	0.503
1532	0.469	1660	0.543
1532	0.459	1671	0.593
1557	0.432	1671	0.541
1557	0.458	1671	0.571
1557	0.466	1678	0.549
1588	0.482	1678	0.564
1592	0.449	1679	0.562
1593	0.473	1684	0.535
1593	0.467	1686	0.571
1630	0.520	1739	0.600
1630	0.530	1739	0.600
1633	0.538		

$\log K_1 = (0.806 \pm 0.081) - (1782 \pm 131)/T$

TABLE III. Equilibrium constants for the reactions $TaF_4(g) + TaF_3(g) = 2\ TaF_3(g)$ (2), $3/4\ TaF_4(g) + 1/4\ Ta(s) = TaF_3(g)$ (4).

T (K)	K_2	$K_4 \times 10^2$ ($atm^{1/4}$)
1885	49.7	1.43
1885	49.6	1.46
1928	44.4	1.72
1973	41.2	2.13
1975	40.1	2.12
2031	36.5	2.53
2031	35.5	2.56
2063	33.1	3.16
2063	34.3	3.13
2064	34.7	3.27
2110	30.9	3.73
2110	30.5	3.54
2110	31.2	3.54
2149	30.0	4.27
2189	28.8	4.99
2189	27.2	5.03
2234	26.3	5.34

$\log K_2 = -(0.142 \pm 0.037) + (3456 \pm 76)/T$

$\log K_4 = (1.968 \pm 0.072) - (7186 \pm 151)/T$

$TaF_5(g)$ does not yield a stable parent ion, as noted earlier.[6] The presence of $TaF_5(g)$ was obvious, however, from the higher TaF_4^+ dissociative ionization threshold. Measurements of TaF_5 in the presence of TaF_4 were made under conditions in which $P(TaF_5) > P(TaF_4)$, so that the parent contribution to TaF_4^+ could be readily extrapolated to higher energies and separated from the larger TaF_3^+/TaF_5 dissociative contribution. The Ta–SF_6 reaction yielded $TaSF_3(g)$ in high abundance, but this species did not interfere with determinations of the TaF_n equilibria since the latter were monitored at low ionizing electron energies.

By choosing temperature ranges in which the species of interest overlapped, it was possible to study the reaction equilibria

$$TaF_5(g) + TaF_3(g) = 2\ TaF_4(g)\ , \quad (1)$$

$$TaF_4(g) + TaF_3(g) = 2\ TaF_3(g)\ , \quad (2)$$

$$TaF(g) + TaF_3(g) = 2\ TaF_2(g)\ , \quad (3)$$

and

$$\tfrac{1}{4}\,TaF_4(g) + \tfrac{1}{4}\,Ta(s) = TaF_3(g) \quad (4)$$

involving the Ta–F species only. Parent ion intensities were measured at 3 eV above the ionization threshold to eliminate any potential overlap from dissociative

TABLE IV. Equilibrium constants for the reaction $TaF_3(g) + TaF(g) = 2\ TaF_2(g)$ (3).

T(K)	K_3
2294	18.3
2294	17.8
2315	16.9
2315	17.7
2354	17.5
2354	16.9
2356	17.8
2405	15.9
2405	16.5
2427	15.4
2427	16.0

$\log K_3 = (0.246 \pm 0.162) + (2319 \pm 382)/T$

TABLE VI. Estimated values of Φ°_{298} for Ta–F species.[a]

T(K)	TaF	TaF_2	TaF_3	TaF_4	TaF_5
298	57.1	64.4	71.9	79.1	81.1
400	57.4	64.9	72.6	79.9	82.1
600	58.7	67.0	75.2	83.4	86.3
800	60.1	69.2	78.2	87.2	90.9
1000	61.3	71.2	80.9	90.7	95.2
1200	62.4	73.1	83.3	93.8	99.1
1400	63.5	74.8	85.5	96.7	102.6
1600	64.4	76.3	87.6	99.3	105.8
1800	65.2	77.7	89.4	101.7	108.8
2000	66.0	79.0	91.1	103.9	111.5
2200	66.7	80.2	92.7	106.0	114.0
2400	67.4	81.3	94.1	107.8	116.3
2600	68.0	82.3	95.5	109.6	118.4

[a] $\Phi^\circ_{298} = -(G^\circ - H^\circ_{298})/T$; units are cal/deg mol.

ionization processes. Measured in this fashion, the parent ion signals faithfully represented the corresponding neutral abundances. As noted above, the TaF_5 abundance was derived from the TaF_4^+ signal at 3 eV above the dissociative threshold, after correction for the extrapolated TaF_4^+ parent contribution.

The system was checked for attainment of chemical equilibrium by varying the SF_6 flow rate and noting the effect of the resulting composition changes on the derived equilibrium data. For Reaction (2), for example, two different SF_6 flows at 2234 K gave the relative intensities of $TaF_2^+/TaF_3^+/TaF_4^+$ parent ions as 0.234/0.660/0.074 and 1.60/11.3/3.03, yielding equilibrium constants K of 25.2 and 26.3, respectively. Similar results were obtained for the other reactions, satisfying the mass action criterion for equilibrium behavior.

In the studies of Reaction (1), relative abundances of $TaF_5/TaF_4/TaF_3$ were in the approximate ratios 10/0.5/0.07 at 1515 K and 10/3/1.5 at 1735 K. For reaction (2), the ratio $TaF_4/TaF_3/TaF_2$ was about 10/8/0.14 at 1885 K and 10/37/5 at 2234 K. The abundance ratios $TaF_3/TaF_2/TaF$ observed in the study of Reaction (3) were about 10/2/0.02, varying only gradually with temperature. Equilibrium constants evaluated directly from the ion abundance ratios for the isomolecular reactions (1), (2), and (3) are listed in Tables II, III, and IV, respectively. Most of these points were measured twice at each temperature to increase accuracy.

In deriving the absolute equilibrium constants for Reaction (4), the sensitivity constant relating ion intensities to pressure was evaluated from a gold vapor pressure calibration, taking proper cognizance of the dependence on excess ionizing energy. Atomic ionization cross sections were taken from the compilation of Mann,[11] and additivity of the atomic values was assumed in estimating those of TaF_3 and TaF_4; this introduces no error in the derived thermochemical data for Reaction (4), since the latter were obtained from second-law analysis. The equilibrium data so derived are listed also in Table III.

A second-law analysis of the equilibrium data yielded the reaction enthalpy changes ΔH° (II) summarized in Table V. There are no spectroscopic and molecular constant data available for any of the Ta–F species that could be used in a corresponding third-law treatment or in providing heat capacities that could be used in correcting the slope heats to 298 K. In previous studies of the W–F[9] and Mo–F[10] systems, however, it was found that spectroscopic constants estimated in a consistent fashion yielded calculated thermodynamic functions showing remarkably good second- and third-law agreement. It was assumed that the molecular parameters of the Ta–F species would be approximated closely by those of the neighboring W–F species,[9] except for the electronic configurations. As before, only electronic ground states were considered, with even- and odd-electron molecules having singlet and doublet states, respectively. The corresponding entropy and phi $[-(G^\circ - H^\circ)/T]$ functions for a given TaF_n and WF_n species will therefore differ by $R\ln 2$. Values of $\Phi^\circ_{298} = -(G^\circ - H^\circ_{298})/T$ for the Ta–F species, evaluated in this fashion, are listed in Table VI. Third-law enthalpies ΔH°(III) derived using these functions are seen in Table V to be

TABLE V. Thermochemistry of Ta–F reactions.

Reaction	Range (K)	ΔH°_T (II)[a]	ΔH°_{298} (II)[a]	ΔH°_{298} (III)[a]
(1) $TaF_3(g) + TaF_5(g) = 2\ TaF_4(g)$	1515–1735	8.2 ± 0.6	8.2	10.4
(2) $TaF_2(g) + TaF_4(g) = 2\ TaF_3(g)$	1885–2234	−15.8 ± 0.4	−14.1	−15.7
(3) $TaF(g) + TaF_3(g) = 2\ TaF_2(g)$	2294–2427	−10.6 ± 1.8	−12.6	−10.9
(4) $3/4\ TaF_4(g) + 1/4\ Ta(s) = TaF_3(g)$	1885–2234	32.9 ± 0.7	34.9	32.7
(5) $TaF_4(g) + Ca(g) = TaF_3(g) + CaF(g)$	1770–1929	···	···	3.1

[a] In kcal/mol.

in reasonably good agreement, i. e., within 2 kcal/mol, with the second-law values, adjusted to 298 K with heat capacity data calculated from the aforementioned molecular constants. The relatively simple prescription used for estimating molecular constants seems to be an effective one, so that the corresponding thermodynamic functions can be used in practical calculations until the necessary spectroscopic data eventually become available.

The four independent equilibria involving the Ta–F species [Reactions (1) through (4)] are not sufficient to determine the properties of the five Ta–F species; one additional independent equilibrium is required. Some type of exchange reaction involving Ta–F species and the fluorides of another element suggested itself, but because of the high heat of sublimation of Ta and the relatively high Ta–F average bond strength, it proved difficult to devise suitable reaction partners. Molecular fluorides with relatively weak bond strengths provided sufficient energy exchange to gasify Ta when added to the cell, but in general they were completely reduced and only the Ta–F species were observed. With more stable fluoride partners, there was insufficient energy exchange to gasify Ta, and only the gaseous fluoride species of the partner were observed. In the end, it proved possible to carry out two such processes simultaneously by adding $SF_6(g)$ to a Ta cell containing $CaF_2(s)$. At about 1800 K and with a moderate flow of SF_6, the species TaF_3, TaF_4, Ca, and CaF were identified in the cell beam. The Ca and CaF abundances were favored by reducing conditions, while the Ta–F signals were observable only under oxidizing conditions characterized by moderate SF_6 flows. By choosing conditions carefully it was possible to strike a balance so that the equilibrium

$$TaF_4(g) + Ca(g) = TaF_3(g) + CaF(g) \qquad (5)$$

could be studied.

Reaction (5) provides a striking example of the mass action effect, since the Ca and Ta species respond in opposite fashion to the SF_6 flow. Two points at 1770 K with different leak rates of SF_6 gave the parent ion intensity distributions $Ca^+/CaF^+/TaF_3^+/TaF_4^+$, evaluated at 4 eV excess ionizing energy, of 0.13/6.69/0.61/0.795 and 1.18/20.0/0.111/0.049, with calculated K values of 34.2 and 38.4, respectively. The agreement is considered a satisfactory indicator of gaseous equilibration. Eight equilibrium data points measured over the range 1770 to 1929 K are summarized in Table VII, along with derived third-law heats. It was difficult to cover an extended temperature range for reasons noted above, so that, in view of the consistency of the data for Reactions (1) to (4) with the estimated thermodynamic functions, the third-law value is preferred. However, the ΔH°(II) and ΔH°(III) data for Reaction (5) are compatible within experimental error. Functions for $Ca(g)$ and $CaF(g)$ were taken from the JANAF Thermochemical Tables.[12]

TABLE VII. Equilibrium data for the reaction $TaF_4(g) + Ca(g) = TaF_3(g) + CaF(g)$ (5).

T (K)	K_5	ΔH°_{298} (III)
1770	38.4	3.2
1770	39.7	3.1
1808	38.7	3.2
1826	39.3	3.2
1865	41.6	3.0
1865	37.8	3.3
1895	41.3	3.0
1929	42.2	2.9
		Av. 3.1 kcal/mol

$\log K_5 = (1.968 \pm 0.153) - (676 \pm 280)/T$

TABLE VIII. Derived enthalpies of formation and bond dissociation energies.

Gaseous molecule	$\Delta_f H^\circ_{298}$ (kcal/mol)	Bond	D°_{298} (kcal)
TaF	69.2	Ta–F	137
TaF_2	−68.7	FTa–F	157
TaF_3	−194.0	F_2Ta–F	144
TaF_4	−305.2	F_3Ta–F	130
TaF_5	−424.6	F_4Ta–F	138

Estimated uncertainties in $\Delta_f H^\circ_{298}$ and D°_{298} are ±3 kcal/mol.

From the established value $D^\circ_{298}(CaF) = 127.0 \pm 1.0$ kcal/mol[12] and the derived enthalpy changes for Reactions (1) to (5), one can evaluate the standard enthalpies of formation and the bond dissociation energies of the gaseous Ta–F species TaF through TaF_5. For this purpose, the ΔH°_{298}(II) values of Reactions (1) to (4) were used, while for Reaction (5) the more reliable third-law value was selected. Thermochemical data so derived are listed in Table VIII.

As a further check on the internal consistency of the results, several measurements on the equilibrium

$$TaF_5(g) + WF_4(g) = TaF_4(g) + WF_5(g) \qquad (6)$$

gave $K = 2.5 \times 10^{-4}$ at 1600 K. This result leads to ΔH°_{298}(III) = 31 kcal/mol for Reaction (6) and $D^\circ_{298}(F_4Ta–F) = 137$ kcal/mol, in satisfactory agreement with the data in Table VIII.

DISCUSSION

Zmbov and Margrave[6] list the standard enthalpy of formation of $TaF_5(g)$ at 298 K as -437.7 ± 1.0 kcal/mol, some 13 kcal/mol more stable than the value reported here; the selected value[6] is based not on their own experimental studies of $TaF_5(g)$ but on a combination of the standard enthalpy of formation of $TaF_5(s)$ at 298 K (-455.0 ± 0.2 kcal/mol[13]) and a heat of sublimation of 17.4 kcal/mol estimated by Feber[5] from the TaF_5 vapor pressure data of Fairbrother and Frith.[14] The estimation of $\Delta_{sub}H^\circ(TaF_5)$[5] involves the implicit assumption of monomeric vapor, an unlikely situation in view of the subsequent evidence for a high degree of association in TaF_5 and other metal pentafluoride saturated vapors.[15] Our new value for $\Delta_f H^\circ(TaF_5, g)$ implies $\Delta_{sub}H^\circ(TaF_5, g)$

= 30.4 kcal/mol, close to the corresponding values for several other pentafluoride monomers WF_5(37 kcal/mol),[9] MoF_5(36 kcal/mol),[10] and UF_5(39 kcal/mol),[16] additional evidence that saturated TaF_5 vapor is highly associated and that the partial pressure of gaseous monomer is insignificant. There are no experimental determinations on any of the other gaseous Ta–F species some of the earlier estimates[5,6] differ substantially from the thermochemical values reported here.

The new data lead to $D_0^\circ(TaF) = 135.7 \pm 3$ kcal/mol = 5.88 ± 0.13 eV. There are no spectroscopic values available for comparison. The individual bond dissociation energies scatter about the average value 141 kcal/mol in TaF_5, but the substantial difference of 27 kcal between the extremes of $D(F_5Ta-F)$ and $D(FTa-F)$ indicates that the estimation of realistic thermochemical data is still a chancy business. The molecular constants needed for a meaningful ionic model calculation of the binding energies of TaF and some of the polyatomic Ta–F species are not available. However, the ionicity criterion[7] indicates that the degree of charge separation in these molecules is not sufficient for valid application of the electrostatic model.

Philippart *et al.*[4] have measured the temperature dependence of Ta–F product fluxes generated by the reaction of a Ta ribbon with fluorine in a flow reactor. The gaseous products TaF_5, TaF_4, TaF_3, and TaF were identified by mass spectrometry, peaking at different temperatures. They reported heats of atomization of TaF_4 (580 kcal/mol), TaF_3 (430 kcal/mol), and TaF (180 kcal/mol), obtained from second-law slopes of the product fluxes. The values for TaF_4 and TaF_3 are within about 10 kcal/mol of the equilibrium results obtained in this study. However, their result for TaF and the nonobservation of TaF_2 are clearly at odds with our results, and suggest a large systematic error in the product flux measurements at the highest ribbon temperatures.[4]

A useful perspective on the temperature and pressure dependence of species abundances can be gained from a calculation of the equilibrium composition of the Ta–F system for various conditions of interest. These data can be evaluated from the enthalpies of formation in Table VIII, the Φ functions in Table VI, and data for Ta(*s*), F(*g*), and $F_2(g)$ from the JANAF Tables.[12] Compositions were calculated in terms of the species partial pressures in equilibrium with Ta(*s*) at total pressures of 1 and 10^{-6} atm over the range 500 to 2500 K, with the results shown in Figs. 1 and 2. At 1 atm pressure, TaF_5 is the major species over the entire temperature range, although TaF_4 and TaF_3 are gaining rapidly above 2000 K. The situation is of course quite different at 10^{-6} atm, where the partial pressures of the lighter dissociation products are enhanced. At the lower pressure, the major Ta species is TaF_5 up to 2000 K, shifting to TaF_4 at 2100 K, TaF_3 at 2300 K, and TaF_2 at 2500 K. Above 2150 K, however, the most abundant vapor species is atomic fluorine. The equilibrium data corroborate the conclusion of Machiels and Olander[3] that, up to 1000 K and equivalent fluorine pressures between 10^{-6} and 10^{-7} atm, TaF_5 is the sole product of the Ta–F_2 reaction.

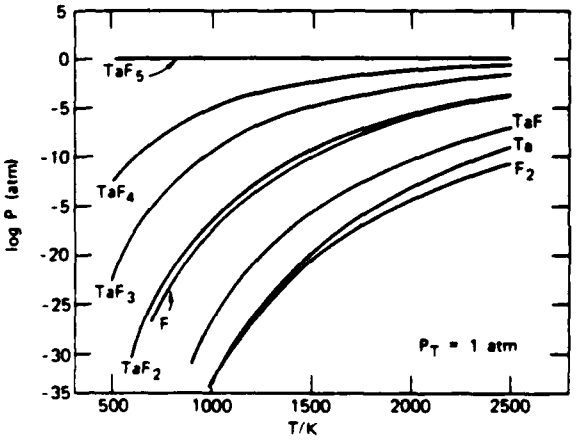

FIG. 1. Equilibrium distribution of gaseous species in the Ta–F system over the range 500 to 2500 K at 1 atm total pressure.

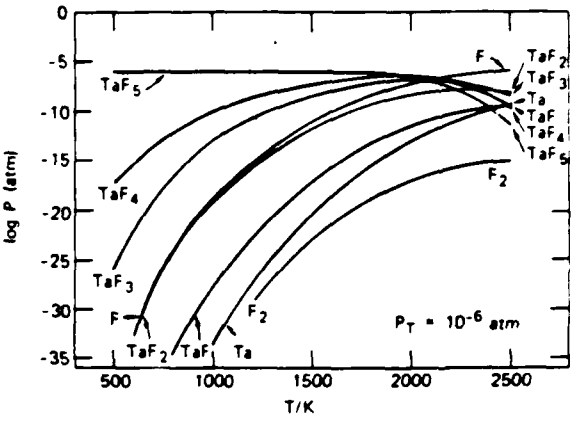

FIG. 2. Equilibrium distribution of gaseous species in the Ta–F system over the range 500 to 2500 K at 10^{-6} atm total pressure.

The calculated compositions at 10^{-6} atm pressure are in qualitative accord with the data of Nordine[1] on the kinetics of gasification of Ta by F atoms at pressures of about 4×10^{-5} to 6×10^{-6} atm. Between 2000 and 2500 K, the observed gasification rate of Ta[1] leveled off and then began to decrease rapidly, consistent with the appearance of atomic fluorine as the major equilibrium gas species and the decline in the abundances of the major Ta–F species above 2200 K, as seen in Fig. 2. Thus, the sharp high temperature falloff found in the F-atom gasification kinetics[1,17] of Pt, Ir, Ta, W, and Mo can be rationalized in terms of the equilibrium thermodynamics as suggested by the QE model,[2] rather than a decreased residence time of adsorbed F atoms at these temperatures.[17] Our calculations suggest that, up to 2000 K, TaF_5 is the only important gaseous reaction product and that, between 2000 and 2100 K, TaF_5 and TaF_4 are roughly comparable; at higher temperatures, F atoms predominate. Thus, it seems unlikely that the

kinetics[1] are influenced by a marked shift in product species to one of the lower Ta fluorides with increasing temperature.

[1]P. C. Nordine, J. Electrochem. Soc. 125, 496 (1978).
[2]J. C. Batty and R. E. Stickney, J. Chem. Phys. 51, 4475 (1969).
[3]A. J. Machiels and D. R. Olander, Surf. Sci. 65, 325 (1977).
[4]J. L. Philippart, J. Y. Caradec, B. Weber, and A. Cassuto, J. Electrochem. Soc. 125, 162 (1978).
[5]R. C. Feber, Los Alamos Scientific Laboratory Report LA-3164, 1964.
[6]K. F. Zmbov and J. L. Margrave, J. Phys. Chem. 72, 1099 (1968).
[7]D. L. Hildenbrand, J. Chem. Phys. 48, 3657 (1968); 52, 5751 (1970).
[8]H. M. Rosenstock, K. Draxl, B. W. Steiner, and J. T. Herron, J. Phys. Chem. Ref. Data 6, Suppl. 1 (1977).
[9]D. L. Hildenbrand, J. Chem. Phys. 62, 3074 (1975).
[10]D. L. Hildenbrand, J. Chem. Phys. 65, 614 (1976).
[11]J. B. Mann, J. Chem. Phys. 46, 1646 (1967).
[12]JANAF Thermochemical Tables, Natl. Stand. Ref. Data Ser. Natl. Bur. Stand. 37 (1971).
[13]E. Greenberg, C. A. Natke, and W. N. Hubbard, J. Phys. Chem. 69, 2069 (1965).
[14]F. Fairbrother and W. C. Frith, J. Chem. Soc. 1951, 3051.
[15]W. E. Falconer, G. R. Jones, W. A. Sunder, M. J. Vasile, A. A. Muenter, T. R. Dyke, and W. Klemperer, J. Fluorine Chem. 4, 213 (1974).
[16]P. D. Kleinschmidt and D. L. Hildenbrand, J. Chem. Phys. (to be published).
[17]D. E. Rosner and H. D. Allendorf, J. Phys. Chem. 75, 308 (1971).

Model Calculations of the Thermochemical Properties of Gaseous Metal Halides

D. L. Hildenbrand

SRI International, Menlo Park, California 94025

ABSTRACT

Two semiempirical models for estimating the thermochemical properties of gaseous metal halides, the Rittner electrostatic model and the ionicity-corrected Birge-Sponer extrapolation, are reviewed, and the areas of applicability of the models are discussed. Possibilities for application of the Rittner model to metal mono-, di-, and trihalide systems are illustrated by examples from the IIA and IIIB metals, and extension to the lanthanide halide series is explored. Over-all, the Rittner model appears to have much promise as a tool for estimating thermochemical data, but proper usage demands that due consideration be given to the inherent limitations of the model. A simple ionicity correction removes much of the uncertainty associated with dissociation energies derived from the linear Birge-Sponer extrapolation, providing another useful tool for estimating thermochemical data.

Our knowledge of the thermochemical properties of metal halide systems is still far from complete, making it necessary to rely on new experimental determinations when critical data needs arise. These new determinations usually cannot be synchronized with the urgent data needs because of the time, expense, and difficulty associated with experimental work. In addition, it is impractical to undertake new thermochemical measurements for every compound of interest. It is important, therefore, to develop modeling schemes that can provide reliable estimates when direct experimental measurements are lacking, or when the available data are conflicting.

Two models that have proved useful in dealing with the thermochemistry of metal halides are the electrostatic polarizable-ion model (1) and the ionicity-corrected Birge-Sponer extrapolation (2). As is always the case, these models have certain inherent limitations and they should not be used indiscriminately. It is the purpose of this paper to point out the important limitations and to indicate the degree of reliability that might reasonably be expected when the models are applied in the proper fashion.

Electrostatic Model

The Rittner polarizable-ion model was originally applied to the gaseous diatomic alkali halide molecules with very satisfactory results (1). A later comparison using critically evaluated experimental data for the alkali halides showed the agreement between calculated and experimental results to be extraordinarily good for the entire series (3). It might logically be expected then that the Rittner model can be successfully applied to other metal halides of interest. However, the model is based on a consideration of the molecule as an assembly of free gaseous ions, each polarized by the field of the other. This implies a high degree of charge separation in the molecule, so that one must apply some type of ionicity criterion to candidate metal halide systems. Metal halide molecules, as a class, cover a wide range of ionic-covalent bonding character, and there are clearly certain molecular species for which the ionic model is inappropriate. Additionally, it should be recognized that the Rittner model is not a comprehensive model in the sense that molecular properties are derived solely from a consideration of the electronic structure, as with a true *ab initio* approach. Rather, properties such as ionic binding energy and dipole moment are derived from electrostatic considerations, using certain other properties (internuclear distance, vibrational force constant, ion polarizabilities) as necessary input.

An especially useful ionicity criterion, used as a guide in the present work, is one based on the hypothetical crossing point of ionic and covalent potential energy curves in the diatomic molecule, r_x, and its relation to the equilibrium internuclear distance, r_e. The rationale underlying this approach has been described by Herzberg (4) and stems from a classification of the ground state potential curves according to their derivation from neutral atoms or ions. The important parameter here is the energy separation between neutral and ionic dissociation limits, which for metal halides is the difference between the first ionization potential (IP_1) of the metal and the electron affinity (EA) of the halogen atom. When (IP_1 − EA) is relatively small, coulombic binding predominates, while covalent binding obtains at large (IP_1 − EA). This distinction can be made more quantitative by considering the ratio r_x/r_e, where r_x can be evaluated from the expression

$$r_x(\text{Å}) = \frac{14.40}{(IP_1 - EA)} \qquad [1]$$

Key words: estimated thermochemical properties, dissociation energies, gaseous metal halides, electrostatic model calculations, Birge-Sponer extrapolation.

with IP and EA in eV. As described by Herzberg (4), molecules for which $r_x/r_e > 2$ exhibit largely ionic binding, while those with $r_x/r_e < 1.5$ are largely covalent. In the intermediate region, both types of binding are important. For this reason, it seems justified to restrict the ionic model calculations to those systems for which $r_x/r_e > 2$. Data to be shown later bear this out. This turns out to be a useful restriction, and helps avoid application of the ionic model into areas of questionable validity.

For diatomic molecules MX, the energy of dissociation to neutral atoms, $D_0°$, can be evaluated from the expression

$$D_0°(MX) = \frac{e^2}{r^2}(r-\rho) + \frac{e^2}{2r^5}(\alpha_1+\alpha_2)(r-4\rho) + \frac{2e^2\alpha_1\alpha_2}{r^6}(r-7\rho) - (IP_1 - EA) \quad [2]$$

which includes terms for charge-charge, charge-induced dipole, and dipole-dipole interaction, and for overlap repulsion. In this expression, e is the electronic charge, r is the equilibrium internuclear separation, α_1 and α_2 are the dipole polarizabilities of M^+ and X^-, respectively, and ρ is the distance parameter in the exponential repulsion term. Other expressions for the repulsion term (*e.g.* r^{-n}) have been used (5), but the exponential formulation exp $(-r/\rho)$ used by Rittner (1) is preferred here because of the relatively direct and systematic way in which ρ is evaluated. Following Rittner, ρ can be evaluated from the expression

$$\rho = \frac{\frac{e^2}{r^2} + \frac{2e^2(\alpha_1+\alpha_2)}{r^5} + \frac{14e^2\alpha_1\alpha_2}{r^6}}{k + \frac{2e^2}{r^3} + \frac{10e^2(\alpha_1+\alpha_2)}{r^6} + \frac{112e^2\alpha_1\alpha_2}{r^9}} \quad [3]$$

where k is the vibrational force constant. Equation [3] is obtained by setting the first derivative of the potential energy function with respect to internuclear separation equal to zero at r_e, the second derivative equal to k, and then solving for ρ. For evaluation of $D_0°$ and ρ, r is set equal to the equilibrium distance, r_e, making it clear that the accuracy is strongly dependent on a reliable value of r_e. The dipole polarizabilities of the halide ions X^- have been determined experimentally, while values for the free ions M^+ often have not. In most instances, $\alpha(M^+)$ can be estimated with acceptable accuracy from the average value of the radius of the valence electron orbit and the IP of M^+, using procedures described previously (6-9). For some diatomic metal halides, the polarization terms can make a substantial contribution to the total energy, making it necessary to use some care in evaluating $\alpha(M^+)$. Values of $\alpha(X^-)$ can be found in the review paper of Dalgarno (10).

Similar expressions can be derived for the binding energies of symmetrical MX_2 and planar symmetric MX_3 molecules. For the dihalides, the energy equation is

$$D_0°(MX_2) = \frac{e^2}{r^2}\left(4 - \frac{1}{2\cos\theta}\right)(r-\rho) + \frac{e^2}{r^5}\left(2\sin^2\theta\alpha_2 + \left[4 + \frac{1}{16\cos^4\theta} - \frac{1}{\cos\theta}\right]\alpha_2\right)(r-4\rho) - IP_1 - IP_2 + 2EA \quad [4]$$

where θ is related to the X-M-X apex angle, φ, by the relation $\theta = 90° - \frac{1}{2}\varphi$. α_2 is the polarizability of M^{++}. When the dihalide is linear ($\theta = 0$), the binding energy equation reduces to

$$D_0°(MX_2)_{linear} = 3.5\frac{e^2}{r^2}(r-\rho) + 3.06\frac{e^2\alpha_2}{r^5}(r-4\rho) - IP_1 - IP_2 + 2EA \quad [5]$$

Likewise for the trihalides, the expression becomes

$$D_0°(MX_3) = 7.27\frac{e^2}{r^2}(r-\rho) + 8.17\frac{e^2}{r^5}\alpha_2(r-4\rho) - IP_1 - IP_2 - IP_3 + 3EA \quad [6]$$

for the planar symmetric configuration. In all instances, $D_0°$ is evaluated at the equilibrium internuclear M-X distance. The metal ion polarizability does not enter into Eq. [5] and [6] because the highly symmetrical configurations preclude any deformation polarization of the metal ion. Although the repulsion parameter ρ can be evaluated in a straightforward manner for diatomic MX, as shown in Eq. [3], the nature of the repulsion term in the triatomic and tetratomic molecules is less clear, and the evaluation of ρ in Eq. [4-6] is more difficult. Until this point is explored more fully, we choose to evaluate ρ for the polyatomic molecules in an empirical fashion, as described below. Values of the successive ionization potentials of most of the metals are available in the compilation of Moore (11), while critically selected values of the electron affinities of the halogen atoms are given by Rosenstock *et al.* (12).

Group IIA halides.—The utility of the Rittner electrostatic model can be illustrated in its application to the thermochemical properties of the Group IIA metal halides. The outstanding success of this model in reproducing the binding energies of the gaseous diatomic alkali halides has already been noted (3). For the IIA monohalides, the necessary molecular constants (internuclear distances and vibrational frequencies) are summarized in the JANAF Tables (13), and the estimated M^+ polarizabilities have been reported (14). In Table I, dissociation energies calculated by means of Eq. [2] and [3] are compared with experimental thermochemical values which are now known for most of the members of this series (9, 14, 15). For these and subsequent comparisons, the calculated values are shown above the experimental values in the tables. $D_0°$ values shown in parentheses for BeBr, BeI, MgBr, and MgI were estimated from related experimental thermochemical data (15), the experimental values have an accuracy of about 2 kcal/mole.

For those molecules lying below the line of demarcation in the table, $r_x/r_e > 2$, and they would be expected to have sufficient ionic character for valid application of the Rittner model. As can be seen, the agreement between calculated and experimental values in that part of the table is quite good. For those molecules in Table I lying above the line, $r_x/r_e < 2$, and the agreement of the ionic model calculations with ex-

Table I. Calculated and experimental dissociation energies of IIA monohalides

	D_{00}, kcal/mole			
	F	Cl	Br	I
Be	117 135	70 92	43 (71)	14 (57)
Mg	100 109	61 75	52 (58)	32 (45)
Ca	120 126	87 94	73 73	58 62
Sr	127 129	92 96	78 79	61 64
Ba	136 139	100 104	84 85	68 73

For each entry, the ionic model calculation is shown above the experimental value.

periment is generally poorer, becoming progressively so as one goes to the least ionic case of BeI. The comparisons tend to bear out the usefulness of the ionicity criterion r_x/r_e, and show that, when applied in the proper domain, the electrostatic model yields reasonably accurate dissociation energies. Bear in mind, however, that the molecular constants of the IIA monohalides are moderately well established, so that relatively little uncertainty is introduced in the input molecular parameters of Eq. [2] and [3]. Krasnov and Karaseva (16) have also treated the IIA monohalides by means of the Rittner model, using a somewhat different approach for evaluating the molecular parameters, and obtain ionic binding energies in close agreement with those calculated in this work. However, their recommended $D_0°(MX)$ values must be viewed with caution because the EA(X) data employed are not consistent with those adopted here. In addition, Krasnov and Karaseva (16) have reached a somewhat different conclusion about the validity of the ionic model, indicating that in most instances it yields only a lower bound to the true $D_0°$. Blue *et al.* (8) have applied the Rittner model to the IIA monofluorides, with results in good agreement with those given here. Over-all, the results for the IIA monohalides provide encouraging support for the Rittner model. It is worth noting that the IIA halides are a more stringent test of the Rittner model than the alkali halides, since with the former the polarization terms contribute substantially more to the binding energy.

Turning now to the IIA dihalides, heats of dissociation were calculated from Eq. [4] using molecular constant data summarized in the JANAF Tables (13). The calculations were limited to the Ca, Sr, and Ba dihalides in view of the results on the monohalides and the ionicity criterion. Note that the molecular geometry varies considerably in this series. Preliminary calculations showed that use of the diatomic ρ values led to consistently low binding energies; on selecting $\rho(MX_2) = 0.8\ \rho(MX)$, one obtains good agreement between calculated and experimental dissociation energies throughout the series. The comparisons are given in Table II, with the X-M-X apex angle used in the calculations shown in parentheses. Experimental values of $D_0°(MX_2)$ are taken largely from the JANAF Tables (13). The dependence of the calculated $D_0°(MX_2)$ on apex angle is small, but not insignificant, due to the increased repulsion between halide ions as the structure deviates from linearity in the simplified model used here. Guido and Gigli (17) have presented a much more detailed treatment of the Rittner model as applied to the IIA dihalides, but the added complexity precludes easy application of the model, and does not yield binding energies in better agreement with experiment. The objective of the present work is to point out the usefulness of a relatively simple approach and to indicate the quality of results that can be obtained when the molecular constants are relatively well established. The data in Table II suggest that an empirical selection of $\rho(MX_2)$ as described above will be satisfactory in other $MX\text{-}MX_2$ systems.

Table II. Calculated and experimental dissociation energies of IIA dihalides

	$D_0°$, kcal/mole							
	F		Cl		Br		I	
Ca	268 266	(140°)	215 214	(180°)	193 186	(180°)	158 155	(180°)
Sr	266 260	(120°)	208 211	(140°)	191 189	(180°)	158 155	(180°)
Ba	269 271	(100°)	217 220	(120°)	195 197	(180°)	167 166	(180°)

$\rho(MX_2) = 0.8\ \rho(MX)$.

Scandium-group fluorides.—Another test of the model is offered by the scandium-group fluorides, which fall well within the ionicity criterion. Taking spectroscopic and molecular constants from several available sources (18, 19), one calculates dissociation energies of the MF, MF_2, and MF_3 species which are in fairly good agreement with the experimental values of Zmbov and Margrave for the Sc-F and Y-F systems (20). The latter contain estimated uncertainties of from 3 to 10 kcal/mole. Agreement with the estimated $D_0°$ values (20) for the La-F series also appears reasonable. Calculated and experimental results are shown in Table III. In calculating the difluoride and trifluoride binding energies from Eq. [4] and [6], it was assumed that $\rho(MX_2) = 0.8\ \rho(MX)$ as found for the IIA dihalides, and that $\rho'(MX_3) = \rho(MX)$. Only for ScF_2 is there an appreciable deviation, and this needs further scrutiny. Note that the required molecular input parameters have been determined for the monofluorides and partially for the trifluorides; values for the difluorides are estimates and therefore contribute an additional uncertainty to the calculations.

Lanthanide monofluorides.—The lanthanide metals are basically an extension of the barium series, in which the inner 5d and 4f orbitals are being filled while maintaining the same outer $6s^2$ valence electron configuration. As such, the ionization energies remain low (21-23) and the gaseous fluorides are expected to fall within the proper ionicity range for valid application of the Rittner model. The few instances in which internuclear distances have been determined (TbF, HoF, YbF) all show that $r_x/r_e >> 2$. Zmbov and Margrave (24) have reported experimental dissociation energies for a few of the lanthanide fluorides and have estimated the remainder. It would be especially instructive to compare these values with the predictions of the Rittner model and to improve the reliability of the estimates, if possible. It may also prove possible later to extend the model calculations to the large number of other lanthanide halides for which no data are available.

In the absence of experimental values, it was assumed that $r_e = 2.00 \pm 0.05$A across the La to Lu series of monofluorides. This agrees with the known values for TbF (25), HoF (26), and YbF (27) and is compatible with the effect of the lanthanide contraction, which causes the molecular constants of these fluorides to be similar to those of SrF. Further, it was assumed that $\alpha(Ln^+)$ would be close to $\alpha(Sr^+)$. With these input data, values of $D_0°(LnF)$ were calculated using the ionic model, and the results are compared with experiment in Table IV; estimates are in parentheses. Agreement with directly measured values is good in all cases except that of GdF; further experimental information, particularly on the spectroscopic constants of GdF, may point up the reasons for the discrepancy. The results appear very promising, and indicate that the calculated values may be more reliable than the estimated $D_0°$ values.

The most critical item here is the lack of information about the equilibrium internuclear distances. As

Table III. Calculated and experimental dissociation energies of scandium group fluorides

	$D_0°$, kcal/mole		
	MF	MF_2	MF_3
Sc	148 141	311 284	439 434
Y	139 144	283 287	458 463
La	148 (143)	279 (288)	432 (452)

For each entry, the ionic model calculation is shown above the experimental value.

Table IV. Calculated and experimental dissociation energies of Lanthanide monofluorides

MF	D_{e0}, kcal/mole: Ionic model	D_{e0}, kcal/mole: Expt.
PrF	139	(138 ± 10)
NdF	137	136 ± 3
PmF	136	(128 ± 10)
SmF	134	134 ± 3
EuF	133	129 ± 2
GdF	123	140 ± 4
TbF	129	(133 ± 10)
DyF	127	125 ± 5
HoF	125	123 ± 4
ErF	123	134 ± 4
TmF	122	(135 ± 10)
YbF	110	(135 ± 10)
LuF	139	(135 ± 10)

Assumes: $r(MF) = 2.0$A, $\alpha(M^+) = 5.0$A^3.

more experimental information becomes available, or as more sophisticated schemes are developed for estimating these distances, the accuracy of the calculations will be improved considerably. It should then be feasible to extend the model calculations to the polyatomic fluorides and to many of the other lanthanide halides as well, provided the ionicity criterion can be met.

Conclusions.—When applied to sufficiently ionic molecular systems, as judged by the ionicity criterion r_x/r_e, the Rittner electrostatic model yields calculated dissociation energies that are in good agreement with experiment for a number of diatomic and polyatomic halides. The accuracy of the calculated values, however, is sensitive to the quality of the molecular input parameters (especially the equilibrium internuclear distance) and the best results are obtained when these parameters have been established experimentally. Whenever estimates of the molecular parameters must be used, it should be recognized that the quality of the calculated results will be strongly dependent on the reliability of those estimates.

At present, there is considerable uncertainty about the nature of the overlap repulsion contribution. Following Rittner, the use of an exponential repulsion term in which the parameter ρ is evaluated from other molecular and atomic constants seems to produce quite good results for the diatomic metal halides. Until a more satisfactory method for evaluating ρ in polyatomic molecules is developed, it appears that an empirical selection based on the value of ρ (diatomic) will be adequate.

Birge-Sponer Extrapolation

An alternate method for estimating the dissociation energies of diatomic molecules is based on the well-known Birge-Sponer extrapolation of vibrational energy levels to the dissociation limit. In many instances, only a few of the lower vibrational levels are known, and this has led to the practice of using a linear extrapolation to estimate the rate of convergence of the higher levels, the so-called linear Birge-Sponer extrapolation (LBX). It has been recognized for some time that the linear extrapolation may be unreliable, and the method has generally fallen into disrepute. A detailed review of the Birge-Sponer extrapolation and its many complexities is given by Gaydon (28).

Recently, however, it has been shown that a systematic correction applied to $D_0°$(LBX) based on the degree of ionic character in the molecule yields estimated $D_0°$ values in fairly good agreement with experiment for a number of molecules of varying ionic character (2). The rationale for this correction derives from the observation that, as a result of the two different types of vibrational potential functions, the vibrational energy levels of a typical covalent molecule converge more steeply than the linear rate, while those of an ionic molecule converge more slowly. Therefore, the $D_0°$(LBX) values of covalent molecules will tend to be too high and those of ionic molecules will be too low. This suggests that the application of a correction to $D_0°$(LBX), related to the degree of ionicity, might yield more reasonable results.

Table V. Comparison of experimental and calculated dissociation energies

MX	D_{e0}(MX), kcal/mole: Expti.	LBX	LBX (corr)	r_x/r_e
CaF	126.4	90	125	2.88
CaCl	94.2	75	95	2.36
CaBr	73.4	67	77	2.04
CaI	62.1	66	68	1.71
SrF	128.7	80	124	3.10
SrCl	95.9	69	97	2.72
SrBr	78.7	65	81	2.28
SrI	63.6	52	67	1.88
BaF	139.5	87	157	3.79
BaCl	104.4	62	102	3.36
BaBr	85.5	64	90	2.71
BaI	71.6	57	69	2.18

One finds that the ratio of the true dissociation energy to the linearly extrapolated value, $D_0°/D_0°$(LBX), correlates very smoothly with the ionicity parameter r_x/r_e and that the analysis of data for a number of metal halides leads to the simple linear relationship

$$D_0°/D_0°(\text{LBX}) \cong 0.374(r_x/r_e) + 0.390 \qquad [7]$$

This approach has been described previously (2), and the details need not be repeated here.

As input data for evaluating $D_0°$(LBX) from the relation

$$D_0°(\text{LBX}) = \frac{\omega_e^2}{4\omega_e x_e} - \tfrac{1}{2}\omega_e \qquad [8]$$

it is especially important to have reliable values of the vibrational anharmonicity constant, $\omega_e x_e$. Values of the vibrational constant ω_e are generally available with sufficient accuracy, but whenever the constants are derived from electronic band spectra using band head positions rather than origins in weakly degraded systems, the resulting value of $\omega_e x_e$ may be unreliable. One should be aware of this potential limitation in evaluating $D_0°$(LBX).

As an illustration of the type of results that can be obtained, the simple and corrected values of $D_0°$(LBX) for the Ca, Sr, and Ba monohalides are compared with experimental results in Table V. The ionicity corrections, using Eq. [7], generally brings the Birge-Sponer values into reasonable agreement with the directly measured values. It is believed that instances of poor correlation (*e.g.*, BaF) can be traced to inaccurate vibrational constants, pointing up the need for due caution in any hasty application of the model. When used with care, it is believed that the modified Birge-Sponer extrapolation can serve as another useful tool for the estimation of reliable thermochemical data.

Acknowledgment

This research was sponsored in part by the Air Force Office of Scientific Research (AFSC), U.S. Air Force, under Contract F44620-73-C-0037.

Manuscript submitted Oct. 13, 1978; revised manuscript received Jan. 25, 1979. This was Paper 389 presented at the Atlanta, Georgia, Meeting of the Society, Oct. 9-14, 1977.

Any discussion of this paper will appear in a Discussion Section to be published in the June 1980 JOURNAL. All discussions for the June 1980 Discussion Section should be submitted by Feb. 1, 1980.

Publication costs of this article were assisted by SRI International.

REFERENCES

1. E. S. Rittner, *J. Chem. Phys.*, **19**, 1030 (1951).
2. D. L. Hildenbrand, in "Advances in High Temperature Chemistry," Vol. 1, L. Eyring, Editor, p. 193, Academic, N.Y. (1967).
3. L. Brewer and E. Brackett, *Chem. Rev.*, **61**, 425 (1961).
4. G. Herzberg, "Spectra of Diatomic Molecules," p. 371, Van Nostrand, Princeton, N.J. (1950).
5. D. Cubicciotti, *J. Phys. Chem.*, 65, 1058 (1961).
6. J. E. Mayer and M. G. Mayer, *Phys. Rev.*, **43**, 605 (1933).
7. L. Pauling and E. B. Wilson, Jr., "Introduction to Quantum Mechanics," p. 387, McGraw-Hill, New York (1935).
8. G. D. Blue, J. W. Green, T. C. Ehlert, and J. L. Margrave, *Nature*, **199**, 804 (1963).
9. D. L. Hildenbrand, *J. Chem. Phys.*, **48**, 3657 (1968).
10. A. Dalgarno, *Adv. Phys.*, 11, 281 (1962).
11. C. E. Moore, *Nat. Stand. Ref. Data Ser. NSRDS-NBS*, **34** (1970).
12. H. M. Rosenstock, K. Draxl, B. W. Steiner, and J. T. Herron, *J. Phys. Chem. Ref. Data*, **6**, Supp. No. 1 (1977).
13. JANAF Thermochemical Tables, *NSRDS-NBS 37* (1971); and supplements.
14. D. L. Hildenbrand, J. Chem. Phys., **52**, 5751 (1970); **66**, 3526 (1977).
15. P. D. Kleinschmidt and D. L. Hildenbrand, *J. Chem. Phys.*, **68**, 28A (1978).
16. K. S. Krasnov and N. V. Karaseva, *Opt. Spectrosc.*, (USSR), *18*, 14 (*1965*).
17. M. Guido and G. Gigli, *J. Chem. Phys.*, **65**, 1397 (1976).
18. B. Rosen, Editor, "Selected Constants—Spectroscopic Data Relative to Diatomic Molecules," Pergamon Press, Oxford (1970).
19. K. S. Krasnov and V. S. Timoshinin, *Teplofiz. Vys. Temp.*, (Engl. Transl.), 7, 333 (1969).
20. K. F. Zmbov and J. L. Margrave, *J. Chem. Phys.*, **47**, 3122 (1967).
21. J. Reader and J. Sugar, *J. Opt. Soc. Am.*, **56**, 1189 (*1966*).
22. J. Sugar and J. Reader, ibid., **55**, 1286 (1965).
23. J. Sugar and J. Reader, *J. Chem. Phys.*, **59**, 2083 (1973).
24. K. F. Zmbov and J. L. Margrave, "Mass Spectrometry in Inorganic Chemistry," p. 267, Adv. Chem. Ser. 72, Am. Chem. Soc., Wash., D.C. (1968).
25. R. F. Barrow, Private communications.
26. D. J. W. Robbins and R. F. Barrow, *J. Phys. B*, **7**, L234 (1974).
27. R. F. Barrow and A. H. Chojnicki, *J. Chem. Soc. Faraday Trans., II*, 71, 728 (1975).
28. A. G. Gaydon, "Dissociation Energies and Spectra of Diatomic Molecules," 2nd ed., Chapman and Hall, London (1953).

Dissociation energies of GdO, HoO, ErO, TmO, and LuO; correlation of results for the lanthanide monoxide series

Edmond Murad

Air Force Geophysics Laboratory, Hanscom Air Force Base, Massachusetts 01731

D. L. Hildenbrand

SRI International, Menlo Park, California 94025
(Received 12 May 1980; accepted 18 June 1980)

High temperature gaseous reaction equilibria involving GdO, HoO, ErO, TmO, LuO, and certain reference oxides have been studied by mass spectrometry, using a molecular effusion beam source. From the reaction thermochemistry, the dissociation energies, D_0°, were derived as 169.5 ± 3 kcal/mol (GdO), 144.1 ± 3 kcal/mol (HoO), 143.9 ± 3 kcal/mol (ErO), 121.8 ± 3 kcal/mol (TmO), and 159.4 ± 2 kcal/mol (LuO). Some of these values differ substantially from previous determinations. However, the new results together with several recent determinations and re-evaluations yield a consistent set of results for the entire series from LaO to LuO. Trends in D_0° values across the series can be correlated remarkably well with changes in the $4f^n 6s^2 \rightarrow 4f^{n-1} 5d 6s^2$ electronic promotion energies in the gaseous metal atoms. Various aspects of the bonding are discussed.

INTRODUCTION

The gaseous monoxides of the 14 lanthanide (rare-earth) metals in the series stretching from cerium to lutetium have been subjected to a number of thermochemical investigations, yet the dissociation energies (D_0^0) of some members of the series remain relatively uncertain. Ames, Walsh, and White[1] carried out the first comprehensive thermochemical study of these monoxides using a combination of mass spectrometric and Knudsen effusion techniques, and recognized the utility of correlating the resulting trends in D_0^0 across the series with the electronic structure of the metal atoms. In particular, the so-called double periodicity in the values of D_0^0 was found to correlate closely with the filling of the lanthanide 4*f* orbitals, and deviations of the D_0^0 values from a common baseline could apparently be accounted for by the changes in $4f^n - 4f^{n-1}5d$ promotion energies of the divalent lanthanide metal ions. Two notable exceptions to this latter correlation, however, were EuO and TmO, where the experimental values of D_0^0 were almost 20 kcal/mol higher than the predicted values. Krause[2] later reviewed the status of the lanthanide monoxide data in detail and reinterpreted some of the measurements; however, the recommended D_0^0 values did not differ appreciably from those reported by Ames, Walsh, and White.[1]

Subsequently, a new thermochemical study[3] yielded a value of D_0^0(EuO) some 22 kcal/mol lower than the result of Ames *et al.*[1] This new result for EuO was corroborated by an Eu + O_2 molecular beam study[4] and by an additional equilibrium study.[5] Further equilibrium measurements[6] on SmO led to a D_0^0 value about 6 kcal/mol lower than that reported earlier,[1] and resolved an inconsistency between D_0^0(SmO) and D_0^0(EuO). On the other hand, re-examination of PrO and NdO by equilibrium mass spectrometry[7] gave results only slightly lower than those of Ames *et al.*[1] And another crossed molecular beam study[8] yielded a value of D_0^0(YbO) about 10 kcal/mol higher than the upper bound reported in the earlier effusion studies.[1]

In order to do a more quantitative evaluation of the promotion energy correlation outlined by Ames *et al.*,[1] it seemed necessary to re-examine several additional monoxides so as to put the model to a fair test. Since a key feature of the model concerns deviations of the experimental D_0^0 values from a baseline defined by those metals with $4f^n 5d\, 6s^2$ ground states (La, Ce, Gd, Lu), it is especially important to fix these benchmarks; D_0^0(LaO) and D_0^0(CeO) are considered to be well established, but the values[6] for GdO and LuO need corroboration. Likewise, the data for HoO, ErO, and TmO appear to be somewhat at odds with the promotional energy model.[1] Accodingly, new experimental determinations of the dissociation energies of GdO, HoO, ErO, TmO, and LuO were undertaken by means of high temperature mass spectrometry. These results, their correlation with the promotional energy model, and the properties of the lanthanide monoxide series as a whole are described in this paper.

EXPERIMENTAL

The desired dissociation energies were derived from high temperature gaseous equilibrium measurements monitored by mass spectrometry. Two separate, but quite similar, instruments were used; these were of the 30.5 cm, 60° sector magnetic deflection type used in previous work.[9] Studies of the GdO, HoO, and ErO systems were done with the AFGL spectrometer, while those on TmO and LuO were done with the SRI instrument.

Effusion oven beams containing the pertinent gaseous species were generated by vaporizing mixtures of the appropriate metals and metal oxides from molybdenum effusion cells. The solid phase mixtures used in the various experiments are summarized in Table I. Samples were of reagent grade quality, but high purity generally is not a critical factor in work of this type since mass analysis provides a selective method for monitoring only the particular gaseous species of interest.

 0021-9606/80/204005-07$01.00

TABLE I. Samples used for generation of effusion beams.

System	Solid phases
Gd–Y–O	Gd_2O_3, Y, Y_2O_3
Gd–Ti–O	Gd, Gd_2O_3, TiO_2
Ho–Er–Ti–O	Ho_2O_3, Er_2O_3, Ti, TiO_2
Tm–Al–O	Tm_2O_3, Al_2O_3
Lu–Y–O	Lu, Lu_2O_3, Y, Y_2O_3

Following customary procedure, the response of each signal to displacement of the molecular beam defining slit was checked to ascertain the effusion cell origin. This slit test proved to be particularly important in the Tm–Al–O studies, where initial vaporization of a Tm_2O_3–Al_2O_3 mixture from a molybdenum cell yielded a Tm^+ parent signal with a neutral beam profile much broader than the normal sharp profile observed with highly condensible species. Inspection showed that the sample had formed a liquid phase which crept onto the outside surface of the cell via the slip fit joint connecting the upper and lower sections of the effusion cell. After enclosing the cell in a cover fabricated from tantalum sheet, the Tm^+ profiles exhibited normal behavior; apparently the Ta shroud effectively trapped the vapors emanating from the outside surface, and no further problems were encountered.

Details of the experimental procedure and interpretation of the data, including determination of ion appearance potentials, temperature measurement, and derivation of reaction equilibrium constants (K_{eq}) from parent ion abundance ratios are given in previous publications.[3,9] As in past work, equilibrium data were taken from parent ion signals measured with low energy ionizing electrons, generally 3 to 5 eV above threshold. In a few instances, higher ionizing energies (20 eV) were used to increase sensitivity, after it was ascertained that the derived equilibrium constant was unaffected by use of the higher energies.

TABLE II. Appearance potentials of ions measured in this study.[a]

Ion	Appearance potential (eV)	Literature value (eV)
Gd^+	6.1 ± 0.1	6.15[b]
GdO^+	6.7 ± 0.5	5.75[c]
Ho^+	6.1 ± 0.5	6.02[b]
HoO^+	6.1 ± 0.5	6.17[c]
Er^+	6.1 ± 0.5	6.11[b]
ErO^+	6.2 ± 0.5	6.30[c]
Tm^+	6.5 ± 1	6.18[d]
TmO^+	6.5 ± 1	6.44[c]
Lu^+	5.5 ± 0.5	5.43[d]
LuO^+	6.5 ± 0.5	6.79[c]
Y^+	6.4 ± 0.5, 6.5 ± 0.3	6.38[e]
YO^+	6.4 ± 0.5, 6.0 ± 0.3	5.85[f]
Ti^+	6.6 ± 0.5, 6.5 ± 0.3	6.82[e]
TiO^+	6.9 ± 0.5, 6.[illegible] ± 0.3	6.70,[g] 6.4[f]
Al^+	6.0 ± 0.5	5.99[e]
AlO^+	9.5 ± 0.5	9.53[h]

[a] Appearance potentials were evaluated using the vanishing current method.
[b] Reference 10.
[c] Reference 11.
[d] Reference 12.
[e] Reference 13.
[f] Reference 14.
[g] Reference 15.
[h] Reference 16.

TABLE III. Equilibrium data for the reaction $Gd(g) + TiO(g) = GdO(g) + Ti(g)$.

T/K	K_{eq}	ΔH_0 (III) (kcal/mol)
1957	24.4	−11.7
1973	22.1	−11.4
1977	20.6	−11.2
1981	24.1	−11.8
1990	20.2	−11.2
1995	21.2	−11.4
2005	21.5	−11.5
2009	22.6	−11.7
2018	22.7	−11.8
2024	19.6	−11.3

Average ΔH_0° (III) = −11.5 ± 2 kcal/mol
ΔH_{1993}° (II) = −12.2 ± 7.5 kcal/mol

RESULTS

Gaseous species present in the effusion beams were identified from the masses and appearance potentials of the ions formed by electron impact. The observed appearance potentials are summarized in Table II, and compared with values of the ionization potentials of the corresponding neutrals. The magnitudes of the appearance potentials and the general accord with literature values provide conclusive evidence for the presence of the metals and metal monoxides in the effusion oven beams. Gaseous equilibria studied and derived results are discussed below. Thermodynamic functions used in the analysis of the equilibrium data were taken from sources described in the Appendix.

The measured reaction equilibrium constants and derived enthalpy changes are presented in Tables III to VII, and a summary of the derived results is given in Table VIII. It is expected that the temperature correction to the second law enthalpies will be relatively small, so that the slope values at the average experimental temperatures can be compared directly with the third law values of ΔH_0°. For the Lu–Y–O system, where the molecular electronic levels are believed to be known reasonably well, the correction to ΔH_T° from 1900 to 0 K is 0.8 kcal/mol. Although the second law enthalpies are not sufficiently precise and accurate to stand alone as definitive determinations, the accord with third law values is in most instances sufficient to corroborate the choice of spectroscopic constants for the lanthanide oxides. The derived thermochemical data presented here, therefore, are based entirely on third law analysis.

The principal sources of error in the third law enthalpies arise from uncertainties in the evaluation of the reaction equilibrium constants and in the thermodynamic

TABLE IV. Equilibrium data for the reaction $Gd(g) + YO(g) = GdO(g) + Y(g)$.

T/K	K_{eq}	ΔH_0° (III) (kcal/mol)
1908	1.13	0.8
1909	1.13	0.8
1924	1.12	0.8
1930	1.13	0.8
1937	1.08	1.0
1940	1.09	0.9
1941	1.06	1.0
1947	1.11	0.9
1951	1.12	0.8
1953	1.14	0.8
1961	1.09	0.9
1961	1.08	1.0
1965	1.12	0.8
1970	1.14	0.75
1977	1.14	0.75

Average ΔH_0° (III) = + 0.9 ± 3 kcal/mol
ΔH_{1946} (II) − 0.1 ± 2.3 kcal/mol

functions of the lanthanide monoxides. In going one step further to derive the dissociation energies of the lanthanide oxides, an additional uncertainty stems from possible errors in the D_0^0 values of the reference oxides YO, TiO, and AlO. The estimated errors take these sources into account, and yield uncertainties of ± 2 kcal/mol in ΔH_0^0 and ± 3 kcal/mol in D_0^0(MO). Selected D_0^0 values of the reference oxides used in this work are also given in the Appendix.

DISCUSSION

The newly determined values of D_0^0 derived from the results of this research are D_0^0 (GdO) = 169.5 ± 3 kcal/mol; D_0^0(HoO) = 144.1 ± 3 kcal/mol; D_0^0(ErO) = 143.9 ± 3 kcal/mol; D_0^0(TmO) = 121.8 ± 3 kcal/mol; and D_0^0(LuO) = 159.4 ± 2 kcal/mol. The value for GdO does not differ significantly from that originally reported by Ames *et al.*[1] (173.0 kcal/mol) or from the selected value of Krause[2] (169 kcal/mol) based on a re-evaluation of the literature in 1974. However, the new values for HoO, ErO, TmO, and LuO are 8, 8, 17, and 8 kcal/mol, respectively, lower than the selected results of Ames *et al.*,[1] and are similarly lower than the revised data of Krause[2] for all but LuO, where a somewhat lower value of 162 kcal/mol was chosen. There is as yet no fully satisfactory explanation for the differences but recent redeterminations on EuO[3] and SmO[6] suggest that interactions between sample and container adversely affected some of the earlier Knudsen mass effusion rate measurements,[1] and that some of the mass spectrometric equilibrium data obtained in those same studies[1] contained significant systematic errors. The D_0^0(MO) data reported here are believed to be accurate within the estimated errors and are selected as "best values" along with the more recent data on PrO,[7] NdO,[7] and EuO.[3-5]

For the remaining oxides in the LaO–LuO series, the value D_0^0(LaO) = 190 ± 1 kcal/mol is selected largely from the equilibrium studies of Ackermann and Rauh,[17] while a recommended value D_0^0(YbO) = 95 ± 5 kcal/mol is chosen

TABLE V. Equilibrium data for the reactions $Er(g) + TiO(g) = ErO(g) + Ti(g)$ (1), and $Ho(g) + TiO(g) = HoO(g) + Ti(g)$ (2).

T/K	K_{eq} (1)	ΔH_0° (III) (kcal/mol)	K_{eq} (2)	ΔH_0° (III) (kcal/mol)
1855	0.053	14.5	0.066	13.6
1884	0.067	13.8	0.063	14.0
1973	0.054	15.3	0.083	13.6
2012	0.079	14.1	0.070	14.5
2078	0.072	15.0	...	...
2094	0.072	15.1	0.070	14.5
2108	0.094	14.0	0.080	14.6
2136	0.087	14.6	0.073	15.2
2153	0.085	14.8	0.104	13.8
2165	0.104	14.0	0.083	14.9
2178	...	...	0.097	14.3

Reaction (1):

Average ΔH_0° (III) = 14.5 ± 3 kcal/mol
ΔH_{2045} (II) = 13.2 ± 2.9 kcal/mol

Reaction (2):

Average ΔH_0° (III) = 14.3 ± 3 kcal/mol
ΔH_{2056}° (II) = 8.2 ± 2.3 kcal/mol

TABLE VI. Equilibrium data for the reaction $Al(g) + TmO(g) = AlO(g) + Tm(g)$.

T/K	K_{eq}	ΔH_0° (III) (kcal/mol)
2249	0.33	0.0
2292	0.32	0.2
2292	0.37	− 0.4
2303	0.36	− 0.3
2303	0.35	− 0.2
2364	0.36	− 0.3

Average ΔH_0° (III) = − 0.2 ± 3 kcal/mol

TABLE VII. Equilibrium data for the reaction $Lu(g) + YO(g) = LuO(g) + Y(g)$.

T/K	$K_{eq} \times 10^2$	ΔH_0° (III) (kcal/mol)
1849	8.35	10.5
1863	8.09	10.7
1864	8.27	10.6
1867	8.24	10.6
1888	8.45	10.6
1888	8.38	10.7
1906	8.78	10.6
1916	8.89	10.6
1924	9.09	10.6
1924	8.95	10.6
1944	9.62	10.4
1944	9.30	10.6
1944	9.40	10.5
1944	9.19	10.6

Average ΔH_0° (III) = 10.6 ± 3 kcal/mol
ΔH_{1905}° (II) = 11.0 ± 0.9 kcal/mol

TABLE VIII. Summary of reaction thermochemistry and derived results.

Gaseous reaction	ΔH_T° (II) (kcal/mol)	ΔH_0° (III) (kcal/mol)	Results (kcal/mol)
Gd + TiO = GdO + Ti	−12.2 ± 7.5	−11.5	D_0°(GdO) = 169.9
Gd + YO = GdO + Y	−0.1 ± 2.3	+0.9	D_0°(GdO) = 169.1
Ho + TiO = HoO + Ti	(+8.2 ± 2.2)	+14.3	D_0°(HoO) = 144.1
Er + TiO = ErO + Ti	+13.2 ± 2.9	+14.5	D_0°(ErO) = 143.9
Al + TmO = AlO + Tm	(+6.0 ± 6.1)	−0.2	D_0°(TmO) = 121.6
Lu + YO = LuO + Y	+11.0 ± 0.9	+10.6	D_0°(LuO) = 159.4

from the crossed molecular beam studies of Cosmovici *et al.*[9] Our selected value for CeO, D_0°(CeO) = 188 ± 4 kcal/mol, is based on second law studies of the LaO–CeO exchange reaction by Drowart and co-workers[18]; the values D_0°(TbO) = 165 ± 5 kcal/mol and D_0°(DyO) = 148 ± 5 kcal/mol are recalculated from the gaseous equilibrium and vaporization data reported by Ames *et al.*[1] with the thermodynamic functions described in the Appendix. The selected values of D_0° for the entire series, believed to be the most internally consistent and reliable set available, are summarized in Table IX.

Ames and co-workers[1] initially noted the doubly periodic variation in D_0°(MO) across the lanthanide series, and commented on similarities with corresponding variations in the enthalpies of sublimation of the metals. As mentioned above, it was found that the experimental values of D_0°(MO) for those gaseous metal atoms with $4f^n6s^2$ ground states could be correlated with the $4f^n - 4f^{n-1}5d$ excitation energies E of the divalent metal ions determined by Jørgensen[19] from measurements in solution. It was noted that the dissociation energies of the monoxides of those metals with $4f^n5d\,6s^2$ ground states (La, Ce, Gd, Lu) formed a more or less common baseline across the series, and that the D_0° values of the oxides of metals with $4f^n6s^2$ ground states fell below this baseline by an amount approximately equal to ΔE. The rationale for this behavior rests on the assumption that the ionic structure $M^{2+}O^{2-}$ predominates, and that the binding energies of all monoxides with the $4f^n5d$ metal ion configuration vary monotonically across the series. For those metal ions with $4f^n$ ground states, the excitation energy ΔE must then be supplied at the expense of that particular MO bond. According to this model, the dissociation energy D_0° can be predicted from the relation

$$D_0^\circ(\text{predicted}) = D_0^\circ(\text{baseline}) - \Delta E \ . \qquad (1)$$

Relatively poor correlation with this model was observed for EuO and TmO, with the model predicting values of D_0° about 20 kcal/mol lower than the experimental values. It is now apparent that this was due in part to errors in the earlier determinations,[1] since our more recent values of D_0° for EuO and TmO are 22 and 17 kcal/mol lower, respectively. Bergman *et al.*[20] also applied the promotional energy model to a number of the lanthanide monoxides and to the sulfides, selenides, and tellurides as well, and discussed implications of the correlation in terms of the ligand field theory.

The relatively close correlation between experimental values of D_0° and those predicted by Eq. (1), as reported by Ames *et al.*,[1] was in a sense fortuitous, since the solution values of ΔE for the divalent ions given by Jørgensen[19] are relative rather than absolute values. A more logical test of the model can be made by using the $4f^n - 4f^{n-1}5d$ transition energies derived from the spectra of the free gaseous M^{2+} ions, and tabulated by Martin *et al.*[21] The free ion values of ΔE are consistently higher than Jørgensen's relative values[19] by 5000 to 10 000 cm^{-1} (15 to 30 kcal/mol), and the D_0° values predicted by Eq. (1) now fall below the experimental values by comparable amounts. Actually, the transition energies, ΔE, follow similar trends for M^{2+}, M^+, and M; the magnitudes of the transition energies (for $4f^n - 4f^{n-1}5d$) decrease regularly as one proceeds in the series $M^{2+} - M^+ - M$.[21] In fact, the correlation between experimental and predicted values of D_0° is quite good if the free atom values of ΔE are used in Eq. (1), as seen in Fig. 1. The pertinent data are summarized in Table IX. The values of ΔE given in Table IX correspond to the transition from the ground state to the lowest J level of the excited state in $4f^n6s^2 - 4f^{n-1}5d^16s^2$. Baseline values of D_0° used in Eq. (1) were evaluated from a second order polynomial fitted to the data for LaO, CeO, GdO, and LuO. Essentially, the agreement is within experimental error for all the monoxides but SmO and EuO, where the differences amount to 13 and 16 kcal/mol, respectively. It may be that for Sm and Eu higher J levels need to be considered. Moreover, it should be kept in mind that Eu, because of its half-filled f shell,

TABLE IX. Selected dissociation energies of the lanthanide monoxides and model predictions.

Oxide	D_0° (kcal/mol)	ΔE[a] (kcal/mol)	State of excited level[a]	D_0° (predicted)[b] (kcal/mol)
LaO	190 ± 1	···	···	190
CeO	188 ± 4	···	···	188
PrO	176 ± 3	13	$^4I_{9/2}$	171
NdO	167 ± 3	19	$^5L_6$	162
SmO	136 ± 3	52	$^7H_2$	123
EuO	112 ± 3	[77]	$^6D_{3/2}$	96
GdO	170 ± 3	···	···	170
TbO	165 ± 5	1	$^6G_{13/2}$	167
DyO	146 ± 5	22	$^7H_6$	144
HoO	144 ± 3	24	$(8, \frac{15}{2})\ J = \frac{17}{2}$	140
ErO	144 ± 3	20	$(\frac{17}{2}, \frac{15}{2})\ J = 6$	143
TmO	122 ± 3	38	$(6, \frac{15}{2})\ J = \frac{13}{2}$	123
YbO	95 ± 5	66	$(\frac{1}{2}, \frac{15}{2})\ J = 2$	94
LuO	159 ± 3	···	···	159

[a] Energy of atomic transition $4f^n6s^2 - 4f^{n-1}5d^16s^2$ from Ref. 21. Transition to lowest J level of the excited atom is considered.

[b] Calculated using Eq. (1): D_0° (baseline) = 190.6 − 3.75N + 0.0936N^2 kcal/mol; N = atomic number (Z) − 57.

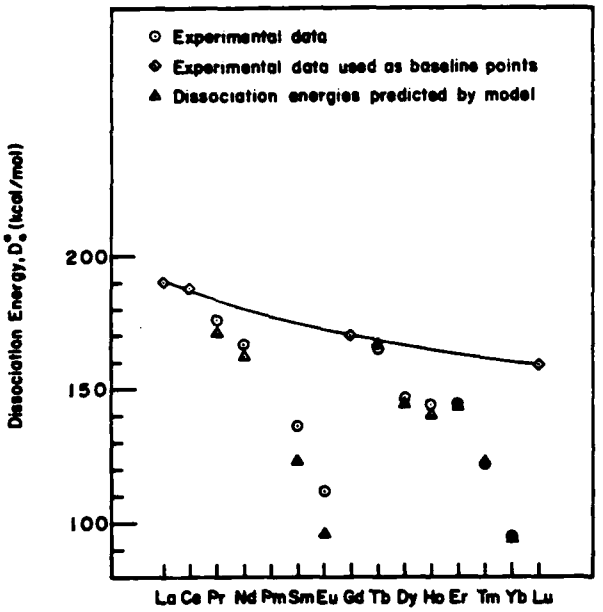

FIG. 1. Variation of the dissociation energies of the lanthanide monoxides with increasing atomic number.

is somewhat anomalous by comparison with the other rare earth oxides. With a ground state of ^8S it resembles, in many ways, Ba, and it is possible that in the case of Eu, at least, ionic forces play important roles. It seems certain, however, that the $4f^n - 4f^{n-1}5d$ excitation energy plays a major role in determining the energetics of most of the lanthanide monoxide bonds.

The poor quantitative correlation of the experimental D_0^0 values with the transition energies of the M^{2+} free gaseous ions casts some doubt on the suitability of describing the bonding in the gaseous monoxides in terms of the $M^{2+}O^{2-}$ ionic configuration. This point is difficult to check via an electrostatic model calculation, as has been done for many gaseous metal halides,[22,23] since the internuclear distances of only a few of the monoxides have been determined, and, perhaps more importantly, the electron affinity $EA(O-O^{2-})$ which is needed to convert the ionic dissociation energy to that of the neutral atoms, is highly uncertain. In two recent studies[11,24] examining the applicability of the electrostatic model to the lanthanide monoxides, assumed values of 7.72 and 6.63 eV were used for $EA(O-O^{2-})$. Despite this large difference, and the use of diverse approaches to evaluating the polarization term, the two sets of calculated dissociation energies agreed with each other to within 0.2 eV or better in most instances, and with the experimental values as well. In these instances, the polarization term is essentially being used as an adjustable parameter, making up for the difference in $EA(O-O^{2-})$.

Although it may at first glance seem significant that the ionic model yields D_0^0 values reflecting the same trends with atomic number as the experimental values, this is a direct consequence of the assumptions in both calculations that the M^{2+} ion polarizabilities vary inversely with the $4f^n - 4f^{n-1}5d$ transition energy ΔE. These polarization terms make a substantial contribution to the total binding energy. Thus the resulting correlation of the ionic model data with ΔE is a predetermined feature of the calculations. Whether or not the M^{2+} ion polarizabilities show the assumed variation with ΔE remains to be seen; none of these quantities has been determined experimentally. At the moment it seems that the apparent success of the ionic model[11,24] can be just as well ascribed to a fortuitous adjustment of the estimated input parameters. The ionicity criterion[22] r_+/r_- indicates that the singly charged configuration M^+O^- is not a major contributor to the bonding in the lanthanide monoxides, and this is corroborated by calculations on La^+O^-, where all the input parameters are known reasonably well; in this instance the ionic model yields a D_0^0 value about 0.7 eV lower than the experimental result.

In contrast to the pronounced double periodicity in the dissociation energies of the lanthanide monoxides, as seen in Fig. 1, it is worth noting that this same effect is not apparent in the lanthanide monofluorides. The D_0^0 values of those monofluorides that have been determined experimentally (NdF, SmF, EuF, GdF, DyF, HoF, ErF, and TmF)[25,26] fall within the range 130 ± 10 kcal/mol, quite different from the behavior of the monoxides. The same ionicity criterion[23] shows the monofluorides to have sufficient ionic character for application of the electrostatic model, and the predicted dissociation energies based on a constant M^+ ion polarizability across the series are in good accord with the experimental values. This contrasting behavior may signal substantial differences in the chemical bonding, with the monoxides being largely covalent and the monofluorides largely ionic. Bergman *et al.*[20] noted the unsuitability of the singly and doubly charged ionic models for the lanthanide chalcogenides and suggested the necessity of considering more complex features of the bonding.

The close similarity of the ionization potentials of the lanthanide metals and their monoxides has been noted previously by Ackermann *et al.*[11]; from Fig. 1 of their paper it can be seen that IP(M) and IP(MO) lie generally within at least 0.5 eV of each other. Just as with the metal,[21] the metal monoxide ionization process will then involve the loss of a 6s electron, which in the monoxide must be nonbonding or slightly antibonding. Considering the importance of the $4f^n - 4f^{n-1}5d$ excitation energy and the fact that at least one of the metal 6s electrons is not involved in bonding, it seems likely that the bonding in MO involves a metal $s-d$ hybrid, or possibly a pure d orbital. Because the dissociation energies of the monoxide ions are related to those of the neutral monoxides $[D_0^0(M^+-O) = D_0^0(MO) + IP(M) - IP(MO)]$ the two dissociation energies will be comparable, and the values of $D_0^0(M^+-O)$ will show the same type of double periodicity exhibited by the $D_0^0(MO)$ values. In Table X are summarized the values of $D_0^0(M^+-O)$ calculated from the above relation with the selected $D_0^0(MO)$ data of Table IX and the literature values of[10] IP(M) and IP(MO).[11]

One final remark along these lines can be made, namely that the thermochemical data complement some kinetic measurements which have shown that associative ionization reactions of the type

TABLE X. Dissociation energies of the lanthanide monoxide ions and heats of formation of the gaseous monoxides.

Oxide	$D_0^\circ(M^+-O)^a$ (kcal/mol)	ΔHf_0° (MO, g, 0 K) (kcal/mol)
LaO	205	−28±1.5
CeO	203	−28±5
PrO	189	−32±3
NdO	179	−30±3
SmO	138	−28±3
EuO	93	−11±3
GdO	180	−16±3
TbO	177	−13±5
DyO	145	−18±5
HoO	141	−13±3
ErO	140	−9±3
TmO	116	−7.5±3
YbO	88	+0.5±5
LuO	127	+2±3

[a] $D_0^\circ(M^+-O) = D_0^\circ(MO) + IP(M) - IP(MO)$. Values for $D_0^\circ(MO)$ were taken from Table IX; those for IP(M) were taken from Ref. 10, while those for IP(MO) were taken from Ref. 11.

TABLE XI. Statistical weights of electronic ground states of the lanthanide monoxides.

Oxide	g_0 Ames *et al.*[a]	g_0 This work[b]
YO	2	2
LaO	2	2
CeO	3	6
PrO	4	8
NdO	5	10
SmO	7	12
EuO	8	16
GdO	9	9
TbO	8	20
DyO	7	12
HoO	6	12
ErO	5	10
TmO	4	8
YbO	3	6
LuO	2	2

[a] Reference 1.

[b] Obtained using the model given by Smoes *et al.* (Ref. 29): g_0 is taken to be m if the (M − 1) ion has a ground state of $^m S$ and as $2m$ otherwise.

$$M + O \rightarrow MO^+ + e$$

have large cross sections for[37] Gd and Sm.[38] It is expected that, with the exceptions of Eu and Yb, all the lanthanide elements will undergo similar reactions.

The heats of formation of the gaseous monoxide molecules are summarized in Table X.

ACKNOWLEDGMENT

We thank J.-Cl. Beaufils, M. Dulick, R. W. Field, and C. Linton for communicating to us their results on CeO and PrO prior to publication. We thank P. Bench of AFGL for help in some of the computations. One of us (E. M.) thanks I. Michael for help in some of the measurements on D_0°(GdO) which were presented at the 175th National Meeting of the American Chemical Society. The assistance of K. H. Lau with the measurements on TmO and LuO are gratefully acknowledged. This work was supported in part by the Air Force Office of Scientific Research (AFSC) under Contract No. F49620-78-C-0033.

APPENDIX

For consistency, the thermodynamic functions of YO, LaO, and all the lanthanide monoxides were calculated from the rotational and vibrational parameters utilized by Ames *et al.*[1] With a few of the monoxides, somewhat more accurate spectroscopic constants are now available, but recalculated values of the function Φ_T° [formerly $-(G_T^\circ - H_0^\circ)/T$] with the new constants differed by no more than 0.2 cal/deg mol at 2000 K from the earlier values,[1] a difference considered negligible. Only the electronic ground states of the lanthanide monoxides were considered, and the statistical weights of those states were taken from the scheme used by Smoes *et al.*[29] for the corresponding lanthanide monosulfides; in Table XI, the statistical weights so derived are listed and compared with the values used by Ames *et al.*[1] Recent spectroscopic studies on CeO[30] and PrO[31] indicates that the spectra of these molecules are quite complex. For example, CeO is found to have the following low-lying states, where ϵ_i is given in cm^{-1} and g_i is given in parentheses: 0(2), 80(2), 915(2), 2000(2), 2140(2), and 2615(2). On the other hand, PrO has the following low-lying states: 0(2), 17.7(2), 3 states at ~2060 ($\Sigma g_i = 6$), 2 states at ~2900 ($\Sigma g_i = 4$). Almost certainly, there are other low-lying states which will contribute to the Φ functions. If the states of PrO cited above are used to calculate the Φ function of PrO, then the derived D_0°(PrO) would be lowered by ~1 kcal/mol; this is well within the quoted uncertainties. Additional electronic states would raise the derived D_0°(PrO). Thus it is likely that the statistical weights used in this work are larger than the actual statistical weights of the ground states which tends to increase the Φ function. On the other hand, not including any low-lying states tends to have an opposite effect.

Thermodynamic functions for AlO and TiO were taken from the *JANAF Thermochemical Tables*.[33] Selected dissociation energies of the reference oxides are as follows: D_0°(TiO) = 158.4 ± 2 kcal/mol (Refs. 15 and 32); D_0°(YO) = 170.0 ± 1 kcal/mol (Ref. 33); and D_0°(AlO) = 122.0 ± 1 kcal/mol (Ref. 34). Although there are implications from a recent kinetic study[35] that D_0°(AlO) ≥ 126 kcal/mol, we prefer the aforementioned value, which is corroborated by a variety of spectroscopic and thermochemical determinations. Heats of sublimation of the lanthanide elements were obtained from the compilation by Hultgren *et al.*[36]

[1] L. L. Ames, P. N. Walsh, and D. White, J. Phys. Chem. 71, 2707 (1967).

[2] R. F. Krause, Jr., Natl. Bur. Stand. Rep. No. NBS IR 74-

600, AFOSR-TR-75-0596, October 1974 (unpublished).
[3]E. Murad and D. L. Hildenbrand, J. Chem. Phys. 65, 3250 (1978).
[4]R. Dirscherl and K. W. Michel, Chem. Phys. Lett. 43, 547 (1976).
[5]G. Balducci, G. Gigli, and M. Guido, J. Chem. Phys. 67, 147 (1977).
[6]D. L. Hildenbrand, Chem. Phys. Lett. 48, 340 (1977).
[7]E. Murad, Chem. Phys. Lett. 59, 359 (1978).
[8]C. B. Cosmovici, E. D'Anna, A. D'Innocenzo, G. Leggieri, A. Ferrone, and R. Dirscherl, Chem. Phys. Lett. 47, 3657 (1968).
[9]D. L. Hildenbrand, J. Chem. Phys. 48, 3657 (1968).
[10]E. F. Worden, R. W. Solarz, J. A. Paisner, and J. G. Conway, J. Opt. Soc. Am. 68, 52 (1978).
[11]R. J. Ackermann, E. G. Rauh, and R. J. Thorn, J. Chem. Phys. 65, 1027 (1976).
[12]W. C. Martin, L. Hagan, J. Reader, and J. Sugar, J. Phys. Chem. Ref. Data 3, 771 (1974).
[13]C. E. Moore, Natl. Stand. Ref. Data Ser. NSRDC-NBS 34 (1970) (unpublished).
[14]E. G. Rauh and R. J. Ackermann, J. Chem. Phys. 60, 1396 (1974).
[15]D. L. Hildenbrand, Chem. Phys. Lett. 44, 281 (1976).
[16]D. L. Hildenbrand, Chem. Phys. Lett. 20, 127 (1973).
[17]R. J. Ackermann and E. G. Rauh, J. Chem. Thermodynam. 3, 445 (1971).
[18]J. Drowart, A. Pattoret, and S. Smoes, Proc. Br. Ceram. Soc. 8, 67 (1967).
[19]C. K. Jørgensen, Mol. Phys. 7, 417 (1964).
[20]C. Bergman, P. Coppens, J. Drowart, and S. Smoes, Trans. Faraday Soc. 66, 800 (1970).
[21]W. C. Martin, R. Zalubas, and L. Hagan, Natl. Stand. Ref. Data Ser., NSRDS-NBS-60 (1978) (unpublished).
[22]E. S. Rittner, J. Chem. Phys. 19, 1030 (1951).
[23]D. L. Hildenbrand, J. Electrochem. Soc. 126, 1396 (1979).
[24]M. Guido and G. Gigli, J. Chem. Phys. 61, 4138 (1974).
[25]K. F. Zmbov and J. L. Margrave, in *Mass Spectrometry in Inorganic Chemistry*, Adv. Chem. Ser. No. 72 (Am. Chem. Soc., Washington, D. C., 1978).
[26]P. D. Kleinschmidt, K. H. Lau, and D. L. Hildenbrand, J. Chem. Phys. (to be published).
[27]H. H. Lo and W. L. Fite, Chem. Phys. Lett. 29, 39 (1974).
[28]E. J. Stone, G. M. Lawrence, and C. E. Fairchild, J. Chem. Phys. 65, 5083 (1976).
[29]S. Smoes, P. Coppens, C. Bergman, and J. Drowart, Trans. Faraday Soc. 65, 682 (1976).
[30]C. Linton, M. Dulick, and R. W. Field, J. Mol. Spectrosc. (in press).
[31]M. Dulick, J.-Cl. Beaufils, and R. W. Field, J. Mol. Spectrosc. (in press).
[32]*JANAF Thermochemical Tables*, NSRDS-NBS-37 (U. S. GPO, Washington, D. C., 1971); J. Phys. Chem. Ref. Data 4, 1 (1975).
[33]M. B. Liu and P. G. Wahlbeck, High Temp. Sci. 6, 3854 (1977), and previous references cited therein.
[34]L. Pasternack and P. G. Dagdigian, J. Chem. Phys. 67, 3854 (1977), and previous references cited therein.
[35]A. Fontijn and W. Felder, J. Chem. Phys. 71, 4854 (1979).
[36]R. Hultgren, P. D. Desai, D. T. Hawkins, M. Gleiser, K. K. Kelley, and D. Wagman, *Selected Values of the Thermodynamic Properties of the Elements* (Am. Soc. for Metals, Metals Park, Ohio, 1973).

Thermochemical studies of the BF_2 radical[a)]

K. H. Lau and D. L. Hildenbrand

SRI International, Menlo Park, California 94025
(Received 7 January 1980; accepted 21 January 1980)

The BF_2 radical was generated under equilibrium conditions by the reaction of both $SF_6(g)$ and $BF_3(g)$ with $B(s)$ in an effusion cell at 1600 to 1800 K, and was identified and thermochemically characterized by mass spectrometry. Enthalpy data derived from the analysis of several gaseous equilibria in the B–F and B–Ca–F systems led to concordant results on BF_2, and to the standard enthalpy of formation $\Delta_f H^\circ_{298}(BF_2) = -120.0 \pm 4$ kcal/mol, about 20 kcal/mol less negative (less stable) than the previously accepted value. From electron impact threshold measurements, the ionization potential of BF_2 was evaluated as 8.84 ± 0.10 eV. The results show the FB–F bond to be 70 kcal weaker than the B–F bond, and 59 kcal weaker than F_2B–F in the BF_3 bond dissociation sequence. Implications of the results on the chemical bonding in the B–F system and comparison with a theoretical treatment of BF_2 are discussed briefly.

INTRODUCTION

The spectroscopic and thermochemical parameters of many small inorganic radicals are not well established, primarily because these radicals are relatively minor species under the usual experimental conditions and are therefore not easily identified and characterized. This is particularly true of odd-electron species such as BF_2. Although BF and BF_3 are major species in the high temperature chemistry of the B–F system and were easily observable in beams generated by the fluorination of elemental boron with CaF_2 at elevated temperatures, there was no positive evidence for the presence of BF_2.[1] Subsequently, Srivastava and Farber[2] reported the results of a mass spectrometric study of the reaction of $B(s)$ with $BF_3(g)$ that led to the identification of $BF_2(g)$ and to the derived enthalpy of formation $\Delta_f H^\circ_{298}(BF_2, g) = -141.0 \pm 3$ kcal/mol, as evaluated in the more recent JANAF Thermochemical Tables.[3] This latter observation[2,3] seemed at odds with our earlier work on the B–Ca–F system[1] since it indicated that at 1700 K the equilibrium constant K_{eq} for the reaction

$$BF_3(g) + BF(g) = 2\ BF_2(g) \qquad (1)$$

should be about 0.7, and that BF_2 should have been clearly observable.

Since the sensitivity and degree of sophistication of the mass spectrometric technique have increased appreciably over the last decade, it seemed worthwhile to re-examine the B–F system for additional information about the stability of BF_2. Small molecules of this type are becoming increasingly susceptible to detailed *ab initio* molecular orbital calculations and it is advantageous to have accurate experimental data, particularly energy quantities, available for comparison. Energy quantities calculated by *ab initio* methods tend to be unreliable because of difficulty in accounting for the electron correlation energy, i.e., the energy associated with the interactions among all the electrons in the molecule. From a comparison of calculated results with experimental quantities such as bond dissociation energies and ionization energies, it is possible to evaluate systematic trends in the correlation energy and to develop improved methods of estimating the correlation correction, thereby increasing the usefulness of the theoretical calculations. Such a comparison of calculated and experimental results for BF_2 is given later in this paper. Also, of course, there is the very real need for accurate molecular properties in technological applications such as development of corrosion-resistant materials, chemical vapor deposition of electronic materials, nuclear fuel processing, and chemical propulsion.

Aside from the equilibrium studies,[2] the only other direct information about BF_2 comes from ESR studies of the radical species generated by irradiation of BF_3 trapped in xenon matrices at liquid helium temperatures.[4] We report here the results of new mass spectrometric studies of gaseous equilibria in the B–F system and the implications of these results on the thermochemical properties of the BF_2 radical.

EXPERIMENTAL

Molecular effusion beams containing the species of interest were generated by admitting $BF_3(g)$ or $SF_6(g)$ to the base of a molybdenum cell containing granules of elemental boron. For studies of the B–Ca–F system, powdered $CaF_2(s)$ was mixed with the boron. A thin partition containing several 0.3 mm diameter apertures was placed midway between the solid sample and the 1.5 mm diameter beam exit orifice to increase the number of reactive gas–solid collisions and to promote equilibration. The composition of the beam emerging from the effusion orifice was monitored by mass spectrometry, using the magnetic sector instrument and experimental technique described previously.[5] All signals were checked for their effusion cell origin by noting the response to displacement of the neutral beam defining slit and ascertaining that the normal sharp beam profile was obtained. Threshold ion yield curves were recorded automatically and analyzed as described earlier.[6] All other aspects of the experimental procedure, together with the method for evaluating equilibrium data from the observed ion intensities, have

[a)]Research sponsored by the Air Force Office of Scientific Research (AFSC), United States Air Force, Under Contract F 49620-78-C-0033. The United States Government is authorized to reproduce and distribute reprints for Governmental purposes notwithstanding any copyright notation hereon.

 0021-9606/80/094928-04$01.00

been discussed in earlier publications.[5]

The B(s) and $CaF_2(s)$ samples were of reagent grade purity, while the SF_6 and BF_3 were commercial compressed gas samples obtained from the Matheson Co; the latter were used without further purification.

RESULTS

The initial step in this study was to obtain conclusive information about the possible presence of molecular BF_2 in the high temperature effusion cell beam. When $BF_3(g)$ was admitted to the Mo cell containing B(s) at room temperature, a strong signal with a threshold appearance potential (A. P.) of about 16 eV appeared at m/e 49. This signal, verified by its isotopic counterpart at m/e 48, is clearly BF_2^+ formed by the dissociative ionization process $BF_3 + e - BF_2^+ + F + 2e$.[7] As the cell temperature was raised to 1600 K, a weak low-energy tail with threshold A. P. of about 9.0 eV appeared on the BF_2^+ ion yield curve; this low-energy tail also showed the proper ^{10}B–^{11}B isotopic structure, and is clearly associated with BF_2^+. With SF_6 as the reactive flow gas, an identical low-energy foot with the same threshold A. P. appeared on the BF_2^+ curve. The BF_2^+ signal measured at 13 eV responded sharply to variations in the BF_3 or SF_6 flow rates, and became immeasurably small with termination of the gas flow. In view of the foregoing evidence and the various estimates placing the ionization potential (I. P.) of BF_2 at about 9 ± 1 eV,[3,8,9] the presence of molecular BF_2 in the beam seems clearly established. By monitoring the BF_3 abundance with both parent BF_3^+ and fragment BF_2^+ ions and BF_2 with the parent ion, all measured a few volts above threshold, we estimate that the pressure ratio $[P(BF_2)/P(BF_3)] \cong 1 \times 10^{-3}$ at 1600 K, when $P(BF_3) \cong 1 \times 10^{-2}$ Torr.

The higher fluorine potential in the $SF_6(g) + B(s)$ system yielded substantially larger BF_2 signals than those in the $BF_3(g) + B(s)$ system, and this factor made it possible to determine a reasonably accurate threshold onset energy for parent BF_2^+ and to evaluate I. P. (BF_2). The BF molecule, also observed in these experiments, served as a convenient reference standard since its I. P. is known quite accurately at 11.115 ± 0.004 eV.[3] Three determinations by the extrapolated voltage difference method[6] yielded $\Delta V_0(BF^+ - BF_2^+) = 2.27 \pm 0.03$ eV and I. P. (BF_2) = 11.11 − 2.27 = 8.84 ± 0.10 eV.

In preliminary experiments at 1635 K, evaluation of the BF and BF_2 partial pressures from the parent ion intensities and that of BF_3 from the BF_2^+ fragment and BF_3^+ parent intensities gave an approximate pressure ratio $BF/BF_2/BF_3 = 100/1/380$ and an equilibrium constant of about 3×10^{-5} for Reaction (1), more than four orders of magnitude lower than that reported by Srivastava and Farber.[2] An accurate evaluation of the BF_3 partial pressure cannot be made from parent BF_3^+ alone, since A. P. (BF_2^+/BF_3) ≅ I. P. (BF_2) and $[I(BF_2^+)/I(BF_3^+)] \cong 10$ for BF_3 in the threshold region. A third law calculation with thermodynamic functions from the JANAF Tables[3] indicates $\Delta H_{298}^\circ(1) \cong 50$ kcal/mol and $\Delta_f H_{298}^\circ(BF_2, g) \cong -124 \pm 3$ kcal/mol. Because of the large BF_3 ion source background signal, it proved difficult to make the type of precise BF_3 beam intensity measurements needed for accurate second law analysis. Therefore, studies of Reaction (1) were not pursued further.

TABLE I. Threshold appearance potentials and neutral precursors of ions in the B–Ca–F system.

Ion	A. P. (eV)	Neutral	Literature
B^+	9 ± 1	B	8.30[b]
BF^+	11.3 ± 0.3	BF	11.115[c]
BF_2^+	15.7 ± 0.5	BF_3	15.81,[d] 15.92[e]
	9.0 ± 0.5	BF_2	
	8.84 ± 0.10[a]	B	
BF_3^+	15.5 ± 0.5	B_2	15.55[d]
Ca^+	6.0 ± 0.3	Ca	6.11[b]
CaF^+	5.5 ± 0.3	CaF	6.0[b]

[a]Extrapolated voltage difference method; all others are the vanishing current method.
[b]Reference 7.
[c]Reference 15.
[d]Reference 9.
[e]Reference 10.

On heating the cell to about 2000 K, a weak B^+ parent signal was observed, along with those of BF^+ and BF_2^+. A few measurements with low energy electrons using SF_6 as the flow gas led to an equilibrium constant of about 9×10^6 for the reaction

$$B(g) + BF_2(g) = 2BF(g) \qquad (2)$$

at 1987 K, independent of SF_6 flow rate. This result leads to the third law heat $\Delta H_{298}^\circ(2) \cong -65$ kcal/mol and $\Delta_f H_{298}^\circ(BF_2, g) \cong -123 \pm 5$ kcal/mol, compatible with the data derived from studies of Reaction (1). However, the weak B^+ signal proved to be somewhat erratic and unsuitable for reliable second law studies.

When powdered $CaF_2(s)$ was mixed with the B(s) in the sample chamber, gaseous Ca and CaF were observed in the effusion beam along with the boron species BF_2 and BF. The threshold appearance potentials identifying these species are summarized in Table I. From a series of ion intensity measurements over the range 1640 to 1800 K, equilibrium data for the reaction

$$BF(g) + CaF(g) = BF_2(g) + Ca(g) \qquad (3)$$

were obtained with both BF_3 and SF_6 as reactive gases; the results are given in Tables II and III. Reaction equilibrium constants, estimated to be accurate within a factor of 2, were evaluated directly from the observed ion intensity ratios without further correction, as described previously.[5] In these measurements, the temperature was varied randomly rather than the increasing order shown in Tables II and III. Special attention was devoted to obtaining accurate second law data by repeating most of the intensity measurements made at a given temperature.

The two Series A points at 1683 K, made with different BF_3 flow rates, provide a good check on the mass action criterion for attainment of equilibrium; the B–F

TABLE II. Equilibrium thermochemical data for the reaction[a] $BF(g) + CaF(g) = BF_2(g) + Ca(g)$.

T(K)	$I(BF^+)$	$I(BF_2^+)$	$I(Ca^+)$	$I(CaF^+)$	$K_{eq} \times 10^4$	ΔH°_{298} (kcal/mol)
Series A, BF_3 flow, A. P. + 5 eV						
1646	11.5	0.066	0.189	4.14	2.62	16.2
1646	11.4	0.060	0.174	3.45	2.65	16.2
1654	16.0	0.087	0.228	4.62	2.69	16.2
1654	15.7	0.087	0.219	4.50	2.70	16.2
1671	17.3	0.093	0.405	7.35	2.97	16.0
1683	21.2	0.177	0.156	3.99	3.26	15.9
1683	16.0	0.066	0.393	6.54	2.52	16.7
1701	30.0	0.159	1.14	18.5	3.27	16.0
1701	30.0	0.153	1.14	18.2	3.19	16.1
1730	53.2	0.171	5.58	52.5	3.41	16.2
1730	47.6	0.189	3.69	40.5	3.62	16.0
1730	41.6	0.156	3.21	34.5	3.50	16.1
1736	42.4	0.126	0.261	2.19	3.55	16.1
1737	29.2	0.069	0.453	2.94	3.65	16.0
1737	29.2	0.069	0.411	2.73	3.56	16.1
1783	98.4	0.303	18.9	149.0	3.91	16.2
1783	116.8	0.309	22.9	166.0	3.65	16.4
1785	118.8	0.420	15.3	136.0	3.98	16.1
1785	107.2	0.420	13.9	134.0	4.06	16.1
1814	154.8	0.558	1.0	8.9	4.05	16.4
					Av.	ΔH°_{298}(III) = 16.2
						ΔH°_{298}(II) = 15.8 ± 1.4

[a]Intensities in arbitrary units.

and Ca–F signals respond in opposite fashion to variations in BF_3 flow, yet the derived values of K_{eq} are in reasonable agreement with each other. Additionally, it can be seen from the data points at 1736, 1737, and 1814 K in Table II, the final points of that series taken, that rapid depletion of the CaF_2 sample caused a sharp drop in the Ca^+ and CaF^+ signals; yet the derived gaseous equilibrium data are entirely consistent throughout, still further proof of equilibrium attainment. Moreover,

TABLE III. Equilibrium thermochemical data for the reaction[a] $BF(g) + CaF(g) = BF_2(g) + Ca(g)$.

T(K)	$I(BF^+)$	$I(BF_2^+)$	$I(Ca^+)$	$I(CaF^+)$	$K_{eq} \times 10^4$	ΔH°_{298} (kcal/mol)
Series B, BF_3 flow, A. P. + 4 eV						
1615	35.2	0.111	0.396	5.55	2.25	16.4
1615	33.6	0.120	0.291	4.50	2.31	16.3
1668	47.2	0.165	0.77	10.2	2.64	16.5
1668	47.6	0.192	0.65	10.2	2.57	16.5
1696	80.4	0.279	3.12	38.4	2.82	16.5
					Av.	ΔH°_{298}(III) = 16.4
Series C, SF_6 flow, A. P. + 4 eV						
1652	42.4	0.222	0.315	5.52	2.98	15.8
1659	16.6	0.063	0.036	0.501	2.73	16.2
1659	17.0	0.066	0.036	0.492	2.83	16.1
1695	27.5	0.105	0.168	1.98	3.25	16.0
					Av.	ΔH°_{298}(II) = 16.0

[a]Intensities in arbitrary units.

TABLE IV. Summary of reactions yielding thermochemical data for $BF_2(g)$.

Reaction	ΔH_T (kcal/mol)	$\Delta_f H^\circ_{298}(BF_2)$ (kcal/mol)	Reference
$BF_3(g) + BF(g) = 2BF_2(g)$	17.1 ± 1[d]	−141.0 ± 3	a
	60 ± 3[d]	−124 ± 5	This work
$B(g) + BF_2(g) = 2BF(g)$	−65 ± 2[d]	−123 ± 5	This work
$BF(g) + CaF(g) = BF_2(g) + Ca(g)$	16.2 ± 2[d]	−119.3 ± 4	This work
$BF_2 + h\nu \rightarrow BF_2^+ + F + e$	364.6[e]	−128 ± 6	b
	367.1[e]	−126 ± 6	c

[a]Reference 2.
[b]Reference 9.
[c]Reference 10.
[d]T = 298 K.
[e]T = 0 K.

a few measurements obtained with SF_6 as the reactive gas, shown in Table III, yielded equilibrium data in good agreement with the BF_3 results. Therefore, it can be safely concluded from these various bits of evidence that gaseous equilibrium was attained in the beam source. Although the most extensive series of measurements was made with 5 eV excess ionizing energy (A. P. + 5 eV), a second series made at A. P. + 4 eV gave essentially the same values of K_{eq}, lending further confidence in the results.

A third law (III) treatment of the equilibrium data was made using thermodynamic functions from the JANAF Tables.[3] The spectroscopic constants of BF, Ca, and CaF are all well established, while those of BF_2 are based on the structure inferred from the matrix ESR studies of Nelson and Gordy,[4] together with estimated vibrational frequencies and parameters for the electronic states; uncertainties in the third law enthalpies from this source should not exceed about 0.8 kcal/mol. The most extensive set of data (Series A), led to the average value ΔH°_{298} (3, III) = 16.2 ± kcal/mol compared to the corresponding second law (II) result ΔH°_{298} (3, II) = 15.8 ± 1.4 kcal/mol. Analysis of the less extensive Series B and C data yielded ΔH°_{298} (3, III) = 16.4 and 16.0 kcal/mol, respectively, both ± 2 kcal/mol. From the agreement between second and third law results, it can be concluded that the equilibrium data contain no serious systematic errors. We select ΔH°_{298} (3) = 16.0 ± 2 kcal/mol as "best value" from the studies reported here, which leads to the standard enthalpy of formation $\Delta_f H^\circ_{298}(BF_2, g) = -120.0 \pm 4.0$ kcal/mol.

DISCUSSION

A summary of the reaction thermochemistry leading to derivation of the standard enthalpy of formation of $BF_2(g)$ is given in Table IV. Included are two values obtained from the threshold energetics of BF_2^+ production by photodissociative ionization of BF_3. Agreement among the various values of $\Delta_f H^\circ_{298}(BF_2, g)$ reported here is reasonably good, considering the combined uncertainties, and lends strong support to the selected value of −120.0 ± 4.0 kcal/mol based largely on the studies of Reaction (3). Surprisingly, our new result for BF_2 differs by more than 20 kcal/mol from the selected JANAF Table value $\Delta_f H^\circ_{298}(BF_2, g) = -141 \pm 3$ kcal/mol.[3]

The JANAF data for BF_2 are based solely on third law analysis of the thermochemical studies of Reaction (1) reported by Srivastava and Farber[2]; these latter studies yielded an approximate $BF/BF_2/BF_3$ partial pressure ratio of 1.2/1/1.2 at 1650 K, compared to 100/1/380 inferred in this work for similar conditions. If the BF_3 pressure was monitored with the BF_3^+ parent ion as indicated in the earlier work,[2] then K_{eq} for Reaction (1) would be overestimated by a factor of 10, but this effect can account for only a small part of the difference. Our observed pressure ratios and the approximate value $K_{eq} \cong 3 \times 10^{-6}$ for Reaction (1) at 1635 K are, however, consistent with the failure to observe BF_2 in earlier studies of the B–Ca–F system,[1] since the BF_2^+ parent intensity would have been a factor of 100 lower than that of the BF_2^+/BF_3 fragment in those experiments and just at the detection limit. We conclude that the partial pressure and thermodynamic stability of BF_2 were grossly overestimated in the experiments of Srivastava and Farber.[2]

With the new thermochemical data for BF_2 in hand, one evaluates the bond dissociation energy sequence in BF_3 as follows: $D_0^\circ(F_2B-F) = 169$ kcal/mol; $D_0^\circ(FB-F) = 110$ kcal/mol; and $D_0^\circ(B-F) = 180$ kcal/mol. In these calculations, the enthalpy of sublimation of boron at 298 K is taken to be 135.0 kcal/mol.[11] The alternation in bond dissociation energies in the B–F system is indeed dramatic, showing the bond FB–F to be exceptionally weak compared to the other two relatively strong bonds. Such an alternation could be rationalized here in terms of the excited valence state concept of bonding, since a major valence excitation of the central boron atom would be required on passing from the monovalent s^2p ground state in BF to the trivalent sp^2 hybrid configuration in BF_3 and BF_2. Indeed, the 112° F–B–F bond angle[4] in BF_2 is not greatly different from the 120° angle in planar symmetric BF_3, indicating that the full valence excitation to the trivalent hybrid configuration occurs with formation of the FB–F bond rather than formation of a linear sp hybrid in BF_2. The latter would require further excitation to sp^2 on addition of the third F-atom ligand. This $s^2p \rightarrow sp^2$ promotional energy must then be supplied at the expense of the second bond making $D(B-F) > D(FB-F) < D(F_2B-F)$. Skinner and Pritchard[12] have calculated the energy of the sp^2 valence state of boron to lie about 127 kcal above the ground s^2p state, substantially higher than the difference $[D(B-F) - D(FB-F)] = 70$ kcal. However, an exact description of the valence state in terms of known atomic orbitals cannot be made, and it may be that inclusion of some ground state character may depress the calculated energies, as suggested by Voge[13] for the sp^3 valence state of carbon. In any event, the observed bond energy sequence is in qualitative accord with the valence state concept, since the latter predicts a relatively large difference between $D(FB-F)$ and $D(B-F)$. This difference is perhaps larger than can be accounted for by other models such as an electrostatic bonding model, unless there were substantial changes in B–F bond length with the number of fluorine ligands.

The *ab initio* calculations of Thomson and Brotchie[14] indicate a BF_2 atomization energy of 193 kcal/mol and an ionization potential of about 11.2 eV. Lack of a correlation energy correction no doubt is the reason why the former falls far short of the experimental value of 290 kcal/mol. Likewise, the calculated I.P. evaluated from the difference between calculated total energies of BF_2 and BF_2^+ is too high because of correlation energy differences between the neutral and the ion. Similar calculations[14] on NF_2 gave an I.P. that was 3.4 eV higher than the experimental value. Since our newly determined value I.P.$(BF_2) = 8.84$ eV is close to the I.P. of atomic boron (8.30 eV), it appears that the electron ejected in the ionization of BF_2 comes from a nonbonding p orbital located primarily on the boron atom.

Finally, it is worth emphasizing the large difference between the newly determined value $\Delta_f H_{298}^\circ(BF_2) = -120.0 \pm 4$ kcal/mol and the previously accepted value[3] -141.0 ± 3 kcal/mol which was based on only one experimental determination.[2] This points up clearly the difficulty faced by critical data compilers in evaluating experimental data and attaching uncertainties. Because the stepwise bond dissociation energies in a polyhalide molecule can vary widely and there are no quantitative theoretical guidelines, there is no satisfactory way to judge just how reliable or "reasonable" a single experimental determination may be. Often, it is only when several independent determinations, preferably by different yet reliable experimental techniques, begin to bracket a quantity that the critical evaluator can truly begin to select most probable values and to set meaningful uncertainty limits. In many respects, experimental methods for evaluating the properties of radicals and related minor species are still in a relatively primitive state. Since advances in bonding theory and many technological applications are dependent on the availability of accurate molecular property data, it is important that these methods be continually upgraded and extended.

[1] D. L. Hildenbrand and E. Murad, J. Chem. Phys. 43, 1400 (1965).
[2] R. D. Srivastava and M. Farber, Trans. Faraday Soc. 67, 2298 (1971).
[3] JANAF Thermochemical Tables, Natl. Stand. Ref. Data Ser. Natl. Bur. Stand. 37 (1971); J. Phys. Chem. Ref. Data 3, 311 (1974).
[4] W. Nelson and W. Gordy, J. Chem. Phys. 51, 4710 (1969).
[5] D. L. Hildenbrand, J. Chem. Phys. 48, 3657 (1968); 52, 5751 (1970).
[6] D. L. Hildenbrand, Int. J. Mass Spectrom. Ion Phys. 4, 75 (1970); 7, 255 (1971).
[7] H. M. Rosenstock, K. Draxl, B. W. Steiner, and J. T. Herron, J. Phys. Chem. Ref. Data 6, Suppl. 1 (1977).
[8] W. C. Steele, L. D. Nichols, and F. G. A. Stone, J. Am. Chem. Soc. 84, 1154 (1962).
[9] V. H. Dibeler and S. K. Liston, Inorg. Chem. 7, 1742 (1968).
[10] C. F. Batten, J. A. Taylor, B. P. Tsai, and G. G. Meisels, J. Chem. Phys. 69, 2547 (1978).
[11] The recent studies of E. Storms and B. Mueller, J. Phys. Chem. 81, 318 (1977) indicate that the JANAF Table[3] value for the enthalpy of sublimation of boron at 298 K of 132.8 kcal/mol is several kcal/mol too low.
[12] H. A. Skinner and H. O. Pritchard, Trans. Faraday Soc. 49, 1254 (1953).
[13] H. H. Voge, J. Chem. Phys. 4, 581 (1936); 16, 984 (1948).
[14] C. Thomson and D. A. Brotchie, Chem. Phys. Lett. 16, 573 (1972).
[15] R. B. Caton and A. E. Douglas, Can. J. Phys. 48, 432 (1970).

Thermochemistry of the gaseous fluorides of samarium, europium, and thulium[a)]

P. D. Kleinschmidt, K. H. Lau, and D. L. Hildenbrand

SRI International, Menlo Park, California 94025
(Received 3 December 1979; accepted 17 September 1980)

The gaseous mono-, di-, and trifluorides of the lanthanide metals samarium, europium, and thulium were characterized thermochemically from high temperature equilibrium studies carried out by mass spectrometry. Reaction enthalpies and entropies were derived using second-law analysis throughout, and the results were used to evaluate the enthalpies of formation and bond dissociation energies (BDE) of the gaseous fluorides, and to obtain approximate values for the electronic entropies of the MF and MF_3 species. The dissociation energies of the monofluorides $D_0^\circ(SmF) = 134$ kcal/mole, $D_0^\circ(EuF) = 129$ kcal/mole, and $D_0^\circ(TmF) = 121$ kcal/mole, all ± 2 kcal/mole, are in good agreement with values predicted by the Rittner electrostatic model, whereas values in the polyatomic fluorides show considerable variation and do not seem to follow any clear trends. Although the BDE values in some instances differ from previous estimates, their sums yield trifluoride heats of atomization that are in close accord with values derived from the vaporization thermodynamics of the solid trifluorides.

INTRODUCTION

Despite substantial experimental work, and an extensive literature on the subject, the thermochemical properties of the gaseous fluorides of the 14 lanthanide metals lying between Ce and Lu have been only partially characterized, and in no instance is there sufficient information for detailed calculations of chemical equilibria among the MF, MF_2, and MF_3 species. As summarized in a review paper by Zmbov and Margrave,[1] based on their own collective studies, gaseous equilibrium measurements have been made on systems involving the monofluorides of Nd, Sm, Eu, Gd, Dy, Ho, and Er, and the difluorides and trifluorides of Nd, Gd, Ho, and Er. The results have been used to derive the standard enthalpies of formation and bond dissociation energies (BDE) of these species. Lower bounds to the dissociation energies of SmF and EuF also have been evaluated from beam–gas chemiluminescent reaction studies,[2,3] leading to results consistent with the equilibrium data. Zmbov and Margrave[1] considered the properties of the lanthanide series as a whole, and estimated the bond dissociation energies of those species not determined experimentally. Trends in the available data indicated the BDE sequence $D(F_2M\text{-}F) > D(FM\text{-}F) \geq D(MF)$, and this pattern was assumed to apply throughout the series.

As will be noted later, there is also a substantial amount of information on the vibrational spectra and structures of the lanthanide fluorides that can be used to evaluate the rotational and vibrational contributions to the thermodynamic functions. However, little is known about the configurations and energies of the low-lying electronic states, except that these are expected to contribute significantly to the total thermodynamic functions of many of the M–F species. It is this uncertainty over the magnitudes of the electronic contributions, together with uncertainties in the estimated BDE values, that precludes the calculation of reliable Gibbs energies and equilibrium data.

The objective of the work described here was to obtain a reasonably complete set of thermochemical data for several of the lanthanide fluoride systems so that trends in these properties could be established accurately, and the validity of certain predictive models could be examined. Although the experimental technique employed was to be the familiar one of high temperature mass spectrometry, a major goal of the work was to determine not only reaction enthalpies and BDE values, but also reaction entropies and, if possible, gross information about the molecular constant assignments (particularly the electronic contributions) of the gaseous species. This necessitated extensive second-law measurements, i.e., measurement of equilibrium constants over wide temperature ranges, relatively free from systematic errors. The fluoride systems chosen for study were those of samarium, europium, and thulium. Experimental BDE values are available only for SmF and EuF[2–4]; the difluorides and trifluorides were not studied in Zmbov and Margrave's investigation[4] of the Sm–F and Eu–F systems, and no BDE data have been reported for the Tm–F system. New thermochemical data on these systems will provide an opportunity to check the accuracy of the earlier estimates, and to examine the possible fine structure in the periodic properties of the lanthanide fluorides.

EXPERIMENTAL

All of the measurements reported here were made with the magnetic-deflection mass spectrometer system described previously.[5] This is a 30.5 cm, 60° sector single-focusing instrument equipped with a heated effusion-beam source, and an electron-impact ion source. Both ion pulse counting and conventional electrometer techniques were used for ion detection in various phases of the work, but no distinction is made in reporting the results since the two methods are equivalent. Ionization efficiency curves were recorded automatically using an X–Y plotter arrangement.[6] Continuous recording of the ion yield curves proved to be es-

[a)]Research sponsored by the Air Force Office of Scientific Research (AFSC), United States Air Force, under Contract F 49620-78-C-0033. The United States Government is authorized to reproduce and distribute reprints for Governmental purposes notwithstanding any copyright notation hereon.

 0021-9606/81/010853-08$01.00

TABLE I. Beam sources for generation of gaseous lanthanide fluorides.

Beam source	Cell type	Cell material	Range (K)	Gaseous species
A (SmF_3, CaF_2) + B	Two-stage	Molybdenum	1730–1912	Sm, SmF, Ca, CaF
B CaF_2 + Sm_2O_3	Two-stage	Molybdenum	2136–2334	Sm, SmF, Ca, CaF
C SmF_3, CaF_2, B	One-stage	Graphite	1448–1643	SmF, SmF_2, Ca, CaF
D SmF_3, Zr	One-stage	Graphite	1532–1673	SmF, SmF_2, SmF_3
E SmF_3	One-stage	Platinum	1400–1500	SmF_3
F (EuF_3, CaF_2) + B	Two-stage	Molybdenum	1618–1785	Eu, EuF, EuF_2, Ca, CaF
G CaF_2 + Eu_2O_3	Two-stage	Molybdenum	1878–2014	Eu, EuF, EuF_2, Ca, CaF
H EuF_3, Zr	One-stage	Molybdenum	1330–1470	Eu, EuF, EuF_2
I $WF_6(g)$ + (EuF_3, W)	Gas-inlet	Graphite	1443–1626	EuF_2, EuF_3, WF_4, WF_5
J EuF_3	One-stage	Platinum	1250–1350	EuF_2, EuF_3
K TmF_3, CaF_2, B	One-stage	Graphite	1440–1560	Tm, TmF, TmF_2, TmF_3, Ca, CaF
L (TmF_3, CaF_2) + B	Two-stage	Graphite	1800–1950	Tm, TmF, TmF_2, Ca, CaF
M TmF_3	One-stage	Platinum	1200–1400	TmF_3

pecially advantageous in this work because of the need to distinguish clearly between the parent and fragment contributions to the MF^+ and MF_2^+ ion signals.

It was necessary to use a wide variety of chemical beam sources to observe and study all the gaseous metal fluoride species of interest. As will become apparent in the ensuing discussion, the stabilities of the three metal fluoride systems differed substantially, and each system required unique chemical conditions to maximize the abundances of the particular species to be studied. The beam sources included simple vaporization of the solid trifluorides from platium cells, single stage cells containing a mixture of reactive solids, two stage cells in which material vaporized from a low temperature chamber interacted with a condensed phase at higher temperature, and gas inlet cells in which species were generated by interaction of the added gas with the condensed phase or phases present. A brief description of the essential features of the various effusion beam sources is given in Table I. The main effusion chamber was of the standard 1.27 cm diameter, 2.15 cm length design with 0.15 cm diameter orifice, and was heated by radiation from a tungsten spiral resistance element.[5]

With the complex sources, a central partition containing several small holes was added to increase the number of reactive gas–solid collisions. In each instance, effusion cell temperatures were measured by optical pyrometry, using a black-body cavity in the lid with length-to-diameter ratio greater than 6. Tests for the attainment of chemical equilibrium were made by applying the mass action criterion or by approaching equilibrium from different chemical compositions.[7,11] It was often necessary to experiment with a number of beam source reactions before a suitable one could be found. This was particularly true for studies of the gaseous trifluorides in the presence of the difluorides, complicated by the fact that the trifluorides do not yield stable parent positive ions and must be monitored through the fragment MF_2^+ ions. Because of this limitation, parent and fragment contributions to MF_2^+ can be unfolded accurately only when the low energy parent contribution is small compared to the fragment contribution. Whenever MF_2 and MF_3 were to be measured simultaneously, it was necessary, therefore, to choose conditions such that $P(MF_3) \gg P(MF_2)$.

Following customary practice, the response of each ion signal to displacement of the neutral beam defining slit was checked to ascertain the effusion cell origin. This slit test eliminated any noneffusion cell background contributions, although the latter were generally negligible. Once the effusion beam composition was established, reaction equilibrium constants were evaluated from ion abundance ratios, each signal measured at a small constant increment (3 to 5 eV) above the ionization threshold. By using low energy ionizing electrons and working close to threshold, it was possible to greatly simplify the mass spectra and to obtain ion abundances that faithfully reflected the neutral abundances. Parent ion signals were used as a measure of all neutrals except the trifluorides, where the fragment MF_2^+ was used. As noted above, the correction for the parent ion contribution at energies exceeding the MF_2^+ fragmentation threshold could be made quite accurately because $P(MF_3) \gg P(MF_2)$. The ion current ratios were used without further correction to represent the equilibrium constants K for the various isomolecular reactions, following the rationale described earlier.[5] Although all thermochemical data reported here were derived from second law analysis of the equilibrium measurements, which requires only a quantity proportional to K, an attempt was made to evaluate the absolute equilibrium constants for certain third law comparisons. This necessitated a small additional correction in each system for the fragmentation of MF_2 to MF^+, as indicated by the ionization efficiency curves.

The solid lanthanide trifluorides were of reagent grade quality, 99.5%–99.9% purity, and were obtained from Alfa Division, Ventron Corp. All other materials used were of similar reagent grade purity, obtained from commercial suppliers.

RESULTS

Gaseous effusion-beam species generated with the various beam sources were identified from the masses, threshold appearance potential (A.P.), and isotopic dis-

TABLE II. Threshold appearance potentials and inferred neutral precursors.

Ion	A.P. (eV)	Beam source	Neutral precursor	Literature
Sm^+	24.0 ± 0.5	*E*	SmF_3	26.0[a]
	5.5 ± 0.3	*A, B*	Sm	5.64,[b] 5.56,[f] 5.58[g]
SmF^+	17.5 ± 0.5	*E*	SmF_3	19.0[a]
	11.5 ± 1.0	*C, D*	SmF_2	···
	4.5 ± 0.3	*A, B, C, D*	SmF	5.7[c]
SmF_2^+	13.2 ± 0.3	*E*	SmF_3	13.0[a]
	7.2 ± 0.3	*C, D*	SmF_2	···
Eu^+	5.6 ± 0.3	*F, G, H*	Eu	5.67,[b] 5.61,[f] 5.68[g]
EuF^+	11.0 ± 1.0	*F, G, I*	EuF_2	···
	5.1 ± 0.3	*F, G, H*	EuF	5.9[c]
EuF_2^+	13.0 ± 0.5	*J*	EuF_3	13.5[a]
	8.2 ± 0.3	*F, G, H, I*	EuF_2	···
Tm^+	6.1 ± 0.3	*K*	Tm	6.18,[b] 5.87,[f] 6.11[g]
TmF^+	18.0 ± 0.7	*L*	TmF_3	20.8[a]
	12.0 ± 1	*K*	TmF_2	···
	5.8 ± 0.3	*K*	TmF	···
TmF_2^+	13.15 ± 0.10	*L*	TmF_3	13.5[a]
	6.96 ± 0.10	*K*	TmF_2	···
Ca^+	6.0 ± 0.3	*A, B, C, F, G, K*	Ca	6.11[d]
CaF^+	5.5 ± 0.3	*A, B, C, F, G, K*	CaF	6.0[d]
WF_4^+	10.0 ± 0.3	*I*	WF_4	9.89[e]
WF_5^+	10.0 ± 0.3	*I*	WF_5	10.03[e]

[a]Reference 1.
[b]Reference 8.
[c]Reference 2.
[d]Reference 9.
[e]Reference 10.
[f]Reference 30.
[g]Reference 31.

tribution of the ions formed from electron impact ionization of the beam. Observed threshold A.P.'s, the quantities of primary importance in this identification process, are summarized in Table II, together with pertinent beam source conditions and the neutral precursors inferred from these data. Ionization thresholds were evaluated by the vanishing current method, using the various metal atom signals and background mercury to calibrate the energy scale. Identification of the lanthanide monofluorides and difluorides is unambiguous, in view of the magnitudes of the lowest threshold energies associated with the corresponding ion signals. As noted by Zmbov and Margrave,[1] the ionization energies of the MF species are close to or lower than those of the metal atoms, indicating that the ionizing orbitals are largely nonbonding or antibonding. The ionization energies of the MF_2 species are 1 to 3 eV higher than those of the monofluorides, but are clearly on the order of the values expected for the difluorides.

Since no trifluoride parent ions were observed, it was necessary to establish the characteristic threshold appearance potentials of the fragment ion species in separate experiments by vaporizing the solid trifluorides from platinum effusion cells. The A.P.'s of the major MF_2^+ fragment ions along with values for some of the other fragment ions are listed in Table II. The possibility of deriving (F_2M-F) bond strengths from the MF_2^+ fragment A.P.'s was explored, but the presence of very small amounts of gaseous EuF_2 and SmF_2 in the platinum cell beams yielded weak tails on the ion yield curves that precluded such an approach in those instances. The difluoride tail was just perceptible for SmF_2^+, and moderately strong for EuF_2^+. Even in the latter case, however, it is estimated that $[P(EuF_3)/P(EuF_2)] > 50$. For TmF_3 it was possible to derive $D_0(F_2Tm-F) \leq 13.15 - 6.96 = 6.19$ eV = 142.7 kcal/mol, and $D_{298}(F_2Tm-F) = 143.3$ kcal/mol. By monitoring the EuF_2^+ and SmF_2^+ fragment ions over a range of temperatures, approximate values of 93.8 and 91.7 kcal/mol were derived for the enthalpies of sublimation of EuF_3 and SmF_3 at 1300 and 1400 K, respectively.

In the ensuing thermochemical studies, equilibrium data were derived from ion intensities measured at low ionizing energies to minimize dissociative ionization, as noted earlier. For use in third law calculations, it was necessary to account for the difluoride fragmentation process $MF_2 + e - MF^+ + F + 2e$, as indicated by the ionization efficiency curves of SmF^+, EuF^+, and TmF^+. At low ionizing energies, the difluoride parent and MF^+ fragment intensities are about comparable. This does not complicate the parent MF^+ measurement, however, since the fragment MF^+ has a higher threshold energy, as seen in Table II.

Sm-F system

The reaction equilibrium

$$Sm(g) + CaF(g) = SmF(g) + Ca(g) \quad (1)$$

was studied over the range 1730 to 1912 K with beams generated by the reaction of gaseous SmF_3 and CaF_2 with $B(s)$, and from 2136 to 2334 K by the reaction of $CaF_2(g)$ with $Sm_2O_3(s)$. The two sets of results were internally consistent, and were combined to yield the least-squares expression for the equilibrium constant K:

$$\log K_1 = -(0.398 \pm 0.068) + (1800 \pm 127)/T .$$

By heating a mixture of $SmF_3(s)$, $CaF_2(s)$, and $B(s)$ in a graphite cell, it was possible to study the equilibrium

$$SmF(g) + CaF(g) = SmF_2(g) + Ca(g) \quad (2)$$

over the range 1448 to 1643 K and to derive the relation

$$\log K_2 = -(1.171 \pm 0.188) + (1449 \pm 291)/T$$

from the results. Likewise, vaporization of a mixture of $SmF_3(s)$ and $Zr(s)$ produced sufficient partial pressures of the pertinent species for study of the reaction

$$SmF(g) + SmF_3(g) = 2\,SmF_2(g) \quad (3)$$

at 1532 to 1673 K, yielding the results

$$\log K_3 = (1.016 \pm 0.085) - (634 \pm 135)/T .$$

In these latter experiments, the partial pressure of SmF_3 exceeded that of SmF_2 by a factor of about 5 or more.

Eu-F system

Two separate studies of the reaction equilibrium

$$Eu(g) + CaF(g) = EuF(g) + Ca(g) \quad (4)$$

were carried out; these were not combined for second law analysis, since the two studies were done about a

TABLE III. Equilibrium data for the reaction $Sm(g) + CaF(g) = SmF(g) + Ca(g)$.

T (K)	K_1	T (K)	K_1
1729	4.19	1844	3.54
1735	3.99	1857	4.11
1746	3.93	1857	3.93
1748	4.92	1861	3.26
1767	4.45	1876	3.46
1768	4.08	1912	3.46
1771	4.40	2136	2.85
1775	4.43	2172	2.41
1784	4.72	2177	2.53
1795	3.83	2191	2.45
1798	3.92	2204	2.91
1812	3.89	2218	2.68
1812	3.71	2258	2.38
1818	4.46	2301	2.52
1827	3.46	2334	2.58

year apart and utilized slightly different ionizing energies and ion source conditions. Data obtained by reaction of $CaF_2(g)$ with $Eu_2O_3(s)$ at 1878 to 2014 K yielded

$$\log K_4 = (0.007 \pm 0.256) + (584 \pm 409)/T \ ,$$

while studies with a beam generated by passing $CaF_2(g)$ and $EuF_3(g)$ over $B(s)$ at 1618 to 1785 K gave

$$\log K_4 = -(0.215 \pm 0.118) + (776 \pm 199)/T \ .$$

The difluoride EuF_2 was also observed with the $CaF_2(g) + Eu_2O_3(s)$ source, and the equilibrium

$$EuF(g) + CaF(g) = EuF_2(g) + Ca(g) \qquad (5)$$

was investigated over the range 1824 to 2014 K, with the resulting expression for the equilibrium constants

$$\log K_5 = -(1.132 \pm 0.190) + (537 \pm 365)/T \ .$$

It proved quite difficult to devise a suitable beam source for studies of equilibria involving $EuF_3(g)$ in the presence of other reference species. After observing both gaseous EuF_2 and EuF_3 in the vapor effusing from platinum and graphite cells containing $EuF_3(s)$, it was possible to study the equilibrium

$$EuF_3(g) + WF_4(g) = EuF_2(g) + WF_5(g) \qquad (6)$$

over the range 1443 to 1626 K by adding a coil of tungsten wire to the cell. In order to stabilize the tungsten fluoride species, it was necessary to maintain a weak flow

TABLE IV. Equilibrium data for the reaction $SmF(g) + CaF(g) = SmF_2(g) + Ca(g)$.

T (K)	K_2	T (K)	K_2
1448	0.602	1562	0.562
1450	0.630	1564	0.554
1480	0.663	1581	0.639
1480	0.760	1582	0.569
1514	0.655	1595	0.531
1514	0.622	1595	0.545
1521	0.638	1613	0.521
1541	0.559	1613	0.507
1541	0.583	1637	0.503
1562	0.501	1643	0.542

TABLE V. Equilibrium data for the reaction $SmF(g) + SmF_3(g) = 2\ SmF_2(g)$.

T (K)	K_3	T (K)	K_3
1532	3.98	1600	4.34
1532	4.10	1625	4.21
1545	3.77	1625	4.28
1562	4.13	1650	4.28
1562	4.23	1650	4.19
1570	4.06	1652	4.19
1585	4.10	1663	4.29
1585	4.18	1663	4.37
1600	4.13	1673	4.39

of $WF_6(g)$ through the cell while measurements were in progress; the derived equilibrium constants represented by the relation

$$\log K_6 = (0.625 \pm 0.092) - (2798 \pm 142)/T$$

were independent of the $WF_6(g)$ flow rate, meeting the mass action criterion for equilibrium behavior.

Tm–F system

In contrast to the variety of chemical reaction beam sources needed for the Sm–F and Eu–F systems, vaporization of a mixture of $TmF_3(s)$, $CaF_2(s)$, and $B(s)$ from a single-stage graphite cell yielded all of the gaseous species necessary for studies of the reaction equilibria

$$Tm(g) + CaF(g) = TmF(g) + Ca(g) \ , \qquad (7)$$

$$TmF(g) + CaF(g) = TmF_2(g) + Ca(g) \ , \qquad (8)$$

TABLE VI. Equilibrium data for the reactions $Eu(g) + CaF(g) = EuF(g) + Ca(g)$ and $EuF(g) + CaF(g) = EuF_2(g) + Ca(g)$.

T (K)	K_4	K_5
	Series I	
1618	1.87	
1620	1.85	
1659	1.82	
1687	1.70	
1702	1.64	
1714	1.71	
1732	1.75	
1759	1.75	
1770	1.70	
1785	1.63	
	Series II	
1824	...	0.150
1878	2.13	0.136
1878	1.97	0.138
1899	2.09	0.150
1912	2.22	0.144
1929	1.95	0.129
1935	2.15	0.147
1948	1.96	0.135
1961	1.89	0.138
1980	2.06	0.141
1993	2.01	0.142
2014	2.00	0.134

TABLE VII. Equilibrium data for the reaction $EuF_3(g) + WF_4(g) = EuF_2(g) + WF_5(g)$.

T (K)	$K_6 \times 10^2$	T (K)	$K_6 \times 10^2$
1443	4.61	1528	6.13
1461	4.93	1568	7.22
1461	5.23	1568	6.68
1489	5.76	1580	6.95
1489	5.61	1580	7.19
1499	6.14	1624	8.15
1500	5.63	1625	7.79
1528	6.37	1626	7.89

and

$$TmF(g) + TmF_3(g) = 2\,TmF_2(g) \qquad (9)$$

at 1445 to 1564 K. In order to extend the temperature range for more accurate second law analysis, Reactions (7) and (8) were studied with a two-stage source in which TmF_3 and CaF_2 vapors reacted with $B(s)$, and measurements were made over the range 1797 to 1952 K. The resulting equilibrium constant expressions were

$$\log K_7 = (0.079 \pm 0.030) - (1149 \pm 50)/T\ ,$$

$$\log K_8 = -(0.417 \pm 0.042) + (1201 \pm 68)/T\ ,$$

and

$$\log K_9 = (1.301 \pm 0.293) - (2951 \pm 441)/T\ .$$

The individual equlibrium constant data points for all reactions studied are summarized in Tables III to VIII.

Thermodynamic functions of lanthanide fluorides

For use in subsequent third law comparisons, the thermodynamic functions of the lanthanide fluoride species, exclusive of electronic contributions, were calculated from estimated spectroscopic constants. Although only limited information is available on the spectroscopy of the monofluorides and difluorides of the lanthanides, it is expected that the molecular constants will not vary appreciably across the series since the $6s^2$ outer electron configuration remains constant as the inner $4f$ orbitals are filled. Indeed, the vibrational frequencies and the internuclear distances of the few MF series members studied to date (LaF, TbF, HoF, YbF, LuF)[12,13] fall within the range $\omega_0 \cong 550 \pm 50\ cm^{-1}$ and $r_e = 2.00 \pm 0.05$ Å, and these values were selected for SmF, EuF, and TmF.

As summarized by Drake and Rosenblatt,[14] the weight of evidence favors highly bent structures for the lanthanide dihalides; an apex angle of 100° was selected for SmF_2, EuF_2, and TmF_2, with an estimated M–F internuclear distance of 2.15 Å. Based on the observed vibrational frequencies of EuF_2, SmF_2, and YbF_2,[15,16] a common assignment of 480, 110, and 460 cm^{-1} was selected for the fundamentals of the three difluorides studied here.

Similarly, evidence summarized by Drake and Rosenblatt[14] indicates the strong likelihood of pyramidal C_{3v} structures for all the lanthanide trifluorides, as indicated by earlier spectroscopic evidence.[17] Following the suggestion of Hauge, Hastie, and Margrave,[17] a constant F–M–F angle of 117° was assumed in the MF_3 species, with an estimated M–F bond distance of 2.15 Å to be consistent with values in LaF and LaF_3. A common vibrational assignment of 90, 120(2), 540(2), and 570 cm^{-1} was assumed for all three trifluorides. The rotational and vibrational parameters are similar to those of the MF_3 species estimated by Myers and Graves,[18] with the exception of their use of a symmetry number of 6.

DISCUSSION

Entropy comparisons

Before using the equilibrium data for derivation of standard enthalpies of reaction and bond dissociation energies, it is necessary to evaluate the electronic contributions to the heat capacities of the gaseous fluorides, since these are expected to be nonnegligible. The electronic energy levels of the lanthanide atoms are known, but those of the fluorides are not. One method of gauging the electronic contribution is to evaluate the total entropies of the metal fluorides from the equilibrium data $[S^\circ_T(\text{exp})]$ and then compare with the sum of the translational, rotational, and vibrational entropies $[S^\circ_T(t+r+v)]$ calculated from the molecular constants described in the preceding section. Such a comparison is shown in Table

TABLE VIII. Equilibrium data for the reactions $Tm(g) + CaF(g) = TmF(g) + Ca(g)$, $TmF(g) + CaF(g) = TmF_2(g) + Ca(g)$, and $Tm(g) + TmF_3(g) = 2\,TmF_2(g)$.

T (K)	K_7	K_8	K_9
1445	0.190	...	...
1447	0.193	2.39	0.179
1463	0.183	2.42	0.187
1463	0.196	2.57	0.187
1478	0.192	2.29	0.212
1480	0.204	2.43	0.212
1482	0.194	2.30	...
1482	0.201	2.37	...
1490	0.204	2.38	0.200
1490	0.218	2.50	0.211
1517	0.214	2.33	0.240
1518	0.218	2.39	0.246
1526	0.207	2.52	0.226
1527	0.205	2.52	0.219
1527	0.220	2.64	0.223
1548	0.223	2.26	0.266
1548	0.222	2.24	0.266
1564	0.230	2.37	6.275
1564	0.223	2.49	0.219
1797	0.244	1.80	
1836	0.262	1.67	
1836	0.270	1.89	
1865	0.287	1.73	
1865	0.293	1.70	
1879	0.286	1.67	
1879	0.293	1.74	
1909	0.298	1.54	
1909	0.306	1.52	
1926	0.332	1.51	
1926	0.324	1.58	
1952	0.314		

TABLE IX. Comparison of measured and calculated entropies.[a]

	SmF	EuF		TmF
T (K)	1930	1700	1940	1650
S_T° (exp)	80.2	77.2	79.4	78.5
S_T° ($t+r+v$)	73.4	72.3	73.5	72.3
Diff.	6.8	4.9	5.9	6.2
S_T° (M, electronic)	6.92	4.14	4.14	4.14
	SmF_2	EuF_2		TmF_2
T (K)	1550	1930		1650
S_T° (exp)	96.6	98.5		100.9
S_T° ($t+r+v$)	92.4	95.4		93.5
Diff.	4.2	2.8		7.4

[a]Units are cal/deg mol.

IX for the MF and MF_2 species. For the symmetrical monofluoride exchange reactions, we estimate that the entropies are accurate to within about 1 cal/deg mol, while those involving the difluorides are uncertain by about twice that amount due to fragmentation corrections and uncertain ionization cross section behavior.

The comparison shows that the derived experimental entropies are in all instances larger than the calculated values based solely on the translational, rotational, and vibrational contributions. Furthermore, the differences for the monofluorides are close to the electronic entropies of the gaseous metal atoms $S_T^\circ(M$, electronic). This indicates that the monofluoride bond formation process probably does not split the electronic energy levels of the metal atom appreciably, and that one might expect the electronic heat capacities of M and MF to approximately balance. For the difluoride species, the electronic contributions also appear to be significant and similar in magnitude to those of the metals. It was assumed, therefore, that the electronic heat capacity terms would compensate each other, and that to a first approximation only the translational, rotational, and vibrational terms need be considered in correcting the second law slope heats of the exchange reactions with Ca and CaF to standard reference temperature.

It is more difficult to make meaningful entropy comparisons for the trifluorides because of larger uncertainties in the magnitudes of the absolute equilibrium constants involving those species, and because of propagation of errors in the MF and MF_2 entropies. Therefore, the trifluoride reactions were treated similarly to the others, i.e., the electronic heat capacity terms were assumed to cancel. Any errors introduced by the foregoing approximations are relatively small, and the data can be modified whenever reliable information about the molecular electronic levels becomes available.

In any event, the comparison of experimental and calculated entropies in Table IX shows that, as expected, the electronic contributions to the thermodynamic functions of the Sm, Eu, and Tm fluorides are significant and that these must be accounted for in practical equilibrium calculations. Because of the complexity of the lanthanide halide spectra, however, very little information about the nature of these electronic levels has been obtained to date. Experimental entropies can therefore serve a very useful purpose in gauging the magnitudes of the electronic contributions, and this approach should be pursued vigorously in future studies.

TABLE X. Summary of reaction thermochemistry.

Gaseous reaction	T_{av} (K)	ΔH_T° (kcal/mol)	ΔH_{298}° (kcal/mol)
(1) Sm + CaF = SmF + Ca	1930	−8.2 ± 0.6	−8.2
(2) SmF + CaF = SmF_2 + Ca	1552	−6.6 ± 1.3	−7.7
(3) SmF + SmF_3 = 2 SmF_2	1604	2.9 ± 0.6	4.0
(4) Eu + CaF = EuF + Ca	1940	−2.7 ± 2.3	−2.7
	1705	−3.6 ± 0.9	−3.6
(5) EuF + CaF = EuF_2 + Ca	1929	−2.5 ± 1.7	−3.9
(6) EuF_3 + WF_4 = EuF_2 + WF_5	1536	12.8 ± 0.6	12.7
(7) Tm + CaF = TmF + Ca	1650	5.3 ± 0.2	5.3
(8) TmF + CaF = TmF_2 + Ca	1646	−5.5 ± 0.3	−6.7
(9) TmF + TmF_3 = 2 TmF_2	1509	13.5 ± 2.0	14.6

TABLE XI. Derived enthalpies of formation and bond dissociation energies.

Gaseous fluoride	$\Delta_f H_{298}^\circ$ (kcal/mol)	Bond	D_{298}° (kcal/mol)
SmF	−66.9	Sm−F	135
SmF_2	−182.7	FSm−F	135
SmF_3	−302.5	F_2Sm−F	139
EuF	−69.2	Eu−F	130
EuF_2	−181.2	FEu−F	131
EuF_3	−281.0	F_2Eu−F	119
TmF	−47.3	Tm−F	122
TmF_2	−162.1	FTm−F	134
TmF_3	−291.5	F_2Tm−F	148

Derived thermochemical data

The second law reaction enthalpies obtained from least squares fitting are summarized in Table X, along with values corrected to 298 K using heat capacity data as described in the preceding section. From the reaction enthalpies, the thermochemical properties of the calcium[19] and tungsten[10] fluoride reference species, and the properties of the gaseous lanthanide metals,[20] the standard enthalpies of formation and the bond dissociation energies of the lanthanide fluorides were derived as shown in Table XI. The reference BDE's are D_{298}°(CaF) = 127.0 kcal/mol and D_{298}°(F_4W−F) = 106.0 kcal/mol. Estimated uncertainties in the derived thermochemical quantities, considering errors from all sources, are ± 2 kcal/mol.

Of all the fluorides studied here, only for SmF and EuF have thermochemical data been reported previously. Our results lead to the dissociation energies D_0°(SmF) = 134 kcal/mol (5.81 eV), D_0°(EuF) = 129 kcal/mol (5.59 eV), and D_0°(TmF) = 121 kcal/mol (5.25 eV), all ± 2 kcal/mol. The previous thermochemical results of Zmbov and and Margrave,[1,2] D_0°(SmF) = 126 ± 4 kcal/mol and D_0°(EuF)

= 125 ± 4 kcal/mol, are somewhat lower than the values obtained here, but in fair agreement. The CL lower bounds $D_0^\circ(SmF) \geq 123.6 \pm 2.1$ kcal/mol[3] and $\geq 121.3 \pm 2.4$ kcal/mol[4] are appreciably lower than the present result, while the corresponding value $D_0^\circ(EuF) \geq 129.6 \pm 2.1$ kcal/mol[3] is quite close to our thermochemical result. Such comparison will aid the interpretation of the CL measurements, and may ultimately give a better understanding of the relationship between the CL lower bounds and the true dissociation limits.

Zmbov and Margrave's estimate $D_0^\circ(TmF) = 135 \pm 12$ kcal/mol[1] is well above our new value, but it should be remembered that the data available at that time were not sufficient for an accurate extrapolation to TmF. Similarly, their estimate of the F_2M-F bond strengths for Sm and Eu are too high by 20 and 30 kcal/mol, respectively, while the remaining values for $D(FM-F)$ and $D(F_2M-F)$ are in fair agreement. This comparison again calls attention to the difficulty in estimating reliable thermochemical data, even when a systematic approach is used.

The bond strength data in Table IX illustrate clearly that the successive BDE's do not follow a regular pattern, as presupposed in the earlier work that assumed $D(M-F) \cong D(FM-F) < D(F_2M-F)$.[1] There is evidently a pronounced fine structure in the BDE patterns, rather than a monotonic variation across the series. The detailed nature of this fine structure is, of course, yet to be determined. Although the BDE values of $D(FM-F)$ are comparable for the three metals, the observed sequence $D(F_2Eu-F) \ll D(F_2Sm-F) < D(F_2Tm-F)$ seems at first glance anomalous. However, this sequence is consistent with the known tendency of Eu, Sm, and Yb to form stable condensed difluorides, the only lanthanides to show such behavior. Kaiser *et al.*[21] have commented on this matter and on the relative ease of reduction of the SmF_3, EuF_3, and YbF_3 to the gaseous difluorides, but not with TmF_3. Additional evidence of this type comes from our observation that EuF_3, and to a very slight extent SmF_3, undergoes partial dissociative vaporization to the gaseous difluoride in inert platinum containers, while no difluoride is observed with TmF_3. The chemical importance of the divalent states of Sm and Eu is thus manifested in trends in $D(F_2M-F)$.

As a check, one can evaluate the enthalpies of formation and atomization of the gaseous trifluorides from the thermochemical properties of the solid trifluorides and the corresponding enthalpies of sublimation. Only for $SmF_3(s)$ is a direct experimental determination of $\Delta_f H_{298}^\circ$ available (-398.9 ± 1.1 kcal/mol)[22]; however, values for $EuF_3(s)$ (-385.3 kcal/mol) and $TmF_3(s)$ (-402.5 kcal/mol) have been estimated[23] from lattice energy considerations and should be sufficiently accurate for present purposes. After application of a heat content correction, the slope enthalpies of $EuF_3(g)$ and $SmF_3(g)$ determined here are converted to standard enthalpies of sublimation of 298 K of 104.0 and 100.0 kcal/mol, respectively, in agreement with values reported by Zmbov and Margrave[1]; for $TmF_3(g)$, the corresponding sublimation enthalpy of 108.0 kcal/mol at 298 K, as determined by Biefeld and Eick,[24] is adopted. These data lead to values of -298.9, -281.3, and -294.5 kcal/mol for the standard enthalpies of formation at 298 K of $SmF_3(g)$, $EuF_3(g)$, and $TmF_3(g)$, respectively, in good agreement with the values in Table XI derived from gaseous equilibrium measurements. From another perspective, the sublimation data yield for the atomization process $MF_3(g) = M(g) + 3F(g)$ the values $\Delta H_{298}^\circ = 405$, 380, and 407 kcal/mol for SmF_3, EuF_3, and TmF_3, respectively, while the individual BDE sums from the data in Table XI are 409, 380, and 404 kcal/mol. Finally, the electron impact value of 143 kcal/mol for $D_{298}^\circ(F_2Tm-F)$ noted earlier compares favorably with the equilibrium value of 148 kcal/mol. We conclude from these comparisons that the derived BDE data are internally consistent and free of significant errors.

Electrostatic model calculations

A model that shows some promise for evaluating the dissociation energies of molecular species with sufficiently ionic bonding is the Rittner electrostatic model.[25] As noted earlier, the lanthanide fluorides fall within the proper ionicity range, and the use of the model in estimating values of $D_0^\circ(MF)$ for these species has been described.[26] Although the critical internuclear distances (r_e) and monovalent metal ion polarizabilities (α) have not been determined for most of the lanthanide monofluorides, it is believed that these can be estimated with a fair degree of reliability across the Ba to Lu series, using established values as a guide. On the assumption that $r_e(MF) = 2.0$ Å, $\alpha(M^+) = 5.0$ Å^3, and a vibrational force constant of 3.5 mdyn/Å are representative values for all of the lanthanide monofluorides, a set of binding energies was calculated that yielded D_0° values of 134, 133, and 122 kcal/mol for SmF, EuF, and TmF, respectively.[25] The results of the model calculations are in remarkably good agreement with the new experimental values, particularly as regards the decline in D_0° in going from SmF to TmF at the far end of the series. In this approach, the ionic binding energy is necessarily constant across the series, and any fluctuation in dissociation energies of the neutrals must result from variations in the ionization potentials of the metals [I.P.(M)] since

$$D_0^\circ(MF) = D_0^\circ(M^+F^-) - [\text{I.P.}(M) - \text{E.A.}(F)] ,$$

where E.A.(F) is the electron affinity of the F atom. The only major discrepancy occurs with GdF, where the model[26] predicts $D_0^\circ(GdF) = 123$ kcal/mol as opposed to the experimental value[2] of 140 ± 4 kcal/mol. It remains to be seen if the difference is due to a sharp change in the atomic and molecular constants as the filling of the second half of the 4*f* shell commences at Gd; this is manifested by a sudden rise in I.P.(M) of about 0.5 eV on passing from Eu to Gd. Thus, the spectroscopic, molecular, and thermochemical data for GdF need further detailed scrutiny before it can be concluded that a real discrepancy exists. At the moment, the molecular constants of the polyatomic fluorides are not well enough established to permit a meaningful extension of the ionic model to those species.

Chemi-ionization reactions

The thermochemical information has a bearing on the possibility of gas phase chemi-ionization processes such as $M + F \rightarrow MF^+ + e$ and $M + F_2 \rightarrow MF^+ + F^-$. Thermal energy processes involving O and O_2 with certain metals have been observed to yield ionic products,[27] and the principle has been used as a method for detecting O atoms.[28] The process

$$M + F \rightarrow MF^+ + e \qquad (11)$$

is allowed at thermal energies only if $D_0^\circ(MF) > I.P.(MF)$. From the results of this research, $[D_0^\circ(MF) - I.P.(MF)] = 1.0$, 0.5, and -0.6 eV for SmF, EuF, and TmF, respectively, so that one would expect chemi-ionization to occur with thermal beams of Sm and Eu, but not with Tm. Diebold *et al.*[29] have in fact observed the Sm analog of Reaction (11) and similarly have employed it as an F atom detector.

[1] K. F. Zmbov and J. L. Margrave, in *Mass Spectrometry in Inorganic Chemistry*, Advances in Chemistry Series 72 (American Chemical Society, Washington, D.C., 1968), p. 267.
[2] C. R. Dickson and R. N. Zare, Chem. Phys. 7, 361 (1975).
[3] A. Yokozeki and M. Menzinger, Chem. Phys. 14, 427 (1976).
[4] K. F. Zmbov and J. L. Margrave, J. Inorg. Nucl. Chem. 29, 59 (1967).
[5] D. L. Hildenbrand, J. Chem. Phys. 48, 3657 (1968); 52, 5751 (1970).
[6] D. L. Hildenbrand, Int. J. Mass Spectrom. Ion Phys. 4, 75 (1970); 7, 255 (1971).
[7] D. L. Hildenbrand, "Attainment of Chemical Equilibrium in in Effusive Beam Sources of the Heterogeneous Reaction Type," 10th Materials Research Symposium, National Bureau of Standards, Gaithersburg, MD, September 1978.
[8] E. F. Worden, R. W. Solarz, J. A. Paisner, and J. G. Conway, J. Opt. Soc. Am. 68, 52 (1978).
[9] H. M. Rosenstock, K. Draxl, B. W. Steiner, and J. T. Herron, J. Phys. Chem. Ref. Data 6, Suppl. No. 1 (1977).
[10] D. L. Hildenbrand, J. Chem. Phys. 62, 3074 (1975).
[11] D. L. Hildenbrand, *J. Chem. Phys. 65, 614 (1976).*
[12] K. P. Huber and G. Herzberg, *Molecular Spectra and Molecular Structure IV. Constants of Diatomic Molecules* (Van Nostrand, New York, 1979).
[13] D. J. W. Lumley and R. F. Barrow, J. Mol. Spectrosc. 69, 404 (1978).
[14] M. C. Drake and G. M. Rosenblatt, J. Electrochem. Soc. 126, 1387 (1979).
[15] J. W. Hastie, R. H. Hauge, and J. L. Margrave, High Temp. Sci. 3, 56 (1971).
[16] C. W. DeKock, R. D. Wesley, and D. D. Radtke, High Temp. Sci. 4, 41 (1972).
[17] R. H. Hauge, J. W. Hastie, and J. L. Margrave, J. Less-Common Metals 23, 359 (1971).
[18] C. E. Myers and D. T. Graves, J. Chem. Eng. Data 22, 436 (1977).
[19] JANAF Thermochemical Tables, Natl. Stand. Ref. Data 37 (1971).
[20] R. Hultgren, P. D. Desai, D. T. Hawkins, M. Gleiser, K. K. Kelley, and D. D. Wagman, *Selected Values of the Thermodynamic Properties of the Elements* (American Society for Metals, Cleveland, 1973).
[21] E. W. Kaiser, W. E. Falconer, and W. Klemperer, J. Chem. Phys. 56, 5392 (1972).
[22] Y. C. Kim, J. Oishi, and S. H. Kang, J. Chem. Thermodyn. 9, 973 (1977).
[23] K. Y. Kim and C. E. Johnson, J. Chem. Thermodyn. (submitted).
[24] R. M. Biefeld and H. A. Eick, J. Less-Common Metals 45, 117 (1976).
[25] E. S. Rittner, J. Chem. Phys. 19, 1030 (1951).
[26] D. L. Hildenbrand, J. Electrochem. Soc. 126, 1396 (1979).
[27] W. L. Fite, H. H. Lo, and P. Irving, J. Chem. Phys. 60, 1236 (1974).
[28] C. E. Fairchild, E. J. Stone, and G. M. Lawrence, J. Chem. Phys. 69, 3632 (1978).
[29] G. J. Diebold, F. Engelke, D. M. Lubman, J. C. Whitehead, and R. N. Zare, J. Chem. Phys. 67, 5407 (1977).
[30] K. F. Zmbov and J. L. Margrave, J. Phys. Chem. 70, 3014 (1966).
[31] R. J. Ackermann, E. G. Rauh, and R. J. Thorn, J. Chem. Phys. 65, 1027 (1976).

National Bureau of Standards Special Publication 561, Proceedings of the 10th Materials Research Symposium on Characterization of High Temperature Vapors and Gases held at NBS, Gaithersburg, Maryland, September 18-22, 1978. Issued October 1979.

ATTAINMENT OF CHEMICAL EQUILIBRIUM IN EFFUSIVE BEAM SOURCES OF THE HETEROGENEOUS REACTION TYPE[1]

D. L. Hildenbrand
SRI International
Menlo Park, CA 94025

Effusive beam sources derived from gas-solid reactions provide a very important pathway for widening the scope of high temperature thermodynamic studies, but the attainment of chemical equilibrium within these sources is problematical. Some of the underlying kinetic factors associated with the use of these sources are discussed. As one might expect, it is important to maximize the ratio of reactive surface area to exit orifice area. Equilibrium seems to be achieved more readily among the products of gas-solid reactions than among reactant and products, as suggested by the quasi-equilibrium model. Some experiences with the use of heterogeneous reaction sources are described, and two definitive tests for the establishment of equilibrium are outlined.

1. Introduction

One of the most reliable methods of determining the thermodynamic properties of gaseous molecules stable at high temperatures is based on the study of reaction equilibria in effusive beam sources. In most instances, thermodynamic data are derived from vaporization equilibria using the conventional Knudsen cell technique [1][2], once the identities of the condensed and vapor phases have been established. More recently, the Knudsen technique has been used to study complex gaseous equilibria [2-4], in which case a distribution of gaseous species is generated in the cell by the reaction of two or more condensed phases, and a selective detection method such as mass spectrometry is used to measure the relative abundances of the species. For thermodynamic applications, of course, it is necessary to establish that chemical equilibrium conditions prevail or to provide some means of extrapolating the results to equilibrium. The attainment of vaporization equilibrium within Knudsen cells has been discussed in some detail [5-7], and a useful model has been developed for treating nonequilibrium data [6]. This direct vaporization method has been used

[1]This research was sponsored by the Air Force Office of Scientific Research (AFSC), United States Air Force, under contract F 49620-78-C0033.

[2]Figures in brackets indicate the literature references at the end of this paper.

widely and it has gained acceptance as one of the most powerful methods available for thermodynamic studies. Most of the selected thermochemical data for gaseous metal oxides and halides have been obtained from Knudsen vaporization measurements on solid or liquid samples.

For a number of chemical systems to which one would like to apply the method, particularly with mass spectrometric analysis of the vapor, there are no suitable condensed phases or mixtures of condensed phases that will generate the desired distribution of gaseous species. This is especially true, for example, of many refractory metal halides that do not form stable, involatile condensed halides, and that cannot be generated by halogenation of the metal with another condensed metal halide because of unfavorable thermodynamics. Other examples are the many gaseous metal hydroxides that are stable only in the presence of the metal oxides and relatively high partial pressures of water. For many such systems, the only feasible reaction pathway involves generation of the desired gaseous species by addition of a reactive gas to the Knudsen effusion source containing a suitable condensed phase. Heterogeneous reaction beam sources of this type have been used to study gaseous species such as HBO_2 [8], LiOH [9], BeCl [10], BH [11], and WF_x [12], along with many others, greatly increasing the variety of chemical systems that can be investigated by high temperature mass spectrometry. Unlike the direct vaporization sources, however, there has not been a generally accepted criterion for establishment of chemical equilibrium in gas-solid reaction sources, and there has been some skepticism from time to time about the validity of the results. Stafford [13], in fact, has cited the uncertain status of equilibrium attainment in gas inlet work as one of the major limitations in applying mass spectrometry to high temperature thermodynamic studies. As direct evidence of this, he refers to Knudsen cell studies of the reaction of $H_2(g)$ with $B_4C(s)$ that yielded concentrations of BH_3 and alkylboranes far in excess of predicted equilibrium levels [11], although two other gaseous products, BH and HBC_2, appear to be equilibrated.

Similar considerations apply to double cell experiments in which gaseous species vaporized from a low temperature chamber pass over a second sample in another chamber held at a higher temperature. Reactive vaporization in the hotter chamber yields the distribution of products to be sampled for equilibrium measurements. A good example of the difficulties that can be encountered is offered by two reported studies [14,15] of the gaseous equilibrium Ge + SiO = GeO + Si. First, a double cell study [14] in which GeO and O_2 vaporized from a low temperature chamber containing $GeO_2(s)$ into the high temperature chamber containing Si(s) yielded an apparent equilibrium constant of 3.0×10^{-4} for the gaseous reaction at 1500 K. Inconsistencies with other data on the thermochemical properties of SiO and GeO prompted a reexamination by the single Knudsen cell technique, using a mixture of Si(s), Ge(s) and $SiO_2(s)$ to generate the gaseous products; these single cell measurement [15] gave an equilibrium constant of 4.6×10^{-5} at 1500 K for the SiO - GeO gaseous exchange reaction and removed the earlier discrepancy. Failure to achieve gaseous equilibrium in the double cell experiments is the most probable reason for the difference.

In view of these concerns over the attainment of chemical equilibrium in heterogeneous reaction beam sources, it seemed worthwhile to review some of the pertinent background on

the subject, to discuss some recent experiences with the use of gas-solid reaction sources in thermodynamic studies, and to outline some useful criteria for establishing that chemical reaction equilibrium is attained. The objective is to improve the overall reliability of high temperature equilibrium measurements, thereby increasing the accuracy of the derived thermochemical data. This is an important item because equilibrium studies are one of the most powerful and widely used methods for characterizing high temperature vapors.

2. Typical Gas-Solid Reaction Sources

There are several different ways in which heterogeneous reaction sources can be used for equilibrium studies. In all cases, the experimental arrangement is simple in principle: The reactive gas is added to the base of a conventional Knudsen cell, where it interacts chemically with a condensed sample to produce one or more gaseous products. The resulting gas mixture is emitted from the cell exit orifice in the form of a molecular effusion beam, and is sampled by an instrument such as a mass spectrometer to obtain composition data and reaction equilibrium constants. In this paper we will be dealing exclusively with mass spectrometric detection, but the analysis applies to all other methods as well. The usual experimental procedure and data treatment methods have been described elsewhere [8,10,12], and will not be dealt with here, except as they bear on the equilibrium question. A sketch of a typical effusion cell with gas inlet is given by Meschi, et al. [8]. For convenience in discussing the kinetic aspects of gas-solid reaction sources, a differentiation is made between two types of applications as described below.

In the most obvious application, the added gas is a direct participant in the reaction under study. For example, the reaction $H_2O(g) + B_2O_3(\ell) = 2HBO_2(g)$ was investigated by admitting $H_2O(g)$ to a platinum cell containing $B_2O_3(\ell)$ [8]. Likewise, the gaseous species LiOH and $(OBF)_3$ have been characterized by the reaction of $H_2O(g)$ with $Li_2O(s)$ [9], and $BF_3(g)$ with $B_2O_3(\ell)$ [16]. These cases in which the added gas is a direct participant and must be present at equilibrium levels are labeled as Type I sources.

An important and useful variation is that in which the added gas and perhaps even the condensed phase serve only to generate a distribution of gaseous products by reactive vaporization, and it is the investigation of equilibria among these gaseous products that is of primary interest. As noted earlier, this technique allows one to study certain gaseous species that cannot be generated by the conventional single cell technique. For example W(s) can be fluorinated by $SF_6(g)$ in a carbon or tungsten cell with gas inlet to yield a distribution of W-F and W-S-F gaseous species that varies with cell temperature [12]. With this arrangement it was possible to study gaseous equilibria such as $WF_3 + WF_5 = 2WF_4$, $WF_3 + S = WF_2 + SF$ and $WSF_3 + S = WF_3 + S_2$, and to use this information to characterize the W-F and W-S-F species thermochemically. Other examples are the Mo-F system [$Mo(s) + SF_6(g)$][17], the IIA metal iodides and bromides [$MO(s) + HI(g)$ and $HBr(g)$] [18, 19] and the CF molecule [$C(s) + SF_6(g)$] [20]. Under these conditions, the added gas need not be present at equilibrium levels, nor must the gaseous products necessarily equilibrate with the condensed phases present if only gaseous reactions are being studied; it is necessary only that

gaseous equilibrium be achieved. There have been examples of reaction products generated at partial pressures far above the equilibrium values [21,22], but in one of these it was demonstrated that gaseous equilibrium prevailed among the products [21]. Sources that are used to study equilibria among the gaseous reaction products are designated as Type II sources.

3. Kinetic Implications

Although our concern here is with the use of the gas inlet cell for equilibrium studies, it is worth noting that, at the other extreme, this arrangement has been used for purely kinetic studies. Benson, Golden and associates have developed the Very Low Pressure Pyrolysis (VLPP) technique into an effective kinetic tool [23]. In VLPP studies, a sample gas is admitted to a heated Knudsen cell with relatively large exit aperture under the usual molecular flow condition, and the steady state level of the sample and decomposition products effusing from the reactor are monitored by mass spectrometry. From measurement of the fraction of sample decomposed as a function of temperature for various reactor geometries, information about unimolecular rate constants and activation energies can be derived. It is worth noting that VLPP was conceived as a direct result of reports detailing the difficulties involved in achieving equilibrium in gas inlet work with Knudsen cells [24].

The analysis of Golden, et al. [23] emphasizes the importance of considering the collision number, Z, associated with a specific Knudsen cell reactor. This collision number is the average number of collisions made by a molecule during its transit through the cell, and is defined by the ratio $Z = A_s/A_o$ where A_s is the interior surface area of the cell and A_o is the cell exit orifice area. For heterogeneous reactions, A_s is the surface area of the condensed sample in the cell, which may or may not include the surface of the cell itself. For a purely gas-phase thermal decomposition process, something on the order of at least 50 wall collisions are required before a molecule attains sufficient internal energy to undergo unimolecular reaction. To attain equilibrium, Z values of 10^4 or greater may be required, pointing up the importance of maximizing the ratio A_s/A_o. A strictly gas-phase decomposition process requires the walls to be chemically inert, but Golden, et al. [23] point out that wall effects are seldom a problem because heterogeneous reactions are generally far slower than the re-evaporation of unreacted species. The latter cannot be generally true, and clearly depends on the specific chemistry involved. In any event, the purely gas-phase decomposition process, a special case of the Type I source, is perhaps the most difficult to study under equilibrium conditions. Along these lines, severe difficulties in establishing dissociative equilibrium in Knudsen sources have been reported for gaseous SF_6 [25,26], and B_2H_6 [27].

Experiences with the attainment of chemical equilibrium among the products of gas-solid reactions, i.e., with the Type II source, have been much more favorable. This is in accord with the general kinetic behavior of gas-solid reactions, as exemplified by the quasi-equilibrium (QE) model [28]. According to the QE model, the rate limiting step is the adsorption and equilibration of the impinging gas molecule at the solid interface. Volatile reaction products are in equilibrium with the surface and are emitted in equilibrium proportions, at a rate governed by the rate of adsorption of the incoming reactive molecule.

The QE model appears to correlate the results of several metal oxidation [28] and metal fluorination [29,30] studies at high temperatures and low pressures quite well. In any event, there is kinetic evidence to support the expectation that chemical equilibrium can be achieved with the Type II source under optimum conditions. It must be demonstrated for each individual system, however, that equilibrium is in fact attained.

4. Tests for the Attainment of Equilibrium

One of the most useful and definitive tests for equilibrium can be made by varying the flow or pressure of the reactive gas over a wide range at constant temperature and noting the effects on the derived equilibrium constant, K_{eq}. As pressure is varied, composition of the gas phase changes in accord with the mass action principle, but at equilibrium the values of K_{eq} derived from the species abundances and the reaction stoichiometry must be independent of overall changes in composition. This invariance of K_{eq} with composition defines the fundamental condition of equilibrium in terms of the law of mass action.

As an example of the mass action test, consider the results of some recent studies of the Sr-Al-I gaseous system [31], obtained by admitting HI(g) to a Knudsen cell containing a mixture of SrO(s), Al_2O_3(s) and AlB_{12}(s). The cell contained a perforated partition at the center to prevent molecular streaming, but otherwise involved no special design features. In two measurements at 1762 K with different HI flow rates, the observed parent ion abundances of Sr^+, SrI^+, Al^+ and AlI^+ varied by factors of 1.2, 36, 0.87 and 25, respectively, but the derived equilibrium constants for the gaseous reaction Sr + AlI = SrI + Al were in good agreement (0.0376 and 0.0368), indicating the attainment of equilibrium. For this experiment, the abundances of Sr and Al were essentially fixed by the presence of the solid phases, but the gaseous iodides were dependent on the HI flow. Likewise, with similar studies [31] of the gaseous equilibrium Ba + GaI = BaI + Ga, the abundances of the parent ions Ba^+, BaI^+, Ga^+, and GaI^+ changed by factors of 0.43, 2.4, 4.4 and 25, respectively, by shifting the HI flow at 1711 K but the derived equilibrium constants of 0.708 and 0.698 agree closely. The reader is referred to the original paper [31] for more details of the measurement. Another example of the use of the mass action test is afforded by the results of studies of gaseous equilibria in the Mo-S-F system, generated by the reaction of SF_6(g) and Mo(s) in a Knudsen cell [17]. As noted in the paper [17], a positive indication of equilibrium was obtained. On the negative side, measurements of S-F gaseous reactions generated by passing SF_6(g) through a graphite cell showed that an order of magnitude change in the SF_6 flow yielded apparent equilibrium constants for the reaction $SF_6 + 2S = 3SF_2$ that differed by more than a factor of 100, while concordant results were obtained for the reaction $S + SF_2 = 2SF$ [26]. The mass action criterion is a sensitive one, and it should always be applied as a test for equilibrium in heterogeneous reaction sources, preferably by varying the abundances of the more pressure sensitive species by at least a factor of ten. Departures from equilibrium in the double cell studies [14] of the Si-Ge-O system would have been apparent if the mass action test had been applied there.

A particularly revealing application of the mass action test is given in some recent studies of the heterogeneous reaction 5/6 $MoF_6(g)$ + 1/6 Mo(s) ≈ $MoF_5(g)$ carried out by Knudsen cell mas spectrometry [32]. When $MoF_6(g)$ was admitted to the Mo cell packed with Mo wire initially, the ion current equilibrium quotient $[I^+(MoF_5)]/[I^+(MoF_6)]^{5/6}$ at 440 K showed a substantial flow rate dependence, seen in the series 1 data of table I. After

Table I

EFFECT OF MoF_6 FLOW RATE ON MOLECULAR ABUNDANCES[a] AND DERIVED DATA FOR THE EQUILIBRIUM 5/6 $MoF_6(g)$ + 1/6 Mo(s) = $MoF_5(g)$ at 440 K

$I^+(MoF_6)$	$I^+(MoF_5)$	$\frac{[I^+(MoF_5)]}{[I^+(MoF_6)]^{5/6}}$
	Series I	
2.77	0.054	2.31×10^{-2}
12.01	0.171	2.15×10^{-2}
33.5	0.315	1.69×10^{-2}
66.6	0.408	1.23×10^{-2}
	Series II	
11.3	0.047	6.28×10^{-3}
12.4	0.051	6.26×10^{-3}
36.4	0.151	7.55×10^{-3}
45.0	0.162	6.79×10^{-3}
50.5	0.191	7.27×10^{-3}
106.1	0.365	7.48×10^{-3}

[a]Abundances in arbitrary units.

vacuum outgassing of the cell for an hour at 1300 K and 5 x 10^{-7} Torr, the quotient dropped to a somewhat lower value but was essentially independent of MoF_6 flow rate within experimental error. Apparently the molybdenum surface was initially covered with an oxide film, and this film severely limited the number of surface sites available for reactive vaporization. After vacuum outgassing, equilibrium behavior was observed, probably as a result of the increase in reactive surface sites. This phenomenon could be reproduced repeatedly by alternately exposing the molybdenum surface to background gas at about 10^{-3} Torr, and later outgassing at 1300 K under high vacuum. The results point out the importance of considering the "clean" surface area A_s when maximizing the ratio A_s/A_o. Another implication of these results worth noting is that the chemical rearrangement and bond breaking step in the MoF_6 + Mo reaction is apparently faster than the surface accommodation of the impinging MoF_6 molecule, even at the relatively low temperatures of these experiments. This is contrary to the assumptions of Golden, et al. [23] regarding the relative importance of surface reaction as opposed to re-evaporation, but is in accord with the quasi-equilibrium model of surface reactions.

One further test that can be useful in checking on the attainment of equilibrium involves the approach to the equilibrium position from different chemical compositions. This is a variation of the classical technique of approaching equilibrium from opposite directions: at equilibrium, the rates of the forward and reverse reactions must be equal, so that the derived equilibrium constants will be independent of the direction of approach. For the high temperature reactions of interest here, the reagents and products cannot be added separately, but it is possible to vary the beam source chemistry so as to give definitive information about equilibrium attainment. For example, in studies of the gaseous tungsten fluorides [12], the reactions $WF_3 + WF_5 = 2WF_4$ and $WF_4 + WF_2 = 2WF_3$ were studied by fluorinating W(s) with both $SF_6(g)$ and $WF_6(g)$. Equilibrium data obtained with the two different sources were in close agreement [12]. A similar set of data for the Mo-F system [17], shown graphically in figure 1 provides evidence that the reactions of $MoF_6(g)$ and $SF_6(g)$ with Mo(s) yield identical equilibrium data for reactions among the Mo-F species. In yet another example, equilibrium data for the gaseous reaction Sm + CaF = SmF + Ca were found to be independent of whether approached by the reaction of $CaF_2(g)$ and $Sm_2O_3(s)$ in a double cell or by the reaction of $SmF_3(s)$, $CaF_2(s)$, and B(s) in a single cell [33]. The double cell data yielded an equilibrium constant of 2.60 at 2200 K for the SmF-CaF exchange reaction, compared to a value of 2.49 from the single cell. These examples serve to show that conclusive evidence of equilibrium behavior also can be obtained by varying the beam source chemistry. The extra time required to make these tests is more than offset by the added confidence that can be attached to the results.

In conclusion, it goes without saying that the attainment of equilibrium in effusive sources never should be taken for granted. Fortunately when tests such as those described above are used routinely with gas-solid reaction sources, no assumptions need be made about the establishment of equilibrium.

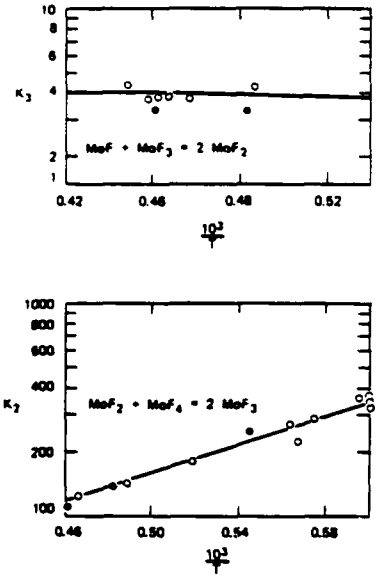

Figure 1. Plot of equilibrium constants for gaseous Mo-F reactions; open circles, $SF_6(g)$ + Mo(s); closed circles, $MoF_6(g)$ + Mo(s).

References

[1] Margrave, J. L., in Physicochemical Measurements at High Temperatures, chap. 10, p. 231 (Butterworths, London, 1959).

[2] Ehlert, T. C., Blue, G. D., Green, J. W., and Margrave, J. L., J. Chem. Phys. 41, 2250 (1964).

[3] Hildenbrand, D. L. and Murad, E., J. Chem. Phys. 43, 1400 (1965).

[4] Ames, L. L., Walsh, P. N., and White, D., J. Phys. Chem. 71, 2707 (1967).

[5] Whitman, C. I., J. Chem. Phys. 20, 161 (1952).

[6] Motzfeldt, K., J. Phys. Chem. 59, 139 (1955).

[7] Stern, J. H. and Gregory, N. W., J. Phys. Chem. 61, 1226 (1957).

[8] Meschi, D. J., Chupka, W. A., and Berkowitz, J., J. Chem. Phys. 33, 530 (1960).

[9] Berkowitz, J., Meschi, D. J., and Chupka, W. A., J. Chem. Phys. 33, 533 (1960).

[10] Hildenbrand, D. L. and Theard, L. P., J. Chem. Phys. 50, 5350 (1969).

[11] Steck, S. J., Pressley, Jr., G. A., and Stafford, F. E., J. Phys. Chem. 73, 1000 (1969).

[12] Hildenbrand, D. L., J. Chem. Phys. 62, 3074 (1975).

[13] Stafford, F. E., High Temperatures-High Pressures 3, 213 (1971).

[14] Hildenbrand, D. L. and Murad, E., J. Chem. Phys. 51, 807 (1969).

[15] Hildenbrand, D. L., High Temperature Science 4, 244 (1972).

[16] Porter, R. F., Bidinosti, D. R., and Watterson, K. F., J. Chem. Phys. 36, 2104 (1962).

[17] Hildenbrand, D. L., J. Chem. Phys. 65, 614 (1976).

[18] Hildenbrand, D. L., J. Chem. Phys. 68, 2819 (1978).

[19] Hildenbrand, D. L., J. Chem. Phys. 66, 3526 (1977).
[20] Hildenbrand, D. L., Chem. Phys. Lett. 32, 523 (1975).
[21] Chupka, W. A., Berowitz, J., Meschi, D. J., and Tasman, H. A., Advan. Mass Spectrom., Vol. 2, p. 99 (Pergamon, London 1963).
[22] Steck, S. J., Pressley, Jr., G. A., Lin, S. S., and Stafford, F. E., J. Chem. Phys. 50, 3196 (1969).
[23] Golden, D. M., Spokes, G. N., and Benson, S. W., Angew. Chem. 12, 534 (1973).
[24] Golden, D. M., Private communication.
[25] Brackmann, R. T., Fite, W. L., and Jackson, W. M., Paper F-1, 18th Annual Conference on Mass Spectrometry and Allied Topics, San Francisco, California (1970).
[26] Hildenbrand, D. L., J. Phys. Chem. 77, 897 (1973).
[27] Sinke, E. J., Pressley, Jr., G. A., Bayliss, A. B., and Stafford, F. E., J. Chem. Phys. 41, 2207 (1964).
[28] Batty, J. C. and Stickney, R. E., J. Chem. Phys. 51, 4475 (1969).
[29] Philippart, J. T., Caradec, J. Y., Weber, B., and Cassuto, A., J. Electrochem. Soc. 125, 162 (1978).
[30] Nordine, P. C., J. Electrochem. Soc. 125, 498 (1978).
[31] Kleinschmidt, P. D. and Hildenbrand, D. L., J. Chem. Phys. 68, 2819 (1978).
[32] Kleinschmidt, P. D., Lau, K. H., and Hildenbrand, D. L., J. Chem. Thermodynamics, in press.
[33] Lau, K. H., Kleinschmidt, P. D., and Hildenbrand, D. L., unpublished data.

Discussion

Question (Cater): Do you have a problem with sorting out the fluoride species because of dissociation in the ion source?

Response (Hildenbrand): Not necessarily, for example in the tungsten case, they all formed parent ions. In some cases there is some fragmentation. But I think there aren't any overriding cases where we cannot sort this out.

Question (Ferron): Is there excess gas in these reactions, I guess at the interface?

Response (Hildenbrand): We are talking about very low pressure conditions. There is a free molecular flow ---.

(Editor's note): The record of this discussion is incomplete but the general concern was with possible nonequilibrium transport effects, the response was that this was usually not a problem.

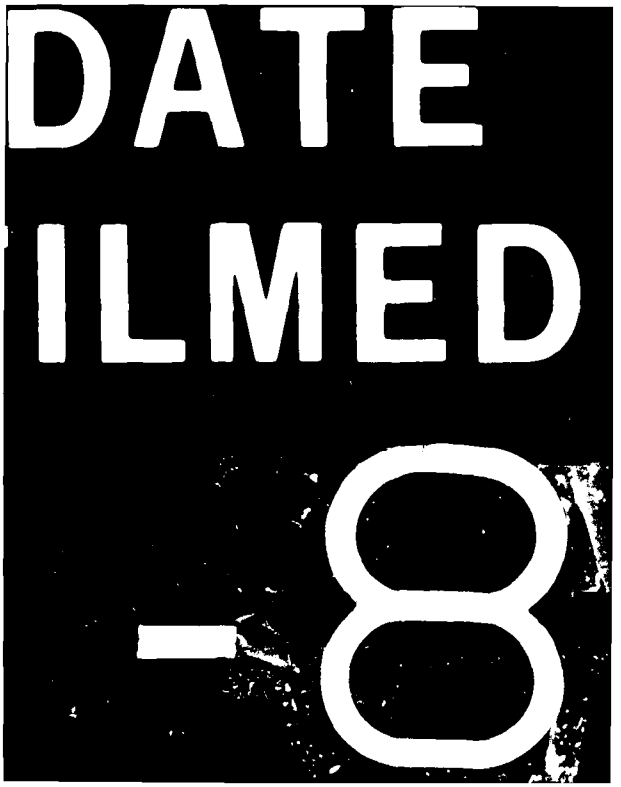
DATE
ILMED
-8